INVESTIGATIONS ON DIFFERENT ASPECTS OF CARDIAC VENTRICULAR REPOLARIZATION: REPOLARIZATION RESERVE AND ADAPTATION TO HEART RATE

Ph.D. Thesis

Zoltán Husti, M.D.

Szeged

2014.

INVESTIGATIONS ON DIFFERENT ASPECTS OF CARDIAC VENTRICULAR REPOLARIZATION: REPOLARIZATION RESERVE AND ADAPTATION TO HEART RATE

Ph.D. Thesis

Zoltán Husti, M.D.

Szeged, 2014.

Supervisor:

István Baczkó M.D., Ph.D.

Department of Pharmacology and Pharmacotherapy

Faculty of Medicine, University of Szeged

Publications related to the subject of the Thesis

I. **Husti Z**, Tábori K, Juhász V, Hornyik T, Varró A, Baczkó I. Combined inhibition of key potassium currents differently affects cardiac repolarization reserve and arrhythmia susceptibility in dogs and rabbits. *Can J Physiol Pharmacol*, 2014, accepted for publication.
Impact Factor (2013) = 1.546

II. Pueyo E, **Husti Z**, Hornyik T, Baczkó I, Laguna P., Varró A., Rodríguez B. Mechanisms of ventricular rate adaptation as a predictor of arrhythmic risk. *Am J Physiol – Heart Circ Physiol*, 2010, 298(5): H1577-1587.
DOI: 10.1152/ajpheart.00936.2009
Impact Factor (2010) = 3.88

List of Abbreviations

AMP	Amplitude of the action potential
APD	Action potential duration
APD_{90}	Action potential duration at 90% repolarization
BCL	Basic cycle length
BVR	Beat-to-beat variability of repolarization
$[Ca^{2+}]_i$	Intracellular calcium concentration
cAVB	Chronic atrioventricular block
CL	Cycle length
DAD	Delayed afterdepolarization
EAD	Early afterdepolarization
HR	Heart rate
$I_{Ca,L}$	Voltage gated L-type calcium current
I_{NaK}	Na^+/K^+ pump current
I_{K1}	Inward rectifier potassium current
$I_{K,ACh}$	Acetylcholine-activated potassium current
I_{Kr}	Rapid component of the delayed rectifying potassium current
I_{Ks}	Slow component of the delayed rectifying potassium current
I_{Na}	Fast voltage gated sodium current
I_{to}	Transient outward potassium current
$[K^+]_o$	Extracellular potassium concentration
LQT	Long QT syndrome
QTc	Frequency corrected QT interval
TdP	Torsades de Pointes chaotic ventricular tachycardia
STV_{QT}	Short-term variability of the QT interval
STV_{RR}	Short-term variability of the RR interval
V_{max}	Maximum upstroke velocity

Table of Contents

1. Introduction

One of the most dreaded side effects of a number of compounds in development and clinically used drugs is their pro-arrhythmic potential causing malignant ventricular arrhythmias including Torsades de Pointes (TdP) polymorphic ventricular tachycardia that can lead to sudden cardiac death. Predicting TdP in clinical settings is a very difficult task since the incidence of drug induced TdP is very low (1:100000). A significant portion of compounds are withdrawn due to their prolonging effect on repolarization and incidence of TdP during the development process.

Drug-induced arrhythmias were generally considered as the consequence of impairment of the cardiac repolarization process that usually leads to QTc prolongation on the ECG. However, recent studies suggest that QTc prolongation is not necessarily associated with the occurrence of TdP and in these cases ventricular repolarization reserve may be reduced without significant changes in the duration of cardiac repolarization. A number of studies suggest that increased short-term variability of QT interval, a novel ECG parameter correlates better with decreased repolarization reserve and the incidence of malignant ventricular arrhythmias.

Another possible predictor of ventricular arrhythmias is the impaired frequency adaptation of the QT interval to sudden heart rate changes. Slow QT interval rate adaptation has been related to increased risk of development of afterdepolarizations and triggered activity, which could eventually result in TdP in a vulnerable substrate (Burashnikov et al. 1998).

1.1 The concept of repolarization reserve

The term “repolarization reserve” was coined by Dan Roden (Roden, 1998) and according to this concept, the complexity of cardiac repolarization process includes some redundancy. As a consequence, the loss of one component of repolarizing currents (e.g. I_{Kr}) does not lead to repolarization abnormalities (i.e. marked QT prolongation) because the other components can compensate for the lost function of the impaired current. On the other hand, in the case of reduced repolarization reserve, even mild inhibition of another repolarizing current can result in excessive repolarization prolongation and serious ventricular arrhythmias. Therefore, decreased repolarization reserve makes the myocardium more sensitive to pro-arrhythmic agents without marked QTc prolongation. Consequently, adequate pro-arrhythmia models with impaired repolarization reserve (mimicking, at least in part, pathological clinical settings) are needed to reliably assess the possible TdP provoking side

effect of pharmaceutical compounds thus contributing to improved prevention of drug-induced sudden cardiac death in humans.

1.2 Cardiac ionic currents and their possible role in repolarization reserve and repolarization adaptation

The action potential of cardiac myocytes is the result of the highly regulated and coordinated function of different transmembrane ionic channels and transporters. The trans-sarcolemmal ionic movement through the pore forming units of transmembrane ion channels is driven by the transmembrane electrochemical gradient. These ion channels can be classified regarding to the mechanisms that regulate their opening: there are voltage gated (e.g inward sodium current (I_{Na})) and ligand gated ion channels (e.g. acetylcholine-activated potassium current ($I_{K,Ach}$)). These channels represent complicated structures consisting of transmembrane proteins with different subunits: the pore forming alpha and channel function modulating beta and/or gamma subunits that regulate the activation and inactivation properties of these channels. It is well known that there are significant apicobasal, transmural as well as chamber specific differences in the expression of these channels and the densities of ionic currents they carry.

1.2.1 Inward sodium current (I_{Na})

The rapid depolarization phase (phase 0) of the action potential and consequently the fast conduction are attributed to the fast inward rectifier sodium current (I_{Na}). The channel possesses double gated properties regulated by the activation and inactivation gates. The sodium channels are closed at resting membrane potential during diastole due to the closed state of the activation gate and rapidly open ($\tau < 0.5$ ms) on membrane depolarization that are more positive than –60 mV while the inactivation gate is slightly slower closing ($\tau \sim$ 0.5-5 ms). Consequently, both gates are open for a short time (1 – 2 ms) and sodium ions flow into the cell driven by the electrochemical gradient resulting in rapid depolarization of the cell (phase 0 depolarization). However, at positive membrane potentials, the inactivation gate closes and remains closed during repolarization until the membrane potential returns to sufficiently negative values (inactive state). After the action potential when the membrane potential returns to the appropriate negative value, the activation gate closes (deactivation) and the inactivation gate opens again ($\tau \sim$ 3 -25 ms) so the channel returns to its resting conformation during diastole (Antoni et al, 1988; Follmer et al, 1987; Fozzard et al, 1985; Varró et al, 1992; Whalley et al, 1995). In addition, a small fraction of the sodium current

inactivates slowly during the plateau phase (window I_{Na}), and this current is relatively potent in Purkinje fibers (Attwell et al, 1979; Carmeliet, 1987). This persistent sodium current functionally opposes repolarizing potassium currents and delays repolarization. In some clinical pathological settings (e.g. long QT syndrome 3, heart failure) this current is augmented resulting in decreased repolarization reserve and prolongation of repolarization leading to malignant ventricular arrhythmias (Schwartz et al, 1995).

1.2.2 L- type inward calcium current ($I_{Ca,L}$)

The operation of the L-type inward calcium current is similar to that of I_{Na}, namely it possesses activation and inactivation gating mechanisms, the channels could be in activated, inactivated and resting states according to the cardiac cycle (Hirano et al, 1989; Isenberg et al, 1982; January et al, 1989; Mitra et al, 1986; Varró et al, 1992; Whalley et al, 1995). The calcium current, like I_{Na}, exhibits both slowly inactivating and window components. The inactivation of the L-type calcium channels are dependent on intracellular calcium concentration ($[Ca^{2+}]_i$): increased $[Ca^{2+}]_i$ accelerates the inactivation of the $I_{Ca,L.}$ (Ca dependent inactivation). Consequently, the $I_{Ca,L}$ are dynamically regulated by the Ca released from the sarcoplasmic reticulum during the cardiac cycle. Since $[Ca^{2+}]_i$ changes dynamically during the cardiac cycle and it is regulated by many other factors (eg. protein kinase A, protein kinase C, phospholamban, ryanodine receptor Ca ATPase, calmodulin) (Bers, 2001), the exact role of the $I_{Ca,L}$ in repolarization and repolarization reserve is difficult to establish. Due to the relatively slow inactivation of calcium channels, $I_{Ca,L}$ plays a very important role in the maintenance of the plateau phase and has a key role in cardiac contraction. In case $I_{Ca,L}$ is augmented, the plateau voltage is shifted to more positive values that may result in enhanced activation of outward potassium currents that may shorten repolarization. In several types of cardiac cells where I_{Na} is not present (sinoatrial node, atrioventricular node) or in seriously damaged cardiac tissue, the L- type calcium current can be responsible for the depolarization and conduction (slow type action potential). An important role is attributed to $I_{Ca,L}$ in the frequency adaptation of the action potential duration and QT interval. The $I_{Ca,L}$ block is associated with slower APD adaptation to heart rate changes that may lead to cardiac arrhythmias.

1.2.3 Rapid delayed rectifier outward potassium current (I_{Kr})

I_{Kr}, that flows through HERG, MIRP and MinK protein constituted channels (Abbott et al, 1999), activates rapidly during depolarization (Gintant, 1996) at membrane potentials more

positive than -30 mV (τ~40 ms). In contrast with I_{Na} and $I_{Ca,L}$, the operation of the channel is regulated by only one gating mechanism, the opening and closing of the activation gate. The opening of the gate is defined as activation and the closing of the gate, as opposed to the double gating mechanism, is called deactivation and not inactivation. The depolarization dependent activation of I_{Kr} channels are preceded by deactivation (Spector et al, 1996), consequently, the channels are largely closed during the plateau phase and open again when membrane potential decreases to around 0 mV and then slowly deactivate at negative membrane potential values. Its special gating properties, namely the fast deactivation and recovery from deactivation, render the channels an apparent inward rectifier and play an important role in the third phase of repolarization. The magnitude of the I_{Kr} current is under direct regulation of the extracellular potassium concentration $[K^+]_o$. Contrary to that might be expected from the Nernst and Goldman-Hodgkin-Katz equation, the I_{Kr} current increases with higher $[K^+]_o$ while reduced $[K^+]_o$ decreases the I_{Kr} current (Sanguinetti and Jurkiewicz, 1992; Yang et al, 1997). It has been found recently that the reduction of $[K^+]_o$ promotes the internalization and degradation of the HERG channels in rabbit heart and in human cell lines resulting in prolonged repolarization and decreased repolarization reserve (Guo et al., 2009). These mechanisms may play an important role in the development of malignant arrhythmias following electrolyte disturbances. I_{Kr} may contribute to repolarization lengthening when repolarization is already prolonged (Virág et al., 2009) with a positive feedback mechanism. In the case of longer action potential duration (e.g in bradycardia), there is less I_{Kr} current at isochronal point of the time course of action potential contributing to further prolongation of repolarization. Because of these properties of the I_{Kr} current, repolarization becomes more vulnerable when depolarizing factors are augmented due to LQT3, or other repolarizing factors are reduced (e.g. LQT1). In this setting, a partial decrease of I_{Kr} may result in critical elongation of APD leading to early afterdepolarization (EAD) and TdP ventricular arrhythmia. The major part of APD prolonging antiarrhythmic and non-cardiac drugs exert their effect by inhibition of I_{Kr} current (Roden and Viswanathan, 2005). A significant inhibition of I_{Kr} leads to substantial APD prolongation (Varró et al, 2000; Lengyel et al, 2001; Jost et al, 2005). When inhibition is partial, the I_{Kr} reduction does not necessarily manifest in significant repolarization lengthening due to the compensatory function of other outward currents. However, in the presence of further APD prolonging factors such as bradycardia, excessive APD prolongation may develop. The torsadogenic effect of weak I_{Kr} inhibiting non-cardiac drugs that do not markedly prolong the QT interval could be explained by this

phenomenon. As a result, I_{Kr} is one of the most important currents contributing to repolarization reserve (Varró and Baczkó, 2011).

1.2.4 Slow delayed rectifier outward potassium current (I_{Ks})

The channel proteins of the slow component of the delayed rectifier potassium current constitute KvLQT1 alpha subunits and Mink and MIRP beta subunits. The I_{Ks} activates slowly during the plateau phase (τ~ 500-1000 ms) and deactivates relatively rapidly at negative membrane potentials (τ~ 100-200 ms) (Jost et al, 2007; Virág et al, 2001). As an important consequence of the slow activation kinetics and small amplitude between 0 and +20 mV, the contribution of I_{Ks} to repolarization is not considerable in normal circumstances, at physiological heart rate and action potential duration (Varró et al, 2000; Jost et al, 2005). However, when action potential duration is lengthened or sympathetic tone is increased, I_{Ks} is activated and plays an important role in the shortening of APD and in preventing extreme APD prolongation. The I_{Ks} current activates at positive membrane potential values, thus in the case of APD prolongation when the plateau phase is shifted to more positive values, more I_{Ks} can be activated protecting the cell from the further repolarization lengthening. Pharmacological block of I_{Ks} inhibits this feedback mechanism increasing the risk of arrhythmia. The activation of the I_{Ks} also increases after sympathetic stimuli (Volders et al, 2003; Yazawa and Kameyama, 1990; Walsh and Kass, 1991), moreover, amplification of $I_{Ca,L}$ under sympathetic tone shifts the plateau toward more positive membrane potential values resulting in further I_{Ks} activation and consequent APD shortening (Volders et al, 2003). Thus, inhibition of I_{Ks} during sympathetic activation leads to the loss of adaptive APD shortening (Han et al, 2001) that is further weakened by the activated inward $I_{Ca,L}$ current. Animal experiments carried out in different species suggest that inhibition of I_{Ks} alone does not result in significant APD prolongation and ventricular arrhythmias. However, pharmacological block of I_{Ks} together with I_{Kr} inhibition causes excessive APD prolongation (Varró et al, 2000) and consequent early afterdepolarizations (EAD) leading to malignant ventricular arrhythmias (TdP-VT). Thus, I_{Ks} does not necessarily contribute to repolarization in normal circumstances and low sympathetic tone, but provides a very important protective mechanism against APD prolonging agents in pathological settings and represents a significant reserve outward current and plays a key role in repolarization reserve (Johnson et al, 2010). The density of I_{Ks} channels shows transmural and regional heterogeneity (Gintant, 1995): the expression is significantly stronger in the subepicardial than in the endocardial layer contributing to physiological repolarization heterogeneity already present in normal settings.

However, under certain conditions (e.g. heart failure) these expression differences may be more pronounced due to electrical remodeling causing significant dispersion of repolarization that may lead to increased incidence of malignant arrhythmias.

1.2.5 Inward rectifier potassium current (I_{K1})

I_{K1} flows through Kir2.1, Kir2.2, Kir2.3, Kir2.4 channels (Anumonwo and Lopatin, 2010; Barry and Nerbonne, 1996; Boyett et al, 1996). Its name (inward rectifier) originates from the phenomenon that potassium movement through these channels is larger toward the intracellular space than outward direction if membrane potentials are more negative than -90 mV (Carmeliet, 1993; Harvey and Ten Eick, 1988). However, it is important to note that this phenomenon exists only in experimental settings due to the fact that membrane potentials of myocytes are more positive than the electrochemical potential of K^+ in physiological circumstances. Consequently, potassium current also flows into the outward direction through these channels. The pore forming units of the inward rectifier potassium current (I_{K1}) are open at resting membrane potential during diastole, but the current is decreasing close to zero at membrane potentials above -30mV and the channel is reopening very rapidly when the membrane potential reaches more negative values (inward rectification) contributing to the final repolarization phase. This inward rectification is due to the voltage dependent channel inhibition caused by Mg^{2+} and polyamines (Matsuda et al, 1987). I_{K1} is fully open at rest that plays an important role in the maintenance of the resting membrane potential. As a consequence, presumably, the I_{K1} can oppose any kind of depolarization such as delayed afterdepolarisations (DAD) due to calcium overload, preventing the development of extrasystoles and its propagation to the surrounding myocardium, therefore I_{K1} can play an important role in repolarization reserve (Varró and Baczkó, 2011). It is considered as a special form of repolarization reserve. In addition, impairment of I_{K1} results in prolonged repolarization and more depolarized membrane potential. The density of I_{K1} shows significant differences among species (Jost et al, 2008; Varró et al, 1993): it is strong in dog and rabbit but relatively weak in human ventricles. This means that block of I_{K1} in humans is not reflected in significant APD lengthening but inhibition of this current together with other repolarizing currents (e.g. I_{Kr}) may cause excessively increased repolarization leading to development of EADs and malignant ventricular arrhythmias (Ishihara et al, 2009). Regarding the regional distribution of I_{K1} channels, significant differences are found: I_{K1} is more pronounced in endocardial than epicardial layers and stronger in apical than in basal areas contributing to repolarization inhomogeneity.

1.3 Pro-arrhythmia models based on the impairment of repolarization reserve and possible significance of short term QT variability

Perhaps the most extensively studied *in vivo* pro-arrhythmia model for drug-induced TdP is the dog model featuring chronic atrioventricular block and chronic bradycardia (Chezalvier-Guilbert et al., 1995; Vos et al., 1995). In this setting, the downregulation of several potassium currents was observed, particularly the downregulation of the slow delayed rectifier potassium current (I_{Ks}), that plays a vital role in repolarization reserve and development of arrhythmias and development of TdP (Volders et al., 1999). Downregulation or impairment of I_{Ks} current alone did not markedly influence normal ventricular repolarization in isolated rabbit, dog and human ventricular preparations but obviously plays an important role of repolarization reserve and it can significantly contribute to the safety margin of repolarization (Varró et al., 2000; Lengyel et al., 2001; Volders et al., 2003; Jost et al., 2005; Abi-Gerges et al., 2006).

In the same chronic AVB dog model, it was found that QTc prolongation alone did not correlate with the pro-arrhythmic potential of drugs (Lawrence 2005) and the markedly lengthened QTc interval by I_{Kr} block alone did not significantly increase the incidence of TdP. These results are similar to that observed in human (van Opstal et al., 2001). This model also showed that the incidence or lack of arrhythmia correlated better with the degree of short-term variability (STV) of repolarization (Thomsen et al., 2004).

Several studies suggest that susceptibility to arrhythmias does not dependent only on the spatial but it is also influenced by the temporal inhomogeneity of repolarization (Berger et al., 1997; Hondeghem et al., 2003). Beat-to-beat variability of repolarization (BVR) which is quantified as short-term variability (STV), is a novel biomarker that represents the temporal dispersion of repolarization duration between consecutive beats. BVR can simply be illustrated on a Poincaré plot where each QT or APD value is plotted against its preceding value. The greater the covered area on the Poincaré plot the larger the BVR. The BVR has been therefore suggested to be calculated in drug safety investigations, expressed as STV. This parameter has already been used in dog and rabbit pro-arrhythmia models as well as in some small clinical studies, however, broad clinical application is still lacking. It was demonstrated in a chronic atrioventricular block dog model (cAVB dog) that the known pro-arrhythmic drug, D-sotalol, increased both the QTc interval and STV_{QT}, however, amiodarone that is less frequently associated with TdP, caused a similar and marked QT prolongation but did not increase STV (Thomsen et al., 2004). Nevertheless, numerous studies confirm that following administration of safe drugs the STV remains unchanged despite significant QT

lengthening whereas pro-arrhythmia is associated with STV prolongation (Thomsen et al, 2004; Oros et al, 2010; Antoons et al, 2010; Oros et al, 2006;Thomsen et al, 2006; van Opstal et al, 2001). Importantly, a large number of TdP episodes were induced only when repolarization reserve was previously impaired by chronic atrioventricular block leading to remodeled heart or multiple drug administration. In these cases, the occurence of TdP was associated with a clear increase in STV.

Some clinical studies also demonstrated that STV_{QT} was a more promising predictive parameter for patients with increased risk for impaired repolarization dependent ventricular arrhythmias. Hinterseer at al. have found that in patients known to be at high risk for drug-induced TdP, STV_{QT} was two-fold higher than in controls, however, QTc- intervals were similar in the two groups (Hinterseer et al., 2008). The results of another study by Hinterseer et al. showed that congenital LQTS patients only with manifest tachyarrhythmias had significantly increased STV_{QT} in addition to a prolonged QTc interval (Hinterseer et al., 2009). Similar results were obtained in patients with congestive heart failure and patients with implantable cardioverter-defibrillator for secondary prevention whose STV_{QT} values were the highest among high risk patients (Hinterseer et al., 2010). An increased STV_{QT} was also demonstrated in professional soccer players with athlete's heart during and after exercise despite increased heart rate and decreases heart rate variability (Lengyel at al., 2011) These results indicate that STV_{QT} could be a more reliable marker to identify patients with decreased repolarization reserve and could be a promising parameter to predict possible malignant ventricular arrhythmias in the clinical setting.

Experiments in our laboratory carried out on a conscious dog and anaesthetized rabbit TdP model also showed that increased QTc interval following the administration of the I_{Kr} blocker dofetilide did not lead to a high incidence of TdP but simultaneous decrease of repolarization reserve by application of the I_{Ks} blocker HMR 1556 resulted in significant increase in STV_{QT} and incidence of TdP (Lengyel et al., 2007). Based on the above it seems that the reduction of I_{Ks} current and the consequent impairment of repolarization reserve either by experimental AV-block (leading to I_{Ks} downregulation) or pharmacological I_{Ks} block, increases arrhythmia susceptibility and increases the incidence of ventricular arrhythmia development that can be better predicted by increased STV_{QT} than by simple measurements of repolarization prolongation.

On the other hand, repolarization reserve is not limited to I_{Ks} function, and currently there is little data on the relative roles of the other potassium currents, such as I_{K1}, in repolarization reserve and TdP development. It is important to note species differences

regarding to the density of I_{K1}: it is relatively weak in humans (Jost et al., 2008), but strong in dog, rabbit and guinea pig (Varró et al., 1993). Impairment of I_{K1} in humans is not always reflected in significant repolarization and QTc prolongation. In LQT7 (Andersen-Tawil syndrome), loss of function mutations in Kir2.1 channels significantly decrease I_{K1} current, however, the substantially increased pro-arrhythmic risk in these patients is not accompanied by marked QTc prolongation on the ECG (Zhang et al., 2005). However, the impairment of repolarization reserve associated with malfunction of I_{K1} together with the defect of other potassium channels, may lead to excessive lengthening of the APD. Computer modeling studies also support a key role for I_{K1} in ventricles: in these models, reduction of I_{K1} in addition to I_{Kr} block led to EADs (Ishihara et al., 2009). Nevertheless, there is little animal experimental evidence that reduction of repolarization reserve associated with malfunction of I_{K1}, actually predisposes the heart to malignant arrhythmias.

There is considerable variation in the expression of key repolarizing potassium channels in different mammalian species, including dog and rabbit that are frequently used species in pro-arrhythmia models. Therefore, it is reasonable to assume that species specific ion channel expression profiles may result in species dependent alterations in responses to potassium channel blockers. Such differences may significantly influence the value of data obtained in these models for human extrapolation, however, it is unclear how species specific potassium channel expressions translate into differences in arrhythmia development in dogs and rabbits.

1.4 Adaptation of the repolarization to abrupt changes in heart rate

Disturbances in another important aspect of cardiac ventricular repolarization adaptation can also play a significant role in the development of serious cardiac arrhythmias and sudden cardiac death. Rapid changes in heart rate are attended by prompt adaptation of QT interval to restore the proper steady-state level. Clinical, animal experimental and theoretical studies have shown that abrupt changes in heart rate result in a progressive adaptation of the QT interval measured on the ECG due to short-term cardiac memory effects. The short-term cardiac memory defined as the effect of pacing history on action potential duration (APD) (Baher et al., 2007). The term ‘memory’ means a variety of circumstances in which the APD of one action potential does not depend simply on the previous action potential (Rosenbaum et al. 1982; Gilmour et al. 1997; Shvilkin et al. 1998; Wu & Patwardhan, 2004). A part of these changes appear after a few beats while others require hours of stimulation. Cardiac memory is identified on the surface ECG as significant change in T- wave polarity that is seen when sinus rhythm resumes after a period of abnormal myocardial activation. Currently,

although, the ionic mechanisms of short-term cardiac memory are poorly understood, they may have important effects on reentry and fibrillation. Grom et al. have demonstrated in a clinical study that in the case of slow APD adaptation, the suddenly decreased heart rate, as occurs at conversion of atrial fibrillation, the initial APD and QT intervals will be shorter than in the steady-state at the new heart rate (Grom et al., 2005). This may make the myocardium more susceptible to arrhythmias. Similarly, when heart rate suddenly increases, the initial APD and QT will be more prolonged than at steady-state. The prolonged APD is known to be a risk for TdP arrhythmia. Patients exhibiting protracted QT interval heart rate adaptation dynamics have been identified to be at greater risk for developing cardiac arrhythmias and sudden cardiac death. Furthermore, clinical data also suggests that the extent of amiodarone-induced acceleration of QT interval heart rate adaptation could be used as a therapeutic marker of antiarrhythmic drug efficacy (Smetana et al., 2004). Regarding the underlying ionic mechanisms that has been extensively studied in cardiac memory is the transient outward potassium current (I_{to}) (Balzo et al., 1992). Changes in $I_{Ca,L}$ and I_{Kr} are also described in cardiac memory (Plotnikov et al., 2003; Obreztchikova et al., 2006). The APD heart rate adaptation consist of two phases: a fast initial phase with time constant <30 s, mainly related to L-type calcium and slow-delayed rectifier potassium current, and a second slow phase of > 2 min driven by intracellular sodium concentration ($[Na]_i$) dynamics. However, despite strong evidence suggesting an important role of short-term cardiac memory in arrhythmogenesis, the underlying ionic mechanisms are still controversial.

2. Aims of the study

2.1 Aims of studies on repolarization reserve

It is not clear, how species specific potassium channel expressions translate into differences in arrhythmia development in dogs and rabbits, two species frequently used in pro-arrhythmia models. It has been shown previously that repolarization reserve impairment by inhibition of I_{Ks} increased arrhythmia susceptibility during subsequent I_{Kr} inhibition in dogs and rabbits in a similar degree. A possibly important role for I_{K1} has been suggested in repolarization reserve. In the first series of experiments we studied the effects of combined pharmacological inhibition of I_{K1} and I_{Ks}, as well as I_{K1} and I_{Kr} on ECG parameters and the incidence of TdP in conscious dogs and anesthetized rabbits. We also investigated whether TdP development was paralleled by increased short-term variability of the QT interval, a novel ECG parameter suggested for more reliable prediction of drug-induced ventricular arrhythmias.

2.2 Aims of studies on repolarization adaptation to changes in heart rate

The aim of the second series of experiments was to investigate another important aspect of cardiac ventricular repolarization adaptation: we performed studies on the ionic mechanisms of QT interval heart rate adaptation in ventricular tissue and their link to pro-arrhythmic mechanisms. Experiments were carried out to identify the specific mechanisms of ionic transport that determine QT interval rate adaptation and how alterations in those mechanisms might lead to arrhythmic events.

3. Methods

All animal experiments were conducted in compliance with the Guide for the Care and Use of Laboratory Animals (NIH Publication No. 85-23, Revised 1996), and the protocol was approved by the Ethical Committee for the Protection of Animals in Research of the University of Szeged, Hungary (I-74-125-2007 and I-74-5-2012) and by the Department of Animal Health and Food Control of the Ministry of Agriculture and Rural Development (XIII/01031/000/2008 and XIII/1211/2012).

3.1 Conscious dogs

Beagle dogs of either sex weighing 10-15 kg were used for the experiments. The animals were allowed to accomodate to experimental personnel and equipment, including a loosely fitting jacket containing ECG electrodes, every day for a week before the commencement of the actual studies. After a 20 min equilibration period, baseline recordings were obtained. The animals were then randomly assigned to the following four groups as shown on **Figure 1**:

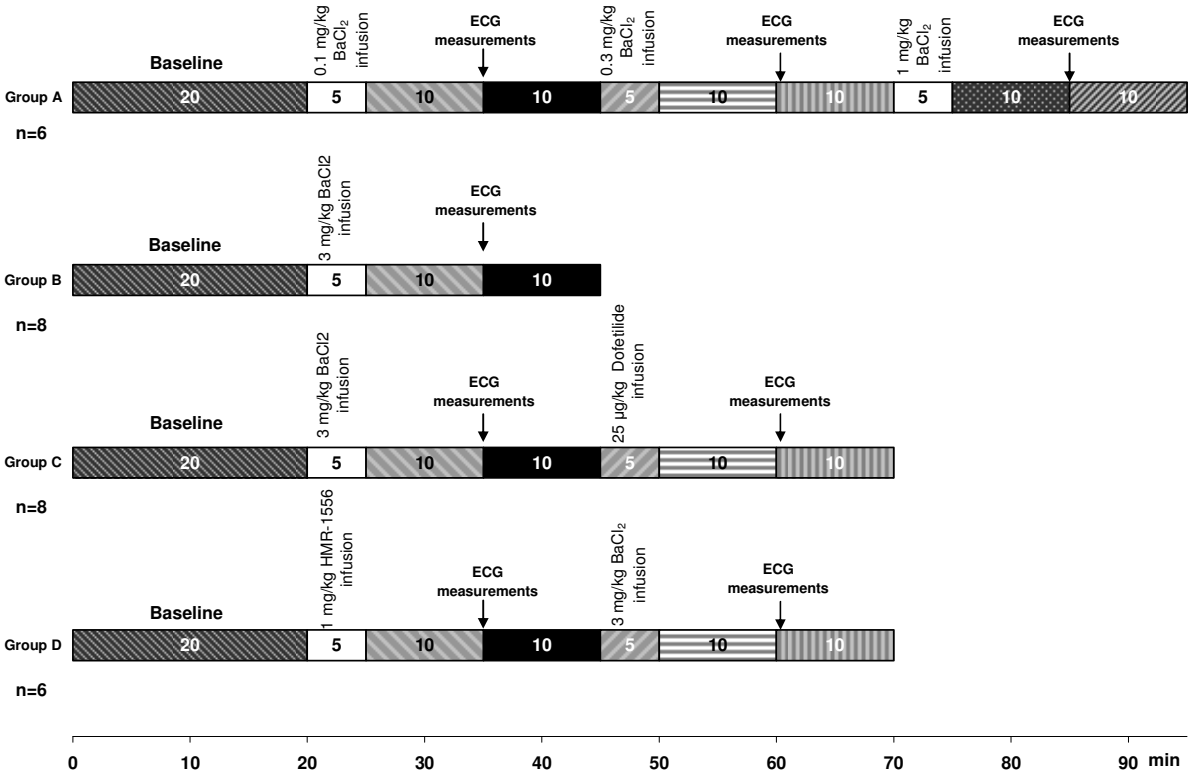

Figure 1. Schematic illustration of drug administration protocols in the different groups of conscious dogs.

(Group A) 6 dogs received $BaCl_2$ intravenously in three different doses: 0.1 mg/kg, 0.3 mg/kg and 1 mg/kg each after a 20 min equilibration period, (Group B) 8 dogs were given 3 mg/kg $BaCl_2$ alone, (Group C) 8 dogs were administered 3 mg/kg $BaCl_2$ followed by 25 μg/kg dofetilide intravenously after a 10 min equilibration period and (Group D) 6 animals received 1 mg/kg HMR 1556 followed by 3 mg/kg $BaCl_2$ intravenously after a 10 min equilibration period. The drugs were administered during a 5 min continuous i.v. infusion (Terufusion TE-3, Terumo Europe, Leuven, Belgium). The electrocardiogram was obtained using precordial leads and was digitized and stored on a computer for later analysis using National Instruments data acquisition hardware (National Instruments, Austin, TX, USA) and SPEL Advanced Haemosys software (v3.2, Experimetria Ltd., Budapest, Hungary). The PQ, RR, QT intervals were measured as the average of 30 consecutive beats (the minimum number of beats required for the calculation of short-term variability of an interval, see below) and the frequency corrected QT interval (QTc) was calculated using a formula recommended for Beagle dogs: $QTc = QT - (0.087 * (RR-1000))$ (Tattersall *et al.*, 2006; Van de Water *et al.,* 1989). The intervals were measured at the following time points during the experiments: (i) 2 min before the start of drug infusion (baseline); (ii) 10 min after the end of drug infusions and (iii) the sinus rhythm ECG section directly preceding the arrhythmia if Torsades de pointes (TdP) or ventricular tachycardia occurred.

3.2 Anaesthetized rabbits

Male New Zealand white rabbits (2-3 kg) were used for the experiments. The animals were anaesthetized with thiopentone (50 mg/kg i.v.) given into the marginal vein of the right ear. A catheter filled with isotonic saline containing 500 IU/ml heparin was inserted into the left carotid artery for the measurement of arterial blood pressure. The right jugular vein was canulated for subsequent i.v. drug administration. The animals were allowed to stabilize for 20 min and baseline measurements were taken. The first group of rabbits received 0.1, 0.3 and 1 mg/kg $BaCl_2$ alone in a volume of 2 ml/kg during a 5 min infusion and each dose were given after a 20 min equilibration period. The second group was administered 0.3 mg/kg $BaCl_2$ followed by 25 μg/kg dofetilide 20 min after HMR administration. The third group received 0.1 mg/kg HMR 1556 followed by 0.3 mg/kg $BaCl_2$ intravenously 20 min after HMR administration. (**Figure 2**):

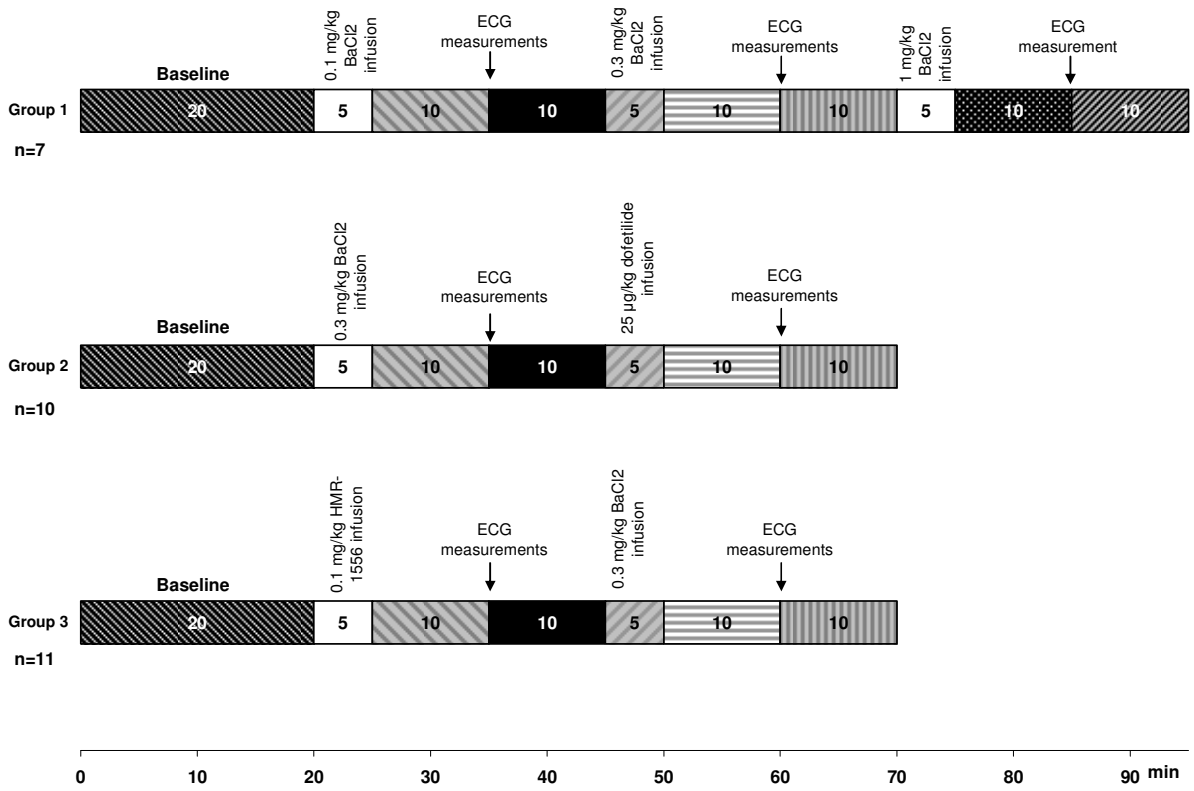

Figure 2. Schematic illustration of drug administration protocols in the different groups of anaesthetized rabbits.

The blood pressure and the electrocardiogram (leads I, II and III) were continuously recorded (at 200 Hz), digitized and stored on a computer for analysis using National Instruments data acquisition hardware (National Instruments, Austin, TX, USA) and SPEL Advanced Haemosys software (v3.2, Experimetria Ltd., Budapest, Hungary). The PQ, RR, QT intervals were measured as the average of 30 beats (the minimum number of beats required for the calculation of short-term variability of an interval, see below). During the measurement of the QT interval in anaesthetized rabbits, the guidelines described by Farkas et al. (2004) were followed. In animals with a significantly faster heart rate than that of humans (e.g. rabbits), QTc calculated with Bazett's formula does not accurately reflect the heart rate dependent changes in QT interval. Therefore, QTc was calculated by a formula specifically suggested for anaesthetized rabbits by (Batey & Coker (2002)) as follows: $QTc = QT - (0.704 * (RR-250)$.

3.3 Short-term beat-to-beat variability of the RR and QT intervals

In order to characterize the instability of beat-to-beat repolarization, Poincaré plots of the QT intervals were constructed where each QT value is plotted against its former value in dogs and rabbits (**Figures 6 and 11**). The plots are the result of 30 consecutive interval measurements in sinus rhythm at a given time point during the experiments. In the case of combined I_{K1} and I_{Kr} or I_{Ks} and I_{K1} block where TdP commonly occurred, the measurements were taken prior to the development of TdP. The beat-to-beat short-term variability (STV) of RR or QT intervals was calculated using the following formula: $STV = \sum|D_{n+1}-D_n| \ (30x\sqrt{2})^{-1}$, where D is the duration of the QT or RR interval. The STV represents the mean orthogonal distance to the line-of-identity on the Poincaré plot, and this estimation of RR and QT interval instability is based on previous analysis of the value of qualitative and quantitative Poincaré plot examination (Brennan *et al*., 2001).

3.4 In vitro study

3.4.1 Standard intracellular microelectrode technique

Action potential measurements were carried out by applying the standard intracellular microelectrode technique in right ventricular papillary muscle preparations isolated from mongrel dogs of either sex weighing 12–20 kg.

After intravenous anaesthesia with thiopentone the hearts were rapidly removed through right lateral thoracotomy and placed in oxygenated modified Locke's solution containing the following (in mM): NaCl 120, KCl 4, $CaCl_2$ 1.0, $MgCl_2$ 1, $NaHCO_3$ 22, and glucose 11. The pH of this solution was set between 7.35 and 7.4 when saturated with the mixture of 95% O_2 and 5% CO_2 at 37^{o}C.

Papillary muscles were obtained from the right ventricle and mounted in a 50 ml of volume tissue chamber. Pacing at cycle length (CL) of 1000 ms, using rectangular pulses of 1ms duration at twice diastolic threshold in intensity was applied until steady-state through bipolar platinum electrodes. Transmembrane potentials were recorded using conventional glass microelectrodes filled with 3 M KCL with a tip resistance of 5-20 MΩ. Electrodes were captured to the high impedance amplifier (Experimetria, type 309, Budapest, Hungary) which was connected to a dual beam oscilloscope. Electrophysiological parameters were measured applying the Action Potential Evaluation Software (APES) running on an IBM compatible computer and data for action potential duration adaptation were evaluated using the EvokeWave software.

3.4.2 Measurements of the action potential parameters

Action potential measurements were carried out using right ventricular papillary muscles. Preparations were paced at basic cycle length (BCL) =1000 ms and allowed to equilibrate for at least 1h until steady state while superfused with oxygenated Locke's solution. The following parameters were recorded during the experiments: The amplitude of the action potential (AMP), the maximum upstroke velocity (V_{max}), resting potential and the action potential duration at 10%, 25%, 50%, 75% and 90% repolarization (APD_{10}, APD_{25}, APD_{50}, APD_{75} and APD_{90}). After control measurements selective I_{K1} (30 μM $BaCl_2$), I_{Kr} (100 nM dofetilide), and I_{Ks} (1μM HMR 1556) blocker drugs were added to the preparations alone and in combination to reduce repolarization reserve.

3.4.3 Measurements of APD adaptation in canine cardiac preparations

Action potential measurements were carried out by applying the standard intracellular microelectrode technique in right ventricular papillary muscle preparations isolated from mongrel dogs of either sex weighing 8–20 kg.

The rate adaptation of the action potential duration at 90% repolarization (APD_{90}) was evaluated. Pacing at cycle length (CL) of 1000 ms was applied until steady state, then CL was changed stepwise to 600 ms for 10 minutes (acceleration) and back to 1000 ms for an additional 10 min (deceleration). Two phases of APD adaptation dynamics were identified: APD_{90} heart rate adaptation following step CL changes consisted of two phases with time constants τ_{fast} and τ_{slow}, calculated from fitting the corresponding portion of APD time course with an exponential function: $f(t) = a + b\, e^{-(t-c)/t}$.

Time constants τ_{fast} and τ_{slow} were obtained both after CL increase and decrease. APD HR adaptation was evaluated both in control and in the presence of $BaCl_2$ (30 μM), HMR 1556 (250 nM), dofetilide (100 nM), $I_{Ca,L}$ blocker (1 μM nisoldipin) and I_{NaK} blocker (600 nM strophantin).

3.5 Compounds

HMR 1556 (Aventis Pharma, Frankfurt am Main, Germany) was dissolved in dimethylsulfoxide (DMSO, 0.1%) as a stock solution of 10 μM. Dofetilide (Gedeon Richter Ltd., Budapest, Hungary) was dissolved in saline as a stock solution of 5 μM. $BaCl_2$ was dissolved in distilled water as a stock solution of 100 mM. Each stock solution was diluted immediately before use.

3.6 Statistical analysis

The incidence of TdP (%) was compared by using the χ^2 test with Yates' correction. All other data are expressed as means + standard deviation (SD). Data within groups were compared after analysis of variance (repeated measures one-way ANOVA) by Bonferroni's post test and the groups were compared in pairs by means of Student's "t" test. A level of $p<0.05$ was considered to be statistically significant.

4. Results

4.1 Studies on repolarization reserve

In these experiments, the effects of the combined inhibition of different potassium currents on drug-induced TdP and several ECG parameters were investigated in conscious dogs and anaesthetized rabbits.

4.1.1 The effect of cumulative doses of $BaCl_2$ alone on RR, QTc interval and STV_{QT} in conscious dogs and anaesthetized rabbits

In order to determine the doses of the I_{K1} inhibitor $BaCl_2$ to be used in our subsequent *in vivo* experiments, especially in the light of the known species specific differences in the composition of ion channels carrying the I_{K1} current, a series of preliminary experiments were performed in conscious dogs and anaesthetized rabbits where cumulative i.v. doses of $BaCl_2$ were administered with continuous ECG registration and evaluation. $BaCl_2$ was used previously in intact dogs in doses up to more than 8 mg/kg (Foster et al., 1977). This dose, however, caused arrhythmias and we did not intend to provoke serious arrhythmias by administration of $BaCl_2$ alone, therefore we tested 0.1, 0.3, 1 and 3 mg/kg i.v. $BaCl_2$ in both dogs and rabbits. Based on these preliminary experiments we chose the applied $BaCl_2$ doses in subsequent experiments, that is a $BaCl_2$ dose that did not provoke significant amount of ventricular arrhythmias.

4.1.1.1 Conscious dogs

Administration of the I_{K1} blocker $BaCl_2$ alone in conscious dogs significantly decreased the heart rate and increased the RR interval in a dose-dependent manner (653.8 ± 69.87 ms, 809.9 ± 124.99 ms and 891.2 ± 136.54 ms after administration of 0.1 mg/kg, 0.3 mg/kg and 1 mg/kg $BaCl_2$ vs. 615.6 ± 145.99 ms at baseline, n=6, $p<0.05$). Interestingly, 3 mg/kg iv. infusion of $BaCl_2$ only showed a tendency to prolong RR intervals, however, these differences proved to be not significant (797.9 ± 191.23 ms after 3 mg/kg $BaCl_2$ vs. 763.3 ± 138.66 ms at baseline, $p>0.05$).

In the dose of 0.1 mg/kg $BaCl_2$ alone did not cause statistically significant QTc prolongation: 256.8 ± 10.59 ms vs 247.9 ± 7.04 ms at baseline, $p>0.05$. The pharmacological block of I_{K1} alone by 0.3, 1, and 3 mg/kg $BaCl_2$ resulted in significant QTc prolongation in conscious dogs. The QTc intervals yielded the following results: 258.55 ± 15.39 ms after 0.3 mg/kg $BaCl_2$, 309.52 ±33.10 ms after 1 mg/kg $BaCl_2$ and 334.9 ± 33.26 ms after 3 mg/kg

$BaCl_2$ vs. 247.9 ± 7.04 ms at baseline, n=6, p<0.05. I_{K1} block alone by 0.1, 0.3, 1 and 3 mg/kg $BaCl_2$ did not significantly influence STV_{QT}: 3.2 ± 1.15 ms, 4.1 ± 1.70 ms, 5.3 ± 3.20 ms and 5.4 ± 1.02 ms vs. 3.8 ± 1.44 at baseline, n=6, all p>0.05.

4.1.1.2 Anaesthetized rabbits

When administered alone in anaesthetized rabbits, the I_{K1} blocker $BaCl_2$ (0.1, 0.3 and 1 mg/kg, i.v.) did not influence the heart rate and RR interval significantly: 234.3 ± 9.29 ms, 236.1 ± 10.67 ms, 247.4 ± 13.07 ms vs. 225.3 ± 9.11 at baseline, n=7, all p>0.05, respectively. The QTc interval was not altered significantly in anaesthetized rabbits by cumulative doses (0.1, 0.3 and 1 mg/kg) of $BaCl_2$: 164.8 ± 3.86 ms, 166.8 ± 5.47 ms, 167.9 ± 4.02 ms vs. control: 161.8 ± 3.84 ms, n=7, all p> 0.05, respectively. There were no significant changes in the short-term variability of QT interval using 0.1, 0.3 and 1 mg/kg $BaCl_2$ alone in anaesthetized rabbits: 3.1 ± 0.49 ms, 3.4 ± 0.50 ms, 3.5 ± 0.40 ms vs. 2.92 ± 0.56 ms at baseline, n=7, all p> 0.05, respectively.

4.1.2 Effect of combined I_{K1} and I_{Kr} inhibition on RR and QTc intervals in conscious dogs and anesthetized rabbits

Both in dogs and rabbits, the administration of the I_{K1} inhibitor $BaCl_2$ alone did not change heart rate and the RR intervals (**Figure 3**). However, infusion of the I_{Kr} inhibitor dofetilide significantly increased RR intervals (**Figure 3**) and decreased heart rate (dogs: 66.9 ± 16.96 vs. 80.5 ± 12.12 beats/min in control; rabbits: 213.9 ± 1.92 vs. 258.6 ± 1.26 beats/min in control, p<0.05) in both species.

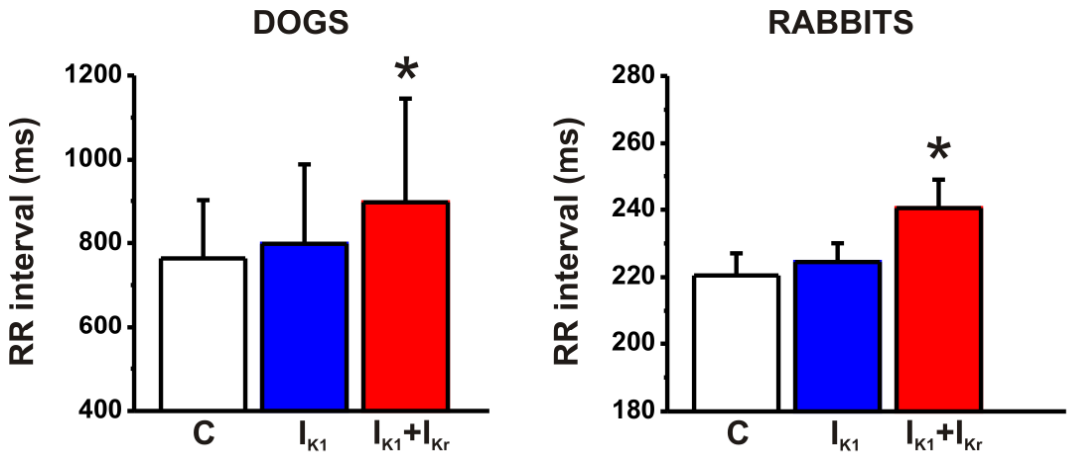

Figure 3. Effect of I_{K1} inhibition (i.v. $BaCl_2$) and combined $I_{K1}+I_{Kr}$ (i.v. $BaCl_2$+dofetilide) inhibition on RR intervals in conscious dogs and anesthetized rabbits. n=7 dogs and 7 rabbits/group; *p<0.05 vs. control values.

In our previous study, the I_{Kr} inhibitor dofetilide administered alone did not alter the RR interval but as expected, significantly prolonged the QTc interval in conscious dogs and anesthetized rabbits (Lengyel et al. 2007). In conscious dogs, I_{K1} inhibition significantly prolonged the frequency corrected QT interval, calculated with the Van de Water formula (Van de Water et al., 1989), and dofetilide infusion caused a further, significant prolongation of the QTc interval (**Figure 4 left panel**). The uncorrected QT intervals yielded similar prolongation: 317.4 ± 47.9 ms after I_{K1} block and 373.5 ± 37.8 ms after combined I_{K1}+I_{Kr} inhibition vs. 221.4 ± 11.7 ms in controls, ($p<0.05$). In anesthetized rabbits, only the combination of I_{K1} and I_{Kr} inhibition resulted in significant QTc interval prolongation (**Figure 4 right panel**). Again, the uncorrected QT intervals showed a similar prolongation only after combined I_{K1}+I_{Kr} inhibition (150.6 ± 5.88 ms after I_{K1} inhibition and 167.8 ± 6.27 ms after $BaCl_2$ and dofetilide combination vs. 147.2 ± 5.46 ms in control).

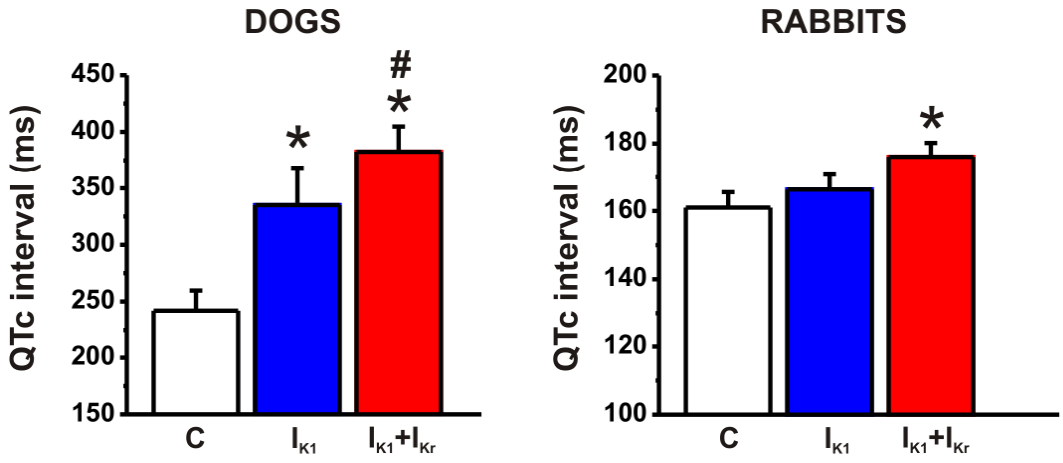

Figure 4. Effect of I_{K1} inhibition (i.v. $BaCl_2$) and combined I_{K1}+I_{Kr} (i.v. $BaCl_2$+dofetilide) inhibition on frequency corrected QT interval (QTc) in conscious dogs and anesthetized rabbits. n=7 dogs and 7 rabbits/group; *$p<0.05$ vs. control values; #$p<0.05$ vs. I_{K1} inhibition.

4.1.3 Effect of combined I_{K1} and I_{Kr} inhibition on the short-term variability of RR (STV_{RR}) and QT intervals (STV_{QT}) in conscious dogs and anesthetized rabbits

Since heart rate affects repolarization duration, the short-term variability of the RR intervals were also calculated in addition to STV_{QT}, the ECG parameter recently suggested for more reliable prediction of ventricular arrhythmias. In conscious dogs, STV_{RR} did not change significantly following I_{K1} and combined I_{K1}+I_{Kr} inhibition (**Figure 5 left panel**). In anesthetized rabbits, the combination of $BaCl_2$ and dofetilide slightly, but significantly increased STV_{RR}, however, the magnitude of these changes (less than 0.5 ms) makes it very

unlikely that this STV_{RR} change markedly influenced repolarization variability (**Figure 5 right panel**).

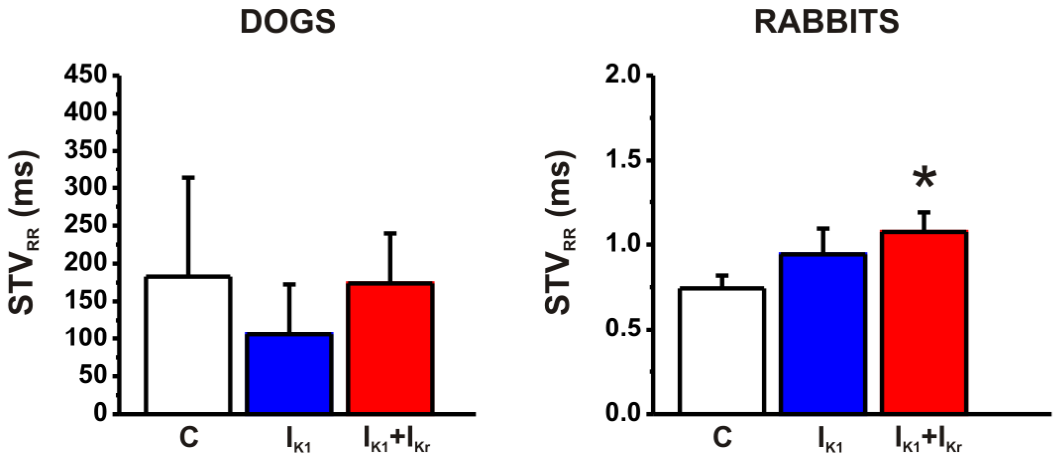

Figure 5. Effect of I_{K1} inhibition (i.v. $BaCl_2$) and combined $I_{K1}+I_{Kr}$ (i.v. $BaCl_2$+dofetilide) inhibition on the short-term variability of the RR interval (STV_{RR}) in conscious dogs and anesthetized rabbits. n=7 dogs and 7 rabbits/group; *p<0.05 vs. control values.

The I_{Kr} inhibitor dofetilide, when administered alone did not alter STV_{RR} in conscious dogs and anesthetized rabbits in our previous study (Lengyel et al. 2007). The Poincaré plots on **Figure 6** illustrate repolarization temporal instability in two individual animals, a conscious dog (**left panel**) and an anesthetized rabbit (**right panel**) following I_{K1} and combined $I_{K1}+I_{Kr}$ inhibition.

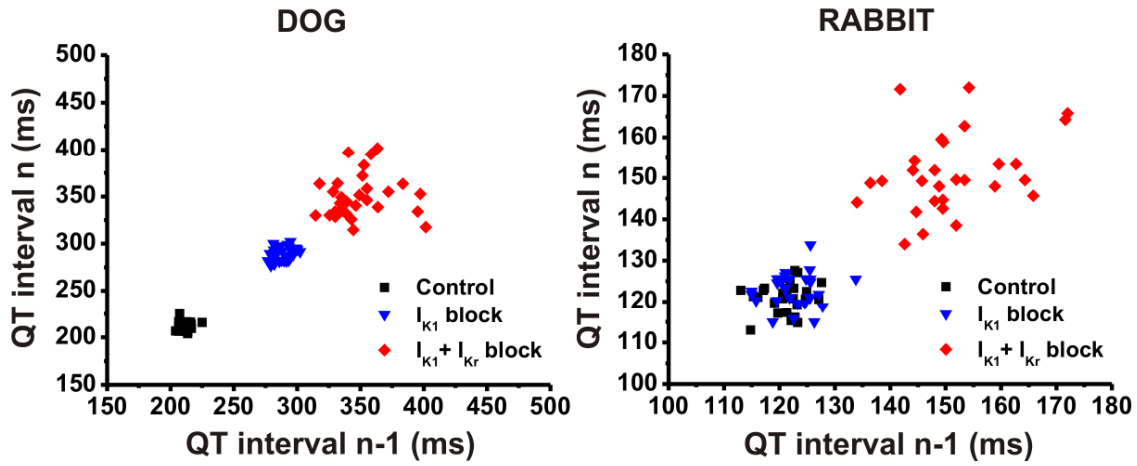

Figure 6. Illustration of the effect of I_{K1} inhibition (i.v. $BaCl_2$) and combined $I_{K1}+I_{Kr}$ (i.v. $BaCl_2$+dofetilide) inhibition on short-term variability of the QT interval (STV_{QT}) in a representative conscious dog (left panel) and an anesthetized rabbit (right panel). For details on Poincaré plot description please refer to the text.

Both animals exhibited TdP arrhythmia as a result of $BaCl_2$ and dofetilide combination, and the scatter of data points covering a large area on the plot following this combination represents large STV_{QT} values in these animals (15.8 ms in the dog and 4.9 ms in the rabbit). Grouped STV_{QT} data showed a significant increase in both species following combined I_{K1}+I_{Kr} inhibition (**Figure 7**). Dofetilide alone did not increase STV_{QT} in conscious dogs, however, it significantly increased STV_{QT} in anesthetized rabbits in our previous study (Lengyel et al. 2007).

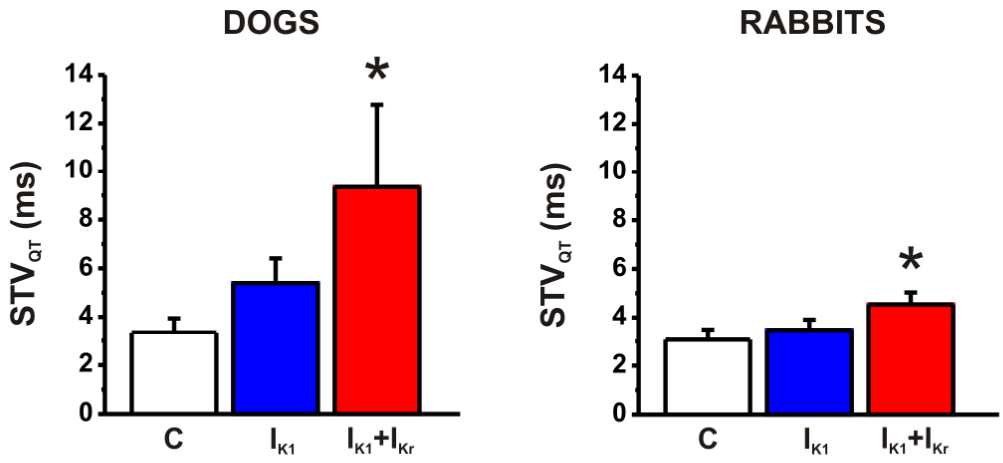

Figure 7. Effect of I_{K1} inhibition (i.v. $BaCl_2$) and combined I_{K1}+I_{Kr} (i.v. $BaCl_2$+dofetilide) inhibition on short-term variability of the QT interval (STV_{QT}) in conscious dogs (left panel) and anesthetized rabbits (right panel). n=7 dogs and 7 rabbits/group; *p<0.05 vs. control values.

4.1.4 Effect of combined I_{Ks} and I_{K1} block on RR and QTc intervals in conscious dogs and anesthetized rabbits

The I_{Ks} inhibitor HMR 1556 did not change the RR interval significantly in conscious dogs or anesthetized rabbits, and this result was in good agreement with our previous observations (Lengyel et al., 2007). The combined inhibition of I_{Ks}+I_{K1}, however, caused a significant increase in RR intervals and decrease in heart rate in rabbits only (**Figure 8 right panel**).

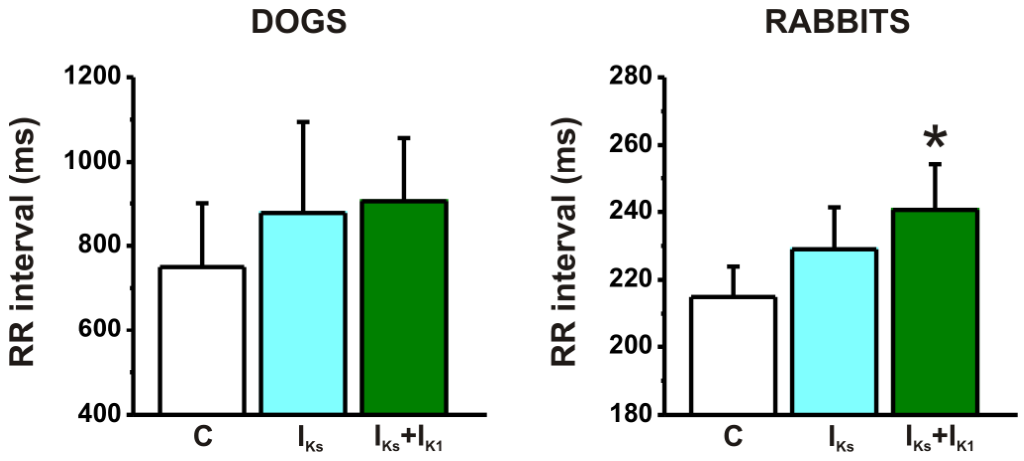

Figure 8. Effect of I_{Ks} inhibition (i.v. HMR 1556) and combined $I_{Ks}+I_{K1}$ (i.v. HMR 1556+$BaCl_2$) inhibition on RR interval in conscious dogs and anesthetized rabbits. n=6 dogs and 7 rabbits/group; *p<0.05 vs. control values.

In conscious dogs, I_{Ks} inhibition significantly increased the frequency corrected QT interval, similarly to our previous observations in conscious dogs (Lengyel et al., 2007). In these animals, subsequent infusion of $BaCl_2$ caused a further, significant QTc prolongation (**Figure 9 left panel**).

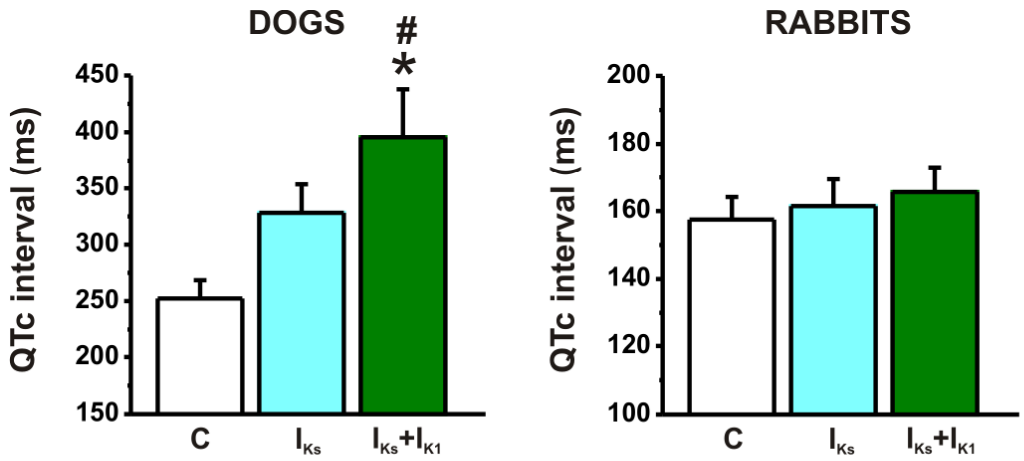

Figure 9. Effect of I_{Ks} inhibition (i.v. HMR 1556) and combined $I_{Ks}+I_{K1}$ (i.v. HMR 1556+$BaCl_2$) inhibition on frequency corrected QT interval (QTc) in conscious dogs and anesthetized rabbits. n=6 dogs and 7 rabbits/group; *p<0.05 vs. control values; #p<0.05 vs. I_{Ks} inhibition.

The uncorrected QT intervals showed similar prolongation: 317.5 ± 35.2 ms after I_{Ks} block and 387.4 ± 45.4 ms after combined $I_{Ks}+I_{K1}$ inhibition vs. 230.5 ± 7.6 ms in controls, (p<0.05). In anesthetized rabbits, I_{Ks} inhibition did not alter QTc, and combined $I_{Ks}+I_{K1}$

inhibition only had a slight tendency to increase QTc but this change did not prove to be statistically significant (**Figure 9 right panel**).

4.1.5 Effect of combined I_{Ks} and I_{K1} inhibition on the short-term variability of RR (STV_{RR}) and QT (STV_{QT}) intervals in conscious dogs and anesthetized rabbits

HMR 1556 did not alter STV_{RR} in conscious dogs or anesthetized rabbits. The combined inhibition of I_{Ks}+I_{K1} caused a significant, but again, very small (less than 1 ms) increase in STV_{RR} in anesthetized rabbits (**Figure 10 right panel**).

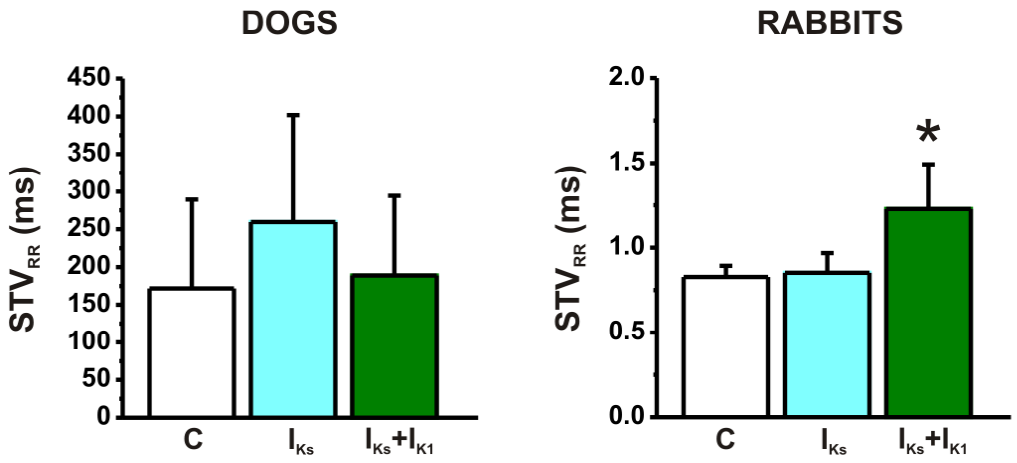

Figure 10. Effect of I_{Ks} inhibition (i.v. HMR 1556) and combined I_{Ks}+I_{K1} (i.v. HMR 1556+$BaCl_2$) inhibition on short-term variability of the RR interval (STV_{RR}) in conscious dogs and anesthetized rabbits. n=6 dogs and 7 rabbits/group; *p<0.05 vs. control values.

The Poincaré plots on **Figure 11** illustrate repolarization temporal instability in two individual animals, a conscious dog (**left panel**) and an anesthetized rabbit (**right panel**) following I_{Ks} and combined I_{Ks}+I_{K1} inhibition. The shift of QT interval data points to the right and upward direction in the conscious dog represent the above described QT prolongation following HMR 1556 administration. Careful evaluation of the plot reveals that in this animal, that later developed TdP after combined I_{Ks}+I_{K1} inhibition, the QT variability only increased after HMR 1556 and $BaCl_2$ combination (**Figure 11 left panel**).

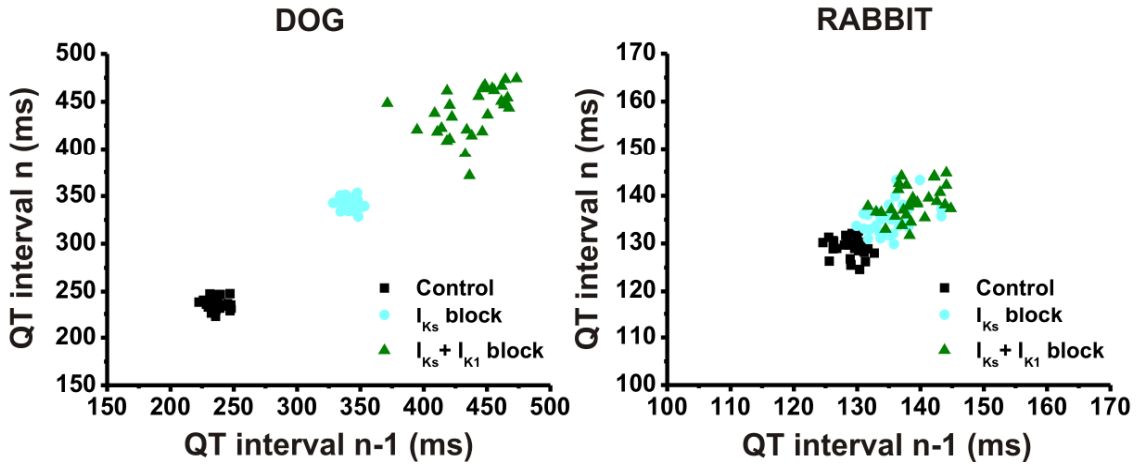

Figure 11. Illustration of the effect of I_{Ks} inhibition (i.v. HMR 1556) and combined $I_{Ks}+I_{K1}$ (i.v. HMR 1556+$BaCl_2$) inhibition on short-term variability of the QT interval (STV_{QT}) in a conscious dog (left panel) and an anesthetized rabbit (right panel). For details on Poincaré plot description please refer to the text.

In accordance with grouped STV_{QT} data represented on **Figure 12** (**right panel**), in the representative rabbit on **Figure 11** (**right panel**) STV_{QT} did not increase significantly after HMR 1556 or HMR 1556+$BaCl_2$ combination in anesthetized rabbits. In contrast, in conscious dogs this combination led to a significant increase in STV_{QT} (**Figure 12 left panel**).

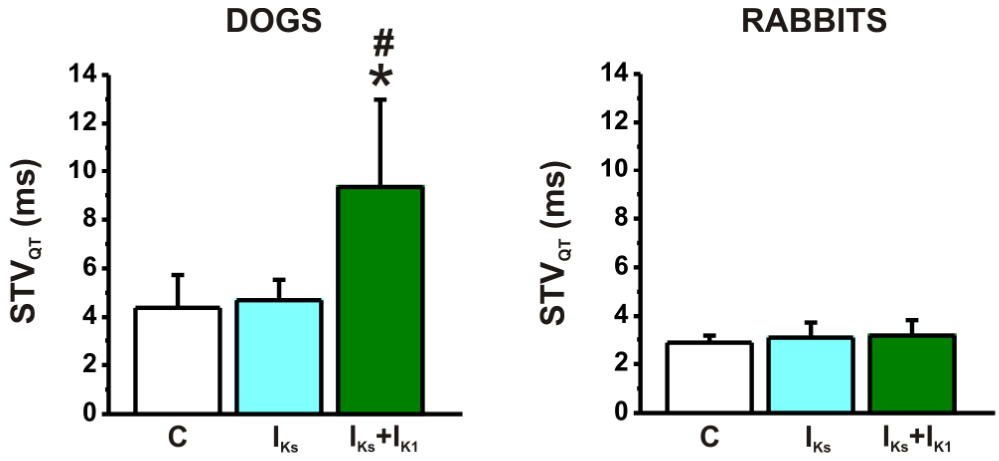

Figure 12. Effect of I_{Ks} inhibition (i.v. HMR 1556) and combined $I_{Ks}+I_{K1}$ (i.v. HMR 1556+$BaCl_2$) inhibition on short-term variability of the QT interval (STV_{QT}) in conscious dogs (left panel) and anesthetized rabbits (right panel). n=6 dogs and 7 rabbits/group; *p<0.05 vs. control values; #p<0.05 vs. I_{Ks} inhibition.

Importantly, in parallel to this STV_{QT} increase, conscious dogs responded to combined $I_{Ks}+I_{K1}$ inhibition with significantly increased TdP incidence, while only one of 7 rabbits developed

TdP following this combination (**Figure 13**), and the rabbit grouped data did not show elevated STV_{QT}.

4.1.6 Effect of combinations of I_{K1} and I_{Kr} inhibition, and I_{Ks} and I_{K1} inhibition on the incidence of TdP in conscious dogs and anesthetized rabbits

As shown on **Figure 13**, inhibition of I_{K1} or I_{Ks} alone did not provoke TdP in any of the animals.

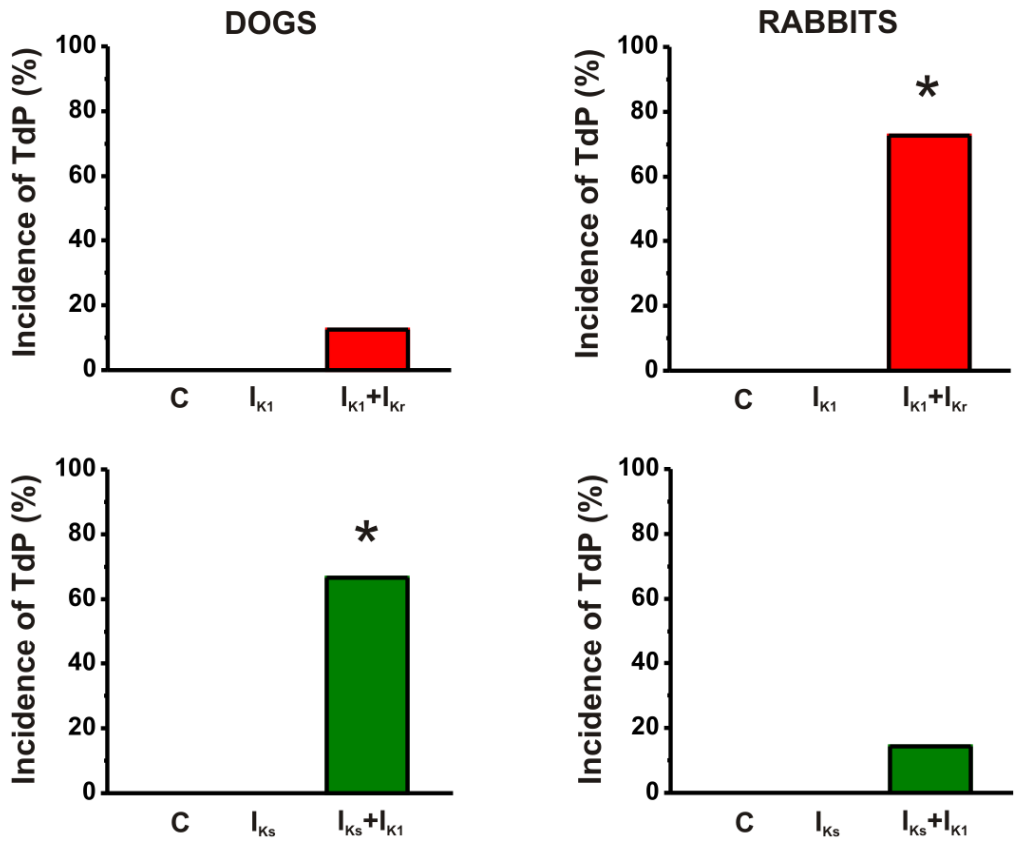

Figure 13. Effect of I_{K1} inhibition (i.v. $BaCl_2$) and combined $I_{K1}+I_{Kr}$ (i.v. $BaCl_2$+dofetilide) inhibition (top panels) and I_{Ks} inhibition (i.v. HMR 1556) and combined $I_{Ks}+I_{K1}$ (i.v. HMR 1556+$BaCl_2$) inhibition (bottom panels) on the incidence of Torsades de Pointes (TdP) chaotic ventricular tachycardia in conscious dogs (left panels) and anesthetized rabbits (right panels). n=7 and 6 dogs, and 7 rabbits/group; *$p<0.05$ vs. control values.

We have shown previously that the I_{Kr} inhibitor dofetilide alone did not cause TdP in conscious dogs and caused TdP in 25% of anesthetized rabbits (Lengyel et al., 2007). Combined inhibition of repolarizing currents, however, led to a significant amount of TdP episodes in both species, albeit in a different manner. Interestingly, conscious dogs and anesthetized rabbits exhibited different TdP incidence following the combined inhibition of key potassium currents: a significant amount of conscious dogs developed TdP following

I_{Ks}+I_{K1} inhibition, while only one rabbit developed TdP after this combination. On the other hand, TdP incidence increased significantly following I_{K1}+I_{Kr} inhibition in rabbits, while only one dog exhibited TdP following $BaCl_2$+dofetilide administration (**Figure 13**).

4.1.7 In vitro studies

4.1.7.1 Effect of combined I_{K1} and I_{Kr} block on action potential parameters in dog right ventricular papillary muscle

As shown on **Figures 14 and 15**, administration of 30 µM $BaCl_2$ and 100 nM dofetilide alone has significantly prolonged the action potential duration at 90% repolarization (APD_{90}). (Control vs. 30 µM $BaCl_2$: 229.9 ± 35.22 ms vs. 285.5 ± 42.75 ms, $p<0.05$; control vs. 100 nM dofetilide: 221.4 ± 23.34 ms vs. 290.8 ± 42.75 ms, $p<0.05$ respectively).

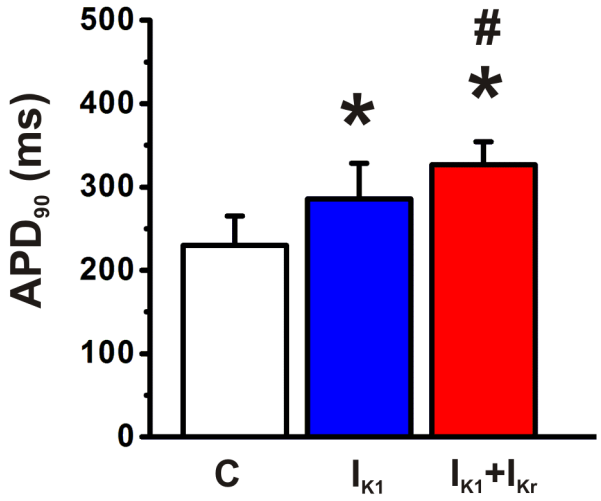

Figure 14. The effect of I_{K1} inhibition alone (by 30 µM $BaCl_2$) and combined I_{K1} and I_{Kr} inhibition (by 30 µM $BaCl_2$ + 100 nM dofetilide) on action potential duration at 90% repolarization (APD_{90}) in dog right ventricular papillary muscle. The I_{K1} blocker $BaCl_2$ significantly prolonged APD_{90}. Dofetilide caused further and marked APD_{90} lengthening when I_{K1} was previously inhibited. n= 5; *$p<0.05$ vs. control, #$p<0.05$ vs. I_{K1} block.

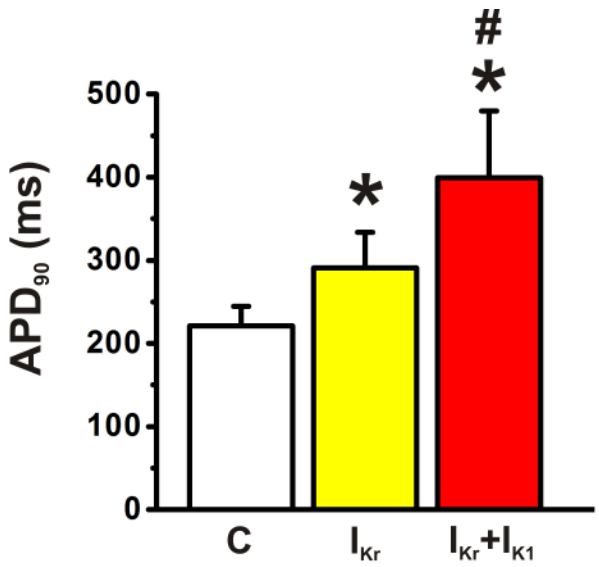

Figure 15. The effect of I_{Kr} inhibition alone (by 100 nM dofetilide) and combined I_{Kr} and I_{K1} inhibition (by 100 nM dofetilide + 30 µM $BaCl_2$) on action potential duration at 90% repolarization (APD_{90}). in dog right ventricular papillary muscle. When dofetilide was administered first, $BaCl_2$ (combined I_{Kr} and I_{K1} block) led to larger APD lengthening than observed on **Figure 14** where $BaCl_2$ was given first. n= 10; *p<0.05 vs. control, #p<0.05 vs. I_{Kr} block.

Further increase of APD_{90} was observed in the case of combined I_{K1} and I_{Kr} block: 100 nm dofetilide caused marked and further APD_{90} prolongation when I_{K1} was first blocked by 30 µM $BaCl_2$ and I_{K1} inhibition resulted in significant further APD_{90} prolongation when I_{Kr} was first blocked by 100 nM dofetilide (control vs. 100 nM dofetilide followed by 30 µM $BaCl_2$: 229.9 ± 35.22 ms vs. 326.5 ± 27.52 ms, p<0.05; control vs. 30 µM $BaCl_2$ followed by 100 nM dofetilide: 221.4 ± 23.34 ms vs. 399.5 ± 79.92 ms, p<0.05 respectively.) Interestingly, the repolarization changes tended to be greater when I_{Kr} was first blocked than in the case of I_{K1} block followed by administration of dofetilide, as illustrated on **Figure 16**. However, these differences were not statistically significant.

In summary, cardiac ventricular repolarization duration was increased by I_{Kr} or I_{K1} block alone and further marked and significant prolongation was observed in the case of combined I_{Kr} + I_{K1} block at 1000 ms basic cycle length.

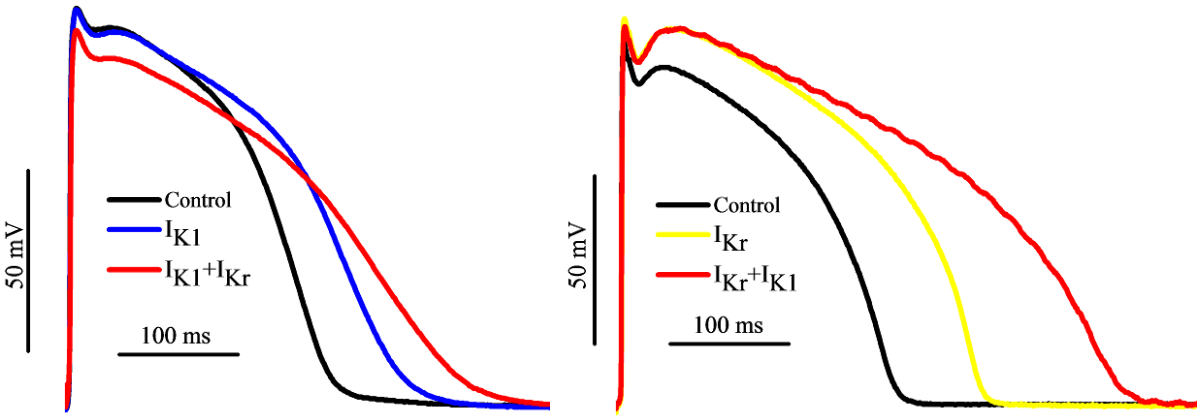

Figure 16. Representative action potentials constructed from an individual dog right ventricular papillary muscle. The left panel demonstrates the effect of I_{K1} block (30 µM $BaCl_2$) and combined I_{K1} and I_{Kr} (100 nM dofetilide) block on action potential when $BaCl_2$ was administered first. The right panel shows representative recordings where dofetilide was administered first, followed by I_{K1} inhibition by $BaCl_2$.

Figures 17 and 18 illustrate the frequency dependent changes of APD_{90} following the administration of 30 µM $BaCl_2$, 100 nM dofetilide alone, and their combination. Both $BaCl_2$ and dofetilide alone prolonged repolarization in a reverse use dependent manner, however, combined I_{Kr} + I_{K1} block caused more pronounced and excessive APD_{90} lengthening at slow heart rates (see cycle lengths 2000, 3000 and 5000 ms).

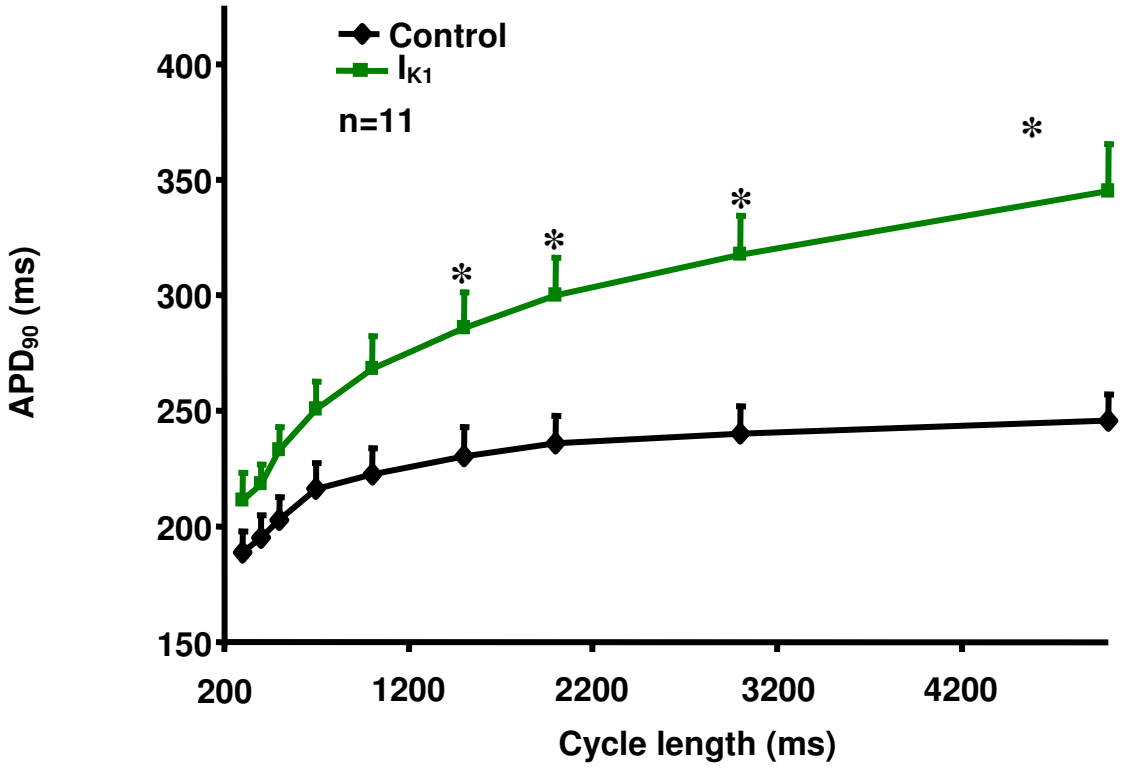

Figure 17. Frequency dependent effect of I_{K1} block alone on dog right ventricular papillary muscle. 30 µM $BaCl_2$ increased the APD that was more pronounced at slow heart rates. *$p<0.05$ vs. control, n= 11

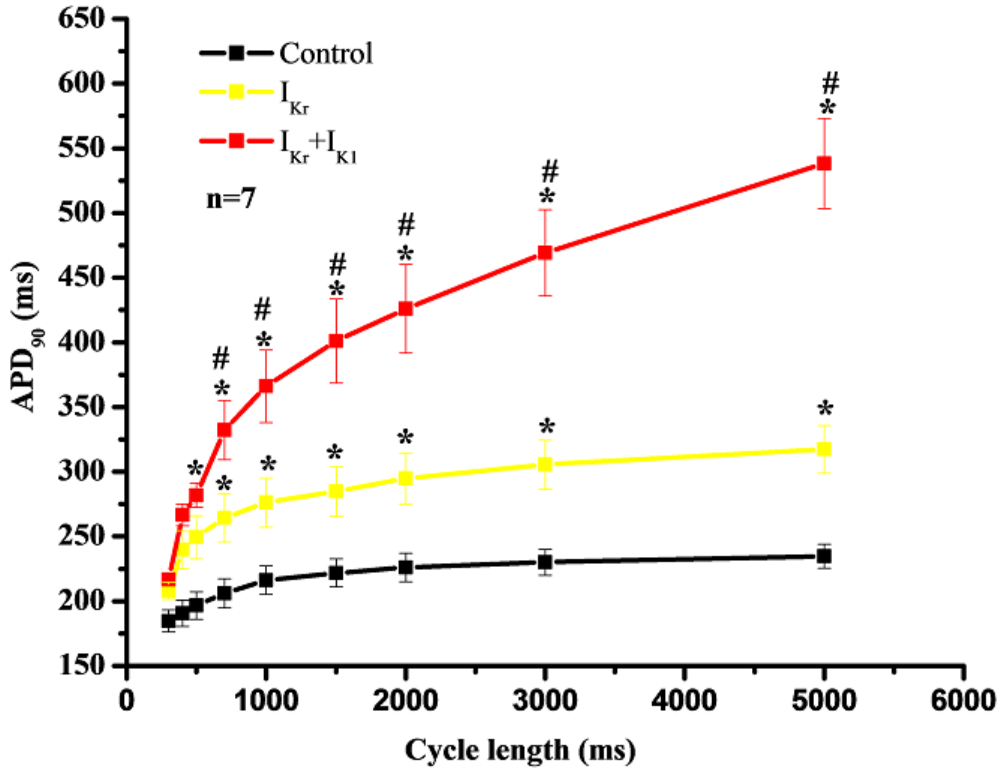

Figure 18. Frequency dependent effect of combined I_{Kr} and I_{K1} block on dog right ventricular papillary muscle. Inhibition of I_{Kr} alone with 100 nM dofetilide prolonged the APD in frequency dependent manner. Additional block of I_{K1} with 30 µM $BaCl_2$ marked APD elongation occurred especially at slow heart rate (reverse frequency dependence). *p<0.05 vs. control, #p<0.05 vs. I_{Kr} block, n= 7

4.1.7.2 Effect of combined I_{Ks} and I_{K1} block on action potential parameters in dog right ventricular papillary muscle

The effect of the I_{Ks} blocker HMR 1556 and the I_{K1} blocker $BaCl_2$ on the action potential in canine papillary muscle is shown on **Figure 19**.

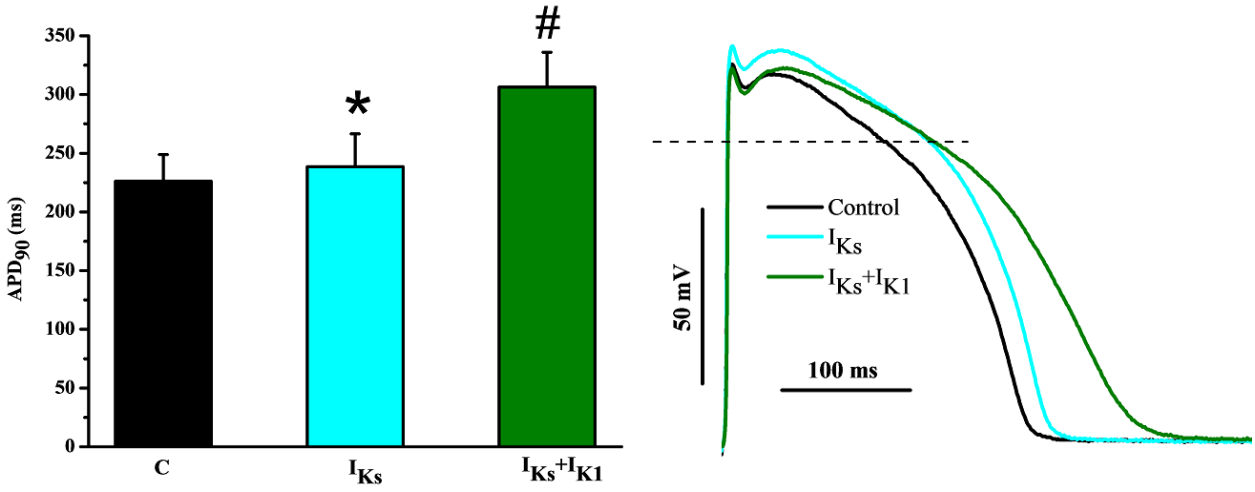

Figure 19. The effect of combined I_{Ks} and I_{K1} block on dog right ventricular papillary muscle at basic cycle length of 1000 ms. Reduction of repolarization reserve with the I_{Ks} blocker HMR 1556 alone

resulted in slight (but statistically significant) APD_{90} prolongation. Additional inhibition of I_{K1} by $BaCl_2$ caused marked APD_{90} increase. *p< 0.05 vs. control, #p<0.05 vs. I_{Ks} block, n= 17. On the right panel representative action potentials constructed from an individual dog right ventricular papillary muscle at BCL= 1000 ms are shown in control, following I_{Ks} and combined I_{Ks} + I_{K1} block.

Small but statistically significant action potential lengthening was induced by 1 µM HMR 1556 at a basic stimulation frequency of 1 Hz (from 226.1 ± 5.54 ms to 238.5 ± 6.82 ms, n=17, p<0.05). In the presence of 1 µM HMR 1556, 30 µM $BaCl_2$ was added to these preparations. The drug induced a marked further lengthening relative to the APD_{90} values measured after the administration of HMR 1556 ($BaCl_2$: 306.3 ± 7.17 ms vs. HMR 1556: 238.5 ± 6.82 ms, n=17, p<0.05), ie. the APD lengthening effect of $BaCl_2$ was significantly augmented in preparations where the repolarization reserve was attenuated by previous application of HMR 1556. Under these circumstances the combined I_{Ks} + I_{K1} block produced reverse rate-dependent APD prolongation (**Figure 20**).

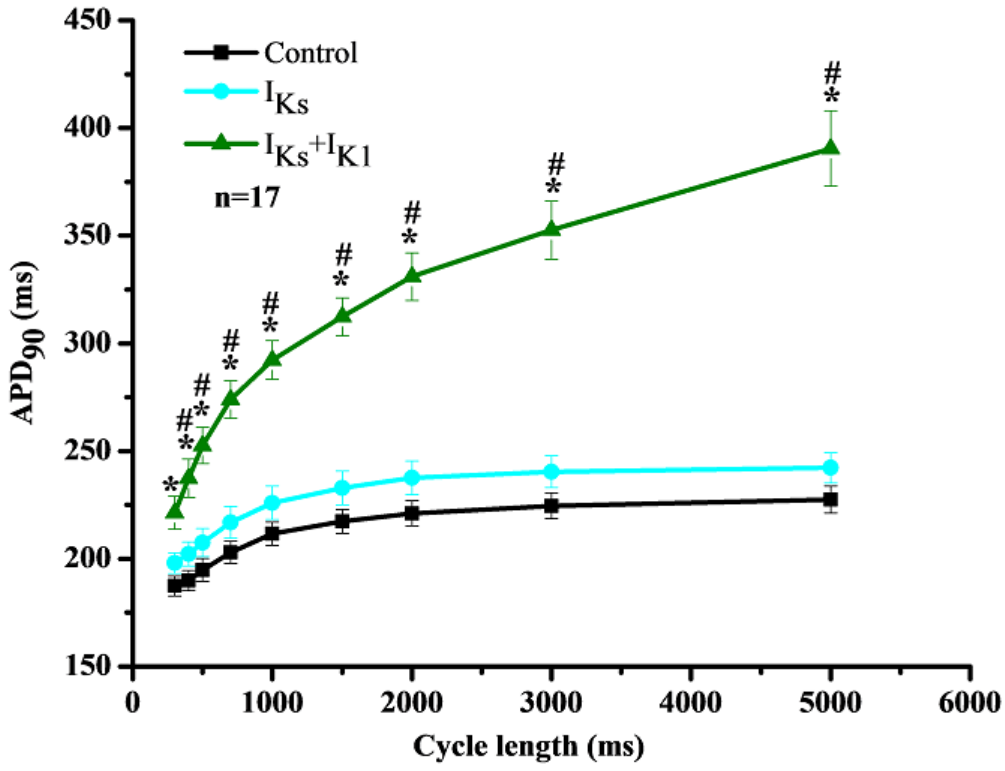

Figure 20. Frequency dependent effect of combined I_{Ks} and I_{K1} block on dog right ventricular papillary muscle. Attenuated repolarization reserve with I_{Ks} block alone did not result in significant APD prolongation in reverse frequency dependent manner, however, additional block of I_{K1} caused marked and significant APD_{90} prolongation at slow heart rates. *p< 0.05 vs. control, #p<0.05 vs. I_{Ks} block, n= 17.

Administration of the I_{Ks} blocker HMR 1556 alone (1 μM) did not cause significant frequency dependent APD_{90} changes on canine papillary muscle. However, with additional block of I_{K1} these changes got more pronounced in a reverse frequency dependent manner (**Figure 20**). In some experiments arrhythmias developed in this setting.

4.2 Results of studies on repolarization adaptation to changes in heart rate

4.2.1 The effects of I_{K1}, I_{Ks}, I_{Kr} $I_{Ca,L}$ and I_{NaK} current inhibition on APD heart rate adaptation

Clinically, the slow adaptation of QT interval to abrupt changes in heart rate (HR), also termed short term cardiac memory, has been proposed as an indicator of arrhythmic risk and sudden cardiac death. In the present study, we investigate the ionic basis of action potential duration at 90% repolarization (APD_{90}) rate adaptation, which is the cellular manifestation of QT heart rate adaptation dynamics.

The results show that the APD heart rate adaptation consists of two phases: a fast initial phase with time constant τ_{fast} 12.9 ± 2.25 / 15.8 ± 3.87 s and a second slow phase with time constant τ_{slow} 176.1 ± 43.41 / 226.1± 51.78.

Following I_{K1} current inhibition by 30 μM $BaCl_2$ decreased τ_{fast} values were measured (**Figure 21**).

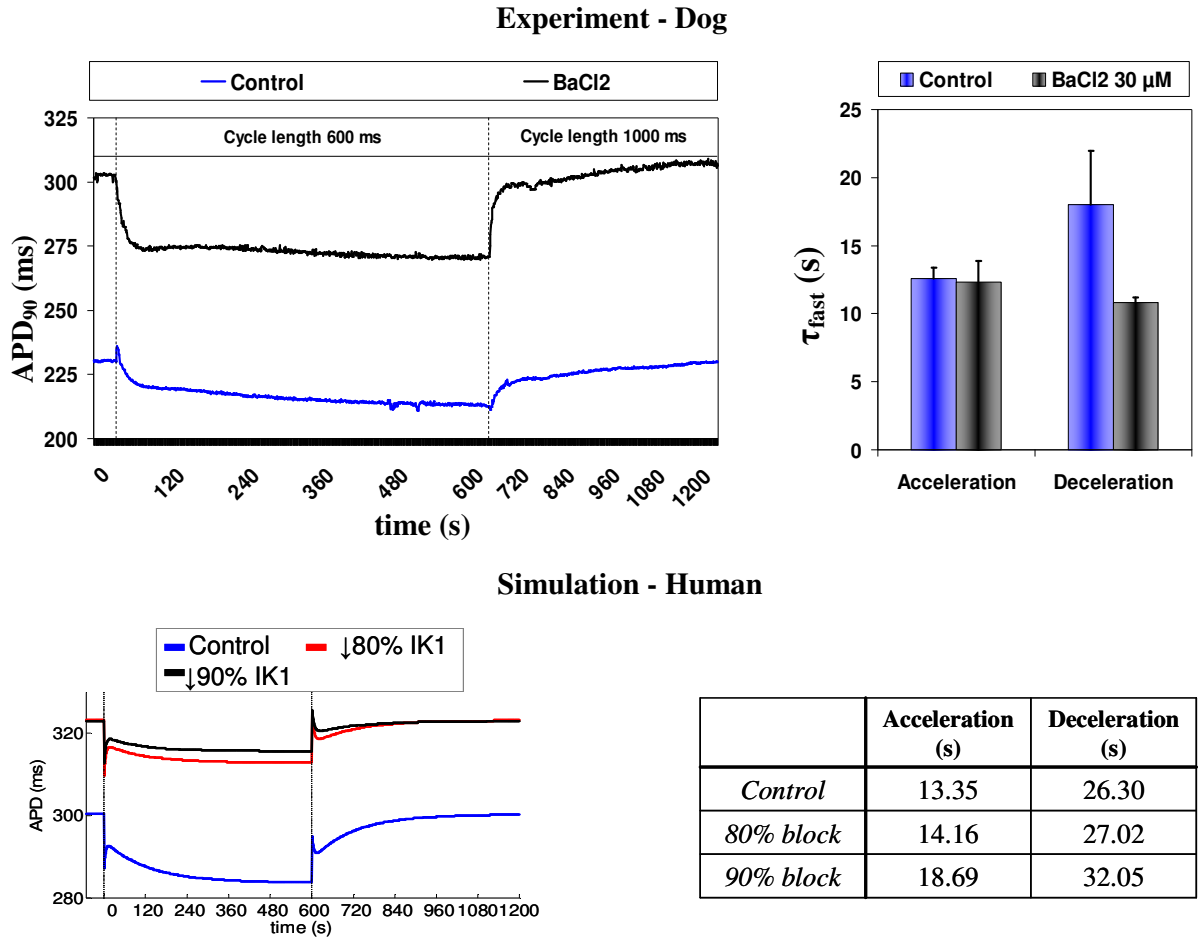

	Acceleration (s)	Deceleration (s)
Control	13.35	26.30
80% block	14.16	27.02
90% block	18.69	32.05

Figure 21. The effect of I_{K1} block on APD_{90} heart rate adaptation. Experimental (top panels) and simulation (bottom panels) study. During acceleration no changes were observed under the effect of I_{K1} block with 30 µM $BaCl_2$. I_{K1} block decreased the τ_{fast} value during deceleration, however, these changes were not statistically significant. n= 5

During acceleration the adaptation kinetics remained unchanged but τ_{fast} decreased from 18.0 ± 3.97 s to 10.8 ± 0.37 s by slowing the heart rate from CL 600 ms to CL 1000 ms. There were opposite changes in the adaptation kinetics after I_{K1} block in the observations of experiments and human simulations. In computer simulations the adaptation was slower (slightly elevated τ_{slow} values) as shown on **Figure 21 (bottom left panel)**, but in the experiment it began faster (reduced τ_{fast} values in deceleration).

By inhibition of the I_{Ks} current in the computer simulation study **(Figure 22 bottom panels)** decresed τ_{fast} values were measured, while there were no clear changes in the experiments with 0.25 µM HMR1556 (**Figure 22 top left and right panel). The** τ_{fast} values slightly increased from 19.9 ± 7.92 s to 24.1 ± 4.77 s during deceleration under the effect of I_{Ks} inhibition impairing the ability of APD adaptation to heart rate changes. In contrast with experiment, an opposite effect was observed in the computer simulation study where τ_{fast}

values were decreased during acceleration and deceleration as shown on **Figure 22 bottom panels.**

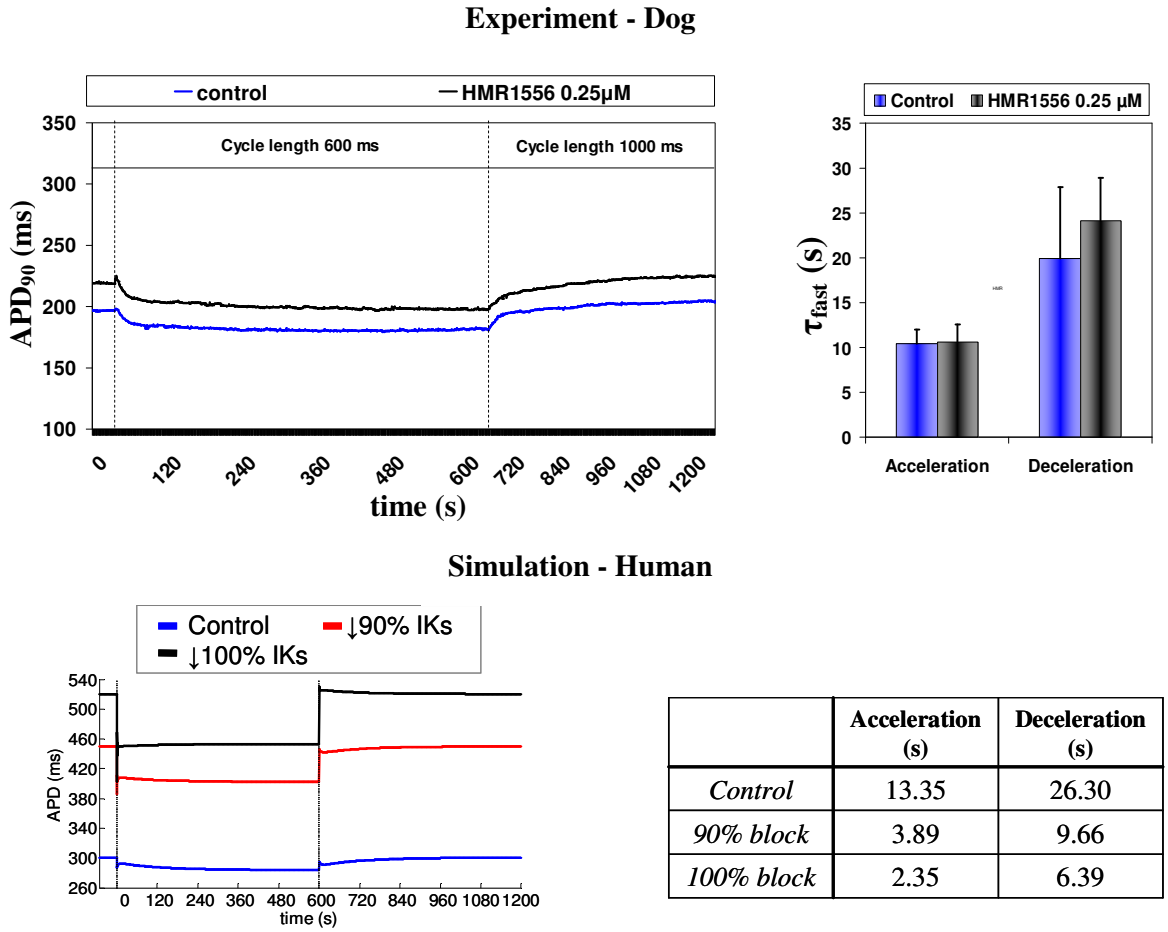

	Acceleration (s)	Deceleration (s)
Control	13.35	26.30
90% block	3.89	9.66
100% block	2.35	6.39

Figure 22. The effect of I_{Ks} block on APD_{90} adaptation kinetics. Experimental (top panel) and computer simulation study (bottom panel). No changes were observed during acceleration in the τ_{fast} values using 0.25 µM HMR 1556. I_{Ks} inhibition increased the τ_{fast} values and delayed the adaptation of repolarization during deceleration. The changes were not found to be significant. Data from computer simulation shows an opposite effect (bottom right panel). n= 5

The APD adaptation kinetics remained unchanged after I_{Kr} block both in simulation and in experiments with application of 100 nM dofetilide. (**Figure 23**)

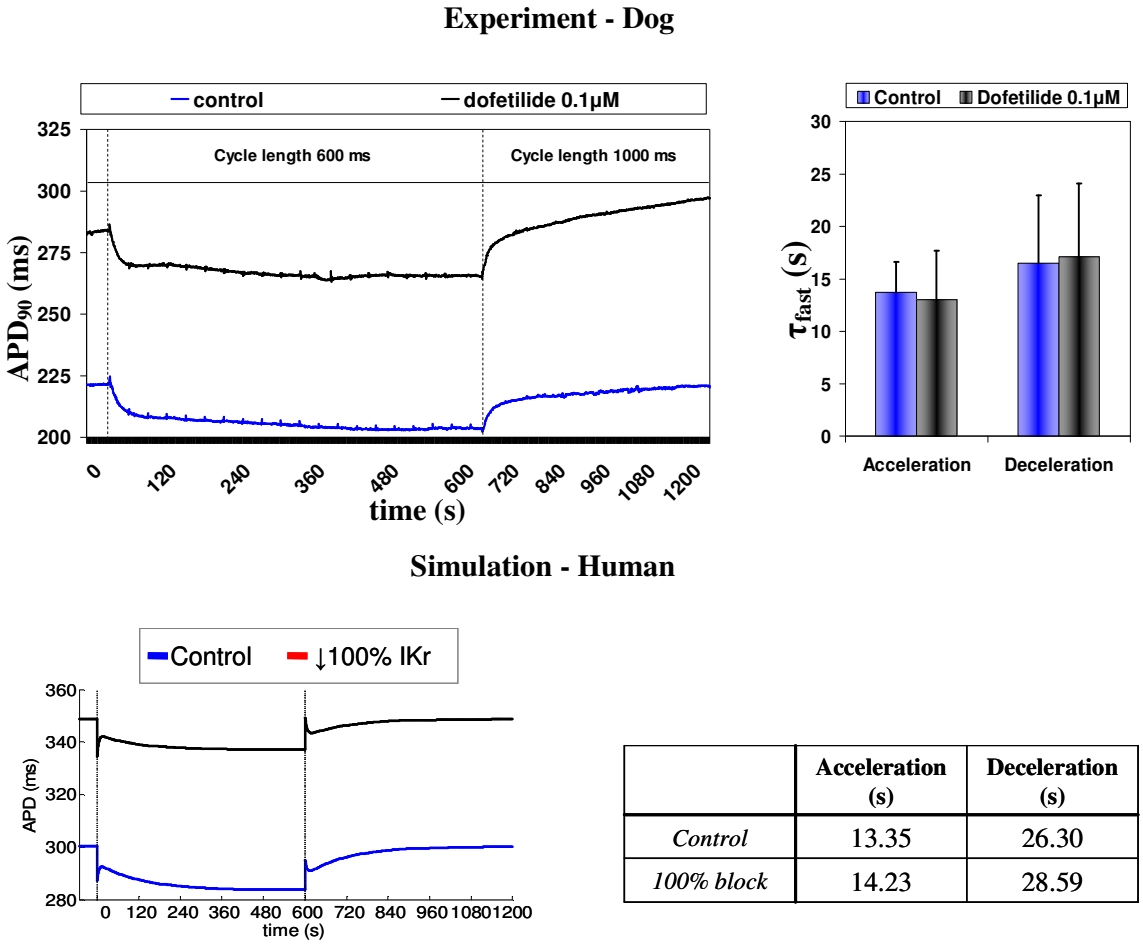

	Acceleration (s)	Deceleration (s)
Control	13.35	26.30
100% block	14.23	28.59

Figure 23: The effect of I_{Kr} block on the APD_{90} adaptation to heart rate changes. There was no alteration under the effect of 100 nM dofetilide in the τ_{fast} value in experimental circumstances (top panels). Concurrently, computer simulation also shows no significant changes in APD HR adaptation (bottom panels). n= 5

In the case of $I_{Ca,L}$ inhibition experiments and computer simulations have provided different results: τ_{fast} values were decreased during acceleration and deceleration from 11.8 ± 1.89 s / 13.6 ± 2.34 s to 8.8 ± 1.95 s / 11.1 ± 1.18 s in experiments associated with faster APD adaptation to heart rate changes, while slower adaptation was present in the computer simulation (see the table on **Figure 24 bottom right panel**). No changes were detected in the slow adaptation phase both in the simulation or experiments.

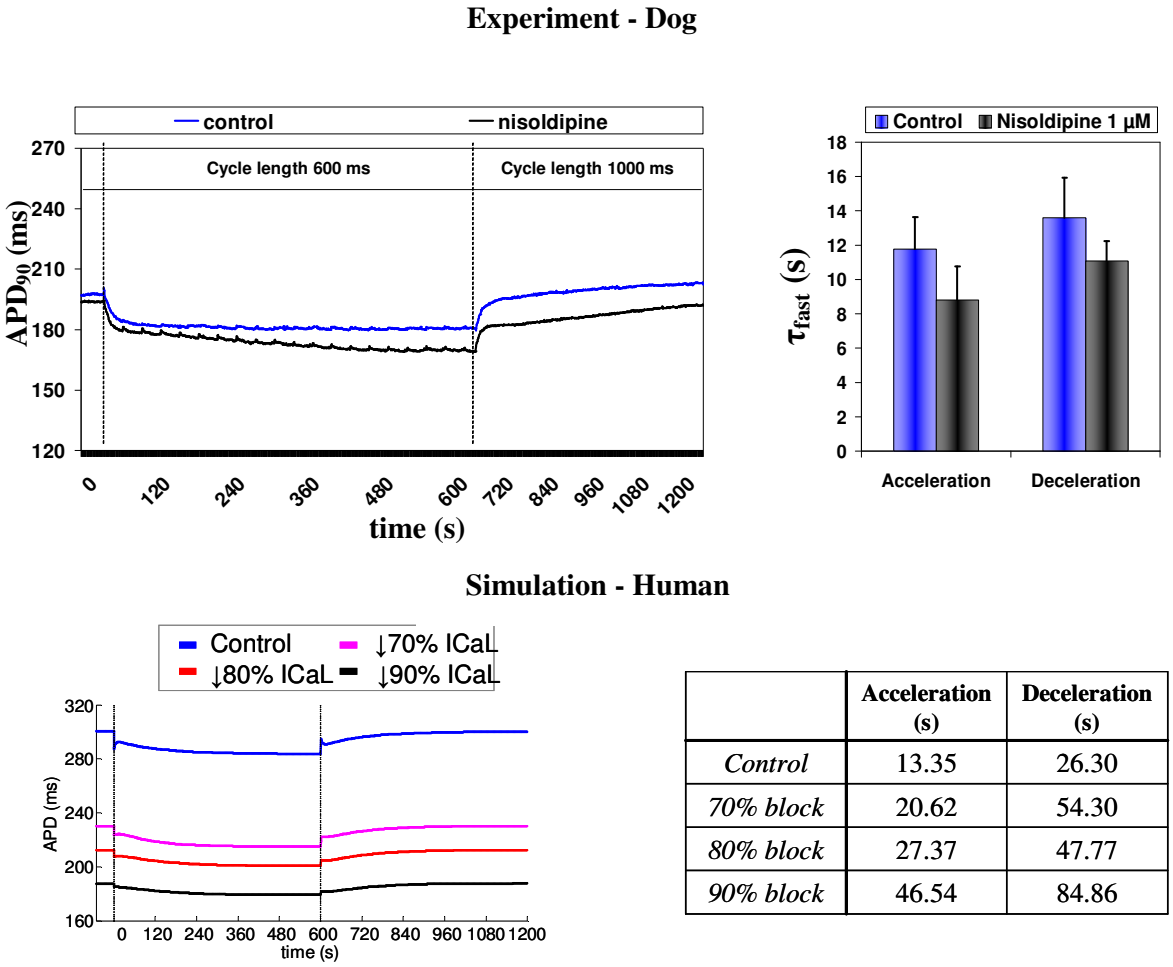

	Acceleration (s)	Deceleration (s)
Control	13.35	26.30
70% block	20.62	54.30
80% block	27.37	47.77
90% block	46.54	84.86

Figure 24. The effect of $I_{Ca,L}$ inhibition on APD HR adaptation. Experimental results are shown on the top panels and simulation study results on the bottom panels. The table indicates the results of the simulation study. n=5

Figure 25 shows the effect of NaK pump inhibition in the presence of 0.6 µM strophantin-G: τ_{slow} values were increased to 258.3 ± 38.08s / 448.9 ± 71.22 s compared with control: 161.1 ± 50.52 s / 245.2 ± 54.07 s, but no changes were observed in the initial fast phase APD adaptation. The τ_{slow} values from the simulation study are presented on the right bottom panel of **Figure 25**. In this case the experiments were confirmed by the computer simulation study.

Experiment - Dog

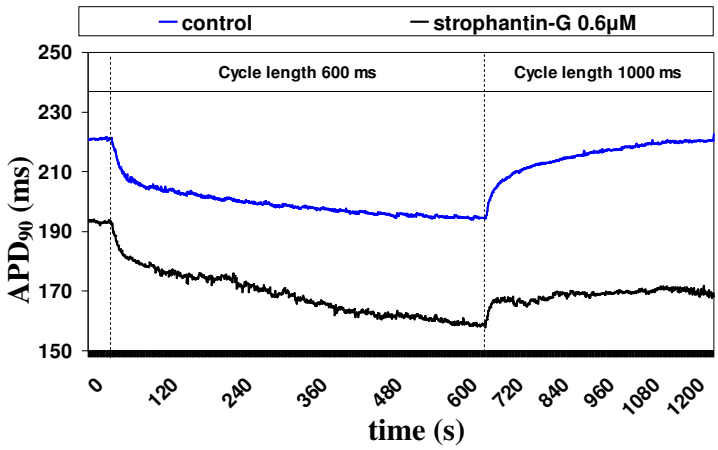

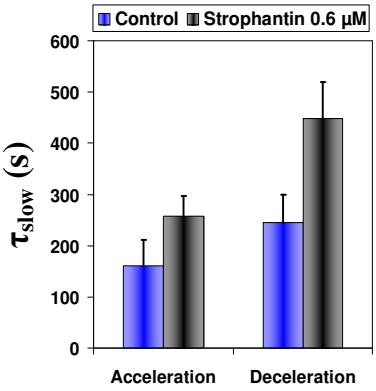

Simulation - Human

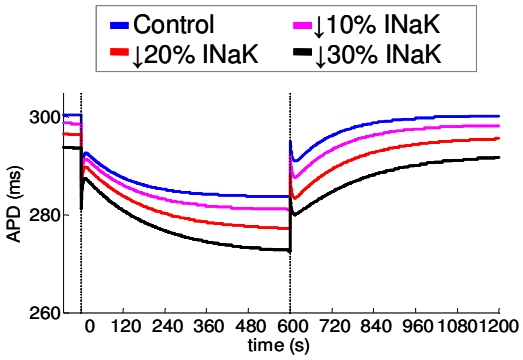

	Tau fast		Tau slow	
	Acceleration (s)	Deceleration (s)	Acceleration (s)	Deceleration (s)
Control	13.35	26.30	125.84	122.71
10% block	13.47	26.12	146.45	137.19
20% block	13.59	26.86	146.45	160.14
30% block	13.90	27.02	194.85	213.74

Figure 25. The effect of I_{NaK} inhibition on APD heart rate adaptation. Experimental results are shown on the top panels and simulation study results on the bottom panels.

5. Discussion

5.1 Studies on repolarization reserve

Here we investigated the effects of repolarization reserve impairment by pharmacological inhibition of I_{K1} in combination with I_{Ks} and I_{Kr} on the incidence of the typical drug-induced arrhythmia, TdP, and different ECG parameters, in a similar experimental setup to a previously published study of out laboratory where the effects of the combined pharmacological inhibition of I_{Ks} and I_{Kr} were characterized in conscious dogs and anesthetized rabbits (Lengyel et al., 2007). In this study we show that combined pharmacological inhibition of other repolarizing potassium currents also leads to repolarization reserve impairment and high incidence of TdP in conscious dogs and anesthetized rabbits. However, dogs and rabbits exhibited markedly different patterns of TdP development in response to combined I_{K1}+I_{Kr} and I_{Ks}+I_{K1} inhibition suggesting that at least some of these currents may play different relative roles in repolarization reserve in dogs and rabbits. In contrast, a previous investigation by our laboratory found that both species responded with a high incidence of TdP paralleled by significant increases of short-term variability of the QT interval following combined I_{Ks}+I_{Kr} inhibition, irrespective of the sequence of I_{Ks} and I_{Kr} blocker administration (Lengyel et al., 2007).

The key role of I_{Ks} in ventricular repolarization reserve has been well established in different animal species as well as in humans (Volders et al. 1999; Varró et al. 2000; Lengyel et al. 2001; Volders et al. 2003; Jost et al. 2005; Abi-Gerges et al. 2006; Lengyel et al. 2007; Jost et al., 2007; Johnson et al., 2010). However, a recent study highlighted that due to lower I_{Ks} densities in human hearts, repolarization reserve may be reduced in humans compared to dogs (Jost et al., 2013). Attributed to low-level I_{Ks} beta-subunit minK expression, a small I_{Ks} and increased TdP susceptibility were described in rabbits (Lu et al., 2001; Zicha et al., 2003). In a recent comparative study, the kinetics of rabbit I_{Ks} have been found more human-like compared to I_{Ks} in guinea-pigs and dogs (Jost et al., 2013b). These data indicate that despite the relatively well characterized role of I_{Ks} in repolarization reserve, the significant differences described in I_{Ks} subunit expression, current densities and kinetics in rabbits and dogs make human extrapolation of results somewhat difficult.

The roles other repolarizing potassium currents may play in repolarization reserve are poorly understood. Among these repolarizing potassium currents, possible roles for I_{to} (Virag et al., 2011) and I_{K1} (Biliczki et al., 2002; Varró and Baczkó, 2011) in repolarization reserve have been suggested. In LQT7 (Andersen-Tawil syndrome), loss of function mutations in

Kir2.1 channels may significantly decrease I_{K1} current, however, the substantially increased pro-arrhythmic risk in these patients is not accompanied by marked QTc prolongation on the ECG (Zhang et al., 2005). Computer modelling studies also support a key role for I_{K1} in ventricles: in these models, reduction of I_{K1} in addition to I_{Kr} block led to early afterdepolarizations (Ishihara et al., 2009). A variety of channel subtypes can be responsible for the I_{K1} current, including alpha-subunits Kir2.1, Kir2.2, Kir2.3, Kir2.4 (for a recent review see Anumonwo and Lopatin, 2010). Significant species-specific differences in the expression of Kir2.x proteins have been reported previously (Wang et al., 1998; Melnyk et al., 2002; Dhamoon and Jalife, 2005). Different heteromeric assembly of Kir2.x proteins leads to different I_{K1} characteristics (Dhamoon et al., 2004) and most likely, to altered overall cardiac electrophysiological responses to drugs. In rabbit cardiomyocytes, a heteromeric assembly of Kir2.1 and Kir2.2 was shown (Zobel et al., 2003). In dogs, Kir2.2 and Kir2.4 levels were minimal, while in humans, Kir2.3 mRNA expression was on a similar level to Kir2.1 and Kir2.1 mRNA expression was found to be three times higher in dogs compared to human (Jost et al., 2013).

In the present study, the short-term variability of the QT interval was calculated to assess temporal instability of repolarization following pharmacological inhibition of repolarizing potassium currents. The STV_{QT} characterizes differences in QT interval durations of consecutive heart beats and has been suggested as a more reliable measure of pro-arrhythmic risk associated with impaired repolarization reserve compared to conventional ECG parameters of repolarization (Berger et al 2003; Varkevisser et al 2012). In this regard, a number of previous *in vivo* and *in vitro* animal experimental and clinical studies (van Opstal et al., 2001; Thomsen et al., 2004; Lengyel et al 2007; Hinterseer et al., 2009; Hinterseer et al., 2010; Antoons et al., 2010) found that STV_{QT} was increased and showed a better correlation with subsequent arrhythmias than QT prolongation in animals or individuals with decreased repolarization reserve later exhibiting serious ventricular arrhythmias. We found in this study that combined inhibition of $I_{K1} + I_{Kr}$ and $I_{Ks} + I_{K1}$ led to increased STV_{QT} in parallel with increased incidence of TdP in most cases, further supporting the role of STV_{QT} determination in ventricular arrhythmia risk estimation. It should be noted that in dogs, following $I_{K1} + I_{Kr}$ inhibition a significant increase in STV_{QT} was found with only one animal showing TdP, however, very short episodes of nonsustained monomorphic ventricular tachycardia were observed in three additional animals.

In the *in vivo* canine TdP model arrhythmias mostly developed following combined I_{Ks} + I_{K1} block, however, following combined I_{Kr} + I_{K1} inhibition a considerable amount of

arrhythmias were not observed. The expression of channel proteins determining the different potassium currents show significant regional (apico-basal, interventricular and atrio-ventricular) and transmural heterogeneity within the myocardium. The density of I_{K1} is higher in the endocardium than epicardium, more potent in the right ventricle than in the left ventricle and more expressed in the apical area than in the basal region (Furukawa et al., 1992; Varro et al., 1993; Brunet et al., 2004; Panama et al., 2007; Dhamoon et al., 2004; Giles et al., 1988; Melnyk et al., 2002). The differences in the delayed rectifier potassium currents are attributable more to I_{Ks} than I_{Kr}. The I_{Ks} current is stronger in the subepicardial than in the subendocardial region (Gintant 1995). These transmural and regional differences already produce an electrical heterogeneity within the myocardium in physiological circumstances. Consequently, since regional differences in I_{Ks} may contribute to electrical inhomogeneity in a greater degree than I_{Kr}, combined block of I_{K1} + I_{Ks} can presumably produce more expressed repolarization heterogeneity leading to the development of reentry arrhythmias more so than in the setting of combined I_{Kr} + I_{K1} block. Moreover, contribution of the I_{Ks} to cycle length dependent changes of cardiac repolarization is more important than that of I_{Kr}. Consequently, the potent respiratory arrhythmia existing in conscious dogs may lead to more excessive regional differences in refractory periods following combined I_{Ks} + I_{K1} block than in the case of combined I_{Kr} + I_{K1} block.

In normal circumstances, conscious dogs show marked respiratory sinus arrhythmia and have larger STV_{RR} and larger STV_{QT} compared to anaesthetized rabbits that exhibited no respiratory arrhythmia and had smaller STV_{RR} and STV_{QT} at baseline. These observations raise the possibility that increased STV_{RR} contributes to STV_{QT} changes in our models. However, following combined potassium current block where STV_{QT} was increased there were no obvious changes in STV_{RR} and a clear influence of STV_{RR} on STV_{QT} was not observed in accordance with previous studies (Thomsen et al., 2007; Lengyel et al. 2011) have also demonstrated in professional soccer players that STV_{QT} remained increased after exercise despite a decrease in heart rate variability. In our experiments, increased STV_{QT} was found after combined potassium current inhibition despite unchanged STV_{RR} in dogs, and the STV_{RR} increases in rabbits were less than, or around 0.5 ms, making it very unlikely that STV_{RR} changes importantly contributed to STV_{QT} alterations.

In our *in vitro* studies on repolarization reserve using dog right ventricular papillary muscle preparations, inhibition of I_{K1} and I_{Ks} alone caused a significant APD_{90} prolongation in a similar degree to the QTc prolongation observed in conscious dogs (**Figures 14, 19, 4 and 9**). Combined inhibition of I_{K1} + I_{Kr} and I_{Ks} + I_{K1} caused a further significant prolongation of

repolarization both *in vivo* and *in vitro* (**Figures 15, 19, 4 and 9**). Interestingly, in our *in vitro* study when I_{Kr} inhibition was followed by combined I_{Kr} + I_{K1} inhibition, the APD_{90} prolongation was larger compared to the experiments where I_{K1} was blocked first followed by combined I_{K1} + I_{Kr} inhibition (**Figures 14 and 15**). The reasons for these observations are not understood, different adaptation mechanisms of repolarization to I_{Kr} and I_{K1} block may be involved. The similar degree in repolarization prolongation and the markedly different TdP incidence in conscious dogs (**Figure 13**) following different potassium channel block combinations again highlight the importance of calculation of STV_{QT} for more reliable drug-induced arrhythmia prediction. The frequency dependent prolongation of APD_{90} following inhibition of different potassium channels was also evaluated. Inhibition of I_{K1} and I_{Kr} alone led to more pronounced APD_{90} prolongation at slow heart rates (increased CL) as shown on **Figures 17 and 18**, however, this reverse frequency dependent prolongation was not observed after I_{Ks} block (**Figure 20**). Combined I_{Kr} + I_{K1} inhibition resulted in a greater reverse frequency dependent APD_{90} prolongation compared to combined I_{Ks} + I_{K1} block (**Figures 18 and 20**). Inhibition of I_{K1}, I_{Kr} or I_{Ks} did not cause any extra "arrhythmic" beats in the in vitro experiments, similarly to our observations in conscious dogs where these interventions did not cause severe ventricular arrhythmias, only some extrasystoles (following $BaCl_2$ and dofetilide) and/or salvos (following dofetilide). In parallel with the *in vivo* results, where combined potassium current inhibition led to serious ventricular arrhythmias, combined I_{Kr} + I_{K1} inhibition and I_{Ks} + I_{K1} block provoked extra beats (beats without stimulation) in canine papillary muscle preparations, and these arrhythmic beats occurred more frequently at CL 3000 ms and CL 5000 ms. Although repolarization was excessively prolonged in these circumstances, early afterdepolarisations (EADs) were not observed using the conventional microelectrode technique. Previous studies suggest that resting membrane potential of ventricular myocytes is maintained by the high resting potassium permeability which flows mainly through I_{K1} (Nichols et al., 1997). By blocking the I_{K1} in combination with other repolarizing currents, enhanced automaticity can occur causing ectopic firing. On the basis of our *in vitro* experiments, enhanced automaticity and ectopic beats may play an important role in arrhythmia generation following combined potassium current block involving I_{K1}. However, experiments using mathematical modeling, inhibition of I_{K1} with combination of I_{Kr} reduction resulted in EADs (Ishihara et al., 2009). The study of Nattel and Quantz suggests that cardiac Purkinje fibers are the likely source of early afterdepolarizations initiating TdP (Nattel & Quantz, 1988). It is possible that I_{K1} block in combination with other potassium

currents inhibition results in formation of EADs in Purkinje fibers, a scenario present in our in vivo setup but not in the in vitro experiments.

In summary, due to stronger I_{K1} and I_{Ks} in dogs compared to rabbits and humans, dogs may exhibit larger repolarization reserve compared to the other two species. Therefore, rabbit pro-arrhythmia models based on pharmacologically impaired repolarization reserve may represent greater arrhythmia susceptibility and may be more useful than canine models in predicting human electrophysiological responses to drugs affecting cardiac ventricular repolarization.

5.2 Studies on adaptation of repolarization to abrupt changes in heart rate

Clinically, the slow adaptation of QT interval to abrupt changes in heart rate (HR), also termed short-term cardiac memory (Arnold et al, 1982; Grom et al, 2005), has been proposed as an indicator of arrhythmic risk and sudden cardiac death. Clinical studies suggest that patients with elongated QT heart rate adaptation dynamics have an increased risk of experiencing cardiac arrhythmias and sudden cardiac death (Grom et al, 2005; Pueyo et al, 2004). In the present study we investigated the ionic basis of APD_{90} rate adaptation which is the cellular manifestation of QT heart rate adaptation dynamics. APD adaptation is defined as protracted when the associated time constant τ_{fast} or τ_{slow} is abnormally long. In the present experiments, 30 μM $BaCl_2$ (estimated 80% I_{K1} block) results in a 28/11% decrease in τ_{fast} (**Figure 21**). Opposite changes in the adaptation kinetics after I_{K1} block were obtained using computer simulation in our cooperative study (Pueyo et al, 2010). Convincing evidence was not found in the present experiments that the block of I_{K1} may significantly influence the initial fast phase of APD heart rate adaptation and may lead to arrhythmias via this mechanism. However, in both simulation and experiments in dog, I_{K1} block was found to have an impact on the slow phase of APD heart rate adaptation. Block of I_{K1} led to 30 % decrease in τ_{slow} in dogs. Consequently, the I_{K1} block alone is not likely to significantly contribute to arrhythmogenesis by slowing the APD and QT adaptation to heart rate changes. It is possible that I_{K1} block in combination with other repolarizing currents indirectly affects the intracellular Ca^{2+} level that mainly determines APD heart rate adaptation. The inhibition of I_{K1} causes membrane depolarization which may lead to changes in the function of the sodium-calcium exchanger (NCX) promoting increase in intracellular calcium levels. Further studies are needed to find out whether the combined block of different potassium currents affect the APD heart rate adaptation and whether decreased adaptation correlates with prolonged short-term QT variability.

Our results also show that QT heart rate adaptation is a manifestation of cellular APD heart rate adaptation. Furthermore, $I_{Ca,L}$ inactivation and I_{Ks} activation kinetics determine the fast phase of HR adaptation while I_{NaK} and $[Na^+]_i$ dynamics are key in the slow and final phase. Regarding the $I_{Ca,L}$ inhibition, computer simulation and experiments carried out on canine right ventricular papillary muscle provided controversial results: simulation showed the increase of τ_{fast} values while decreased τ_{fast} values were experienced in dog papillary muscle associated with faster APD adaptation to heart rate changes. Our experimental results are confirmed by another study where the low incidence of afterdepolarization following administration of amiodarone was related to the ability of the drug to slow $I_{Ca,L}$ and decrease τ_{fast} (Wegener et al, 2006). Furthermore, clinical observations also suggest that patients who benefit from amiodarone therapy, the loss of pro-arrhythmia has been explained by the accelerated adaptation of QT interval to heart rate changes (Smetana et al., 2004). Our experimental results and computer simulation study equally indicate the crucial role of I_{Ks} in the fast phase of APD adaptation as previously suggested. (Carmeliet 2006; Eisner et al., 2009; Faber et al, 2000) 90 % inhibition of the I_{Ks} current during simulation resulted in a 71–82/63–76% reduction in τ_{fast} following acceleration/deceleration in human (Pueyo et al., 2010), while increase were observed in dog ventricular preparations under the effect of 0.25 μM HMR 1556 (~ full block). Alterations in the I_{Ks} current, as showed in experiments and simulation, may be associated with reduced APD HR adaptation causing ventricular arrhythmias. Clinical observations also confirmed the major role of I_{Ks} in arrhythmogenesis: gain of function mutations in the KCNQ1 gene with reduced time constant of I_{Ks} activation gate, causes short QT syndrome associated with high incidence of sudden cardiac death. (Béllocq et al., 2004) Computer simulations and experiments were in good agreement regarding the inhibition of I_{NaK}. Both our experimental and simulation results show the key role of I_{NaK} in the slow phase of APD adaptation. Large τ_{slow} values are also associated with flat APD restitution slopes, which could favor the stability of reentrant circuits and thus could increase arrhythmic risk (Pueyo et al, 2010). Simulations in human and dog also suggest that DADs develop under ~ 60 % I_{NaK} inhibition, the degree of block associated with ischemic heart disease and patient with heart failure treated with digitalis (Pueyo et al., 2010; Bundgaard et al., 1996)**.** Alterations in these mechanisms of transmembrane ionic transport result in protracted APD heart rate adaptation and increased risk of arrhythmias mostly due to increased risk of afterdepolarization development. Thus, our results suggest that slow QT rate adaptation, as measured in surface ECG of patients at high arrhythmic risk, is a reflection of adverse ionic changes, which, upon further deterioration, may facilitate arrhythmia initiation.

6. Conclusions

6.1 Conclusions: studies on repolarization reserve

In conclusion, both rabbits and dogs are susceptible to pharmacological impairment of repolarization reserve and concomitant ventricular arrhythmia induction by compounds that inhibit repolarizing currents. Our results have further confirmed that STV_{QT} may be a better predictor of drug-induced TdP development than conventional ECG parameters characterizing repolarization prolongation. Importantly, however, rabbits are more susceptible to combined inhibition of I_{K1}+I_{Kr} than dogs, and dogs are more susceptible to combined inhibition of I_{K1}+I_{Ks} than rabbits, suggesting different relative roles of I_{K1} and I_{Ks} in repolarization reserve in the two species. These results warrant cautious evaluation of the potential pro-arrhythmic adverse effects and cardiovascular safety of candidate compounds in rabbit and dog models. The different relative roles of repolarizing potassium currents in dogs and rabbits need to be considered when extrapolating animal experimental pro-arrhythmia study results to human clinical situations. In addition, our results also strongly suggest that the I_{K1} current plays an important role in repolarization reserve. The underlying mechanism of arrhythmia generation following impairment of repolarization reserve by inhibition of I_{K1} seems to be increased ectopic firing rather than the development of EADs.

6.2 Conclusions: repolarization adaptation to abrupt heart rate changes

Our experiments strongly suggest (also confirmed by computer simulations) that $I_{Ca,L}$ and I_{Ks} currents determine the fast phase of heart rate adaptation while I_{NaK} dynamics are critical in the slow and final phase. The results also demonstrate that I_{NaK} inhibition, as it occurs in myocardial ischemia and heart failure patients, results in decreased APD adaptation, and might be a pro-arrhythmic risk factor. Large t_{slow} due to I_{NaK} inhibition is associated with an increase in action potential triangulation and may promote $I_{Ca,L}$ reactivation, resulting in an increased risk of delayed afterdepolarization formation. Different outcomes were observed in the case of I_{Ks} and $I_{Ca,L}$. Experiments demonstrate that reduced I_{Ks} is associated with delayed APD adaptation in the fast phase while $I_{Ca,L}$ block correlated with increased fast phase APD adaptation kinetics. It should be noted that experimental results following $I_{Ca,L}$ block were in conflict with computer modeling results, highlighting some existing imperfections in the human action potential computer model. Interestingly, I_{Kr} inhibition had no effect on APD heart rate adaptation kinetics and these results were in agreement with computer simulation

studies. These results provide new insights into the mechanisms of ventricular rate adaptation and its connection to pro-arrhythmic risk.

7. Acknowledgements

I would like to thank Professor András Varró, Head of the Department of Pharmacology and Pharmacotherapy, Faculty of Medicine, University of Szeged, for his support.

I would also like to thank Dr István Baczkó, my tutor and supervisor, who directed my research work for his invaluable help during my Ph.D. studies.

I would like to thank my family for all their help and care.

8. References

1. Abbott GW, Sesti F, Splawski I, Buck ME, Lehmann MH, Timothy KW, Keating MT, Goldstein SA. 1999. MiRP1 forms IKr potassium channels with HERG and is associated with cardiac arrhythmia. Cell. 97(2):175-87. PMID: 10219239, doi: 10.1016/S0092-8674(00)80728-X.
2. Abi-Gerges N, Small BG, Lawrence CL, Hammond TG, Valentin JP, Pollard CE. 2006. Gender differences in the slow delayed (IKs) but not in inward (IK1) rectifier K+ currents of canine Purkinje fibre cardiac action potential: key roles for IKs, beta-adrenoceptor stimulation, pacing rate and gender. Br J Pharmacol. 147(6):653-60. PMID: 16314855, doi: 10.1038/sj.bjp.0706491.
3. Antoni H, Böcker D, Eickhorn R. 1988. Sodium current kinetics in intact rat papillary muscle: measurements with the loose-patch-clamp technique J Physiol. 406: 199-213. PMID: 2855435.
4. Antoons G, Oros A, Beekman JD, Engelen MA, Houtman MJ, Belardinelli L, Stengl M, Vos MA. 2010. Late na(+) current inhibition by ranolazine reduces torsades de pointes in the chronic atrioventricular block dog model. J Am Coll Cardiol. 55(8):801-9. PMID: 20170820, doi: 10.1016/j.jacc.2009.10.033.
5. Anumonwo JM, Lopatin AN. 2010. Cardiac strong inward rectifier potassium channels. J Mol Cell Cardiol. 48(1):45-54. PMID: 19703462, doi: 10.1016/j.yjmcc.2009.08.013.
6. Arnold L, Page J, Attwell D, Cannell M, Eisner DA. 1982. The dependence on heart rate of the human ventricular action potential duration. Cardiovasc Res 16: 547–551, PMID: 7151099, doi: 10.1093/cvr/16.10.547.
7. Attwell D, Cohen I, Eisner D, Ohba M, Ojeda C. 1979. The steady state TTX-sensitive ("window") sodium current in cardiac Purkinje fibres. Pflugers Arch. 379(2):137-42. PMID: 571107, doi: 10.1007/BF00586939.
8. Baher A, Qu Z, Hayatdavoudi A, Lamp ST, Yang MJ, Xie F, Turner S, Garfinkel A, Weiss JN. 2007. Short-term cardiac memory and mother rotor fibrillation. Am J Physiol Heart Circ Physiol. 292(1):H180-9. PMID: 16891403, doi: 10.1152/ajpheart.00944.2005
9. Balzo U, Rosen MR 1992. T wave changes persisting after ventricular pacing in canine heart are altered by 4-aminopyridine but not by lidocaine. Implications with respect to phenomenon of cardiac 'memory'. Circulation. 85(4):1464-72. PMID: 1555287, doi: 10.1161/01.CIR.85.4.1464.
10. Barry DM, Nerbonne JM. 1996. Myocardial potassium channels: electrophysiological and molecular diversity. Annu Rev Physiol. 58:363-94. PMID: 8815800, doi: 10.1146/annurev.ph.58.030196.002051.
11. Batey AJ, Coker SJ. 2002. Proarrhythmic potential of halofantrine, terfenadine and clofilium in a modified in vivo model of torsade de pointes. Br J Pharmacol. 135(4):1003-12. PMID: 11861329, doi: 10.1038/sj.bjp.0704550.
12. Béllocq C, van Ginneken AC, Bezzina CR, Alders M, Escande D, Mannens MM, Baró I, Wilde AA. 2004. Mutation in the KCNQ1 gene leading to the short QT-interval syndrome. Circulation 109: 2394–2397, PMID: 15159330, doi: 10.1161/01.CIR.0000130409.72142.FE.
13. Berger RD, Kasper EK, Baughman KL, Marban E, Calkins H, Tomaselli GF. 1997. Beat-to-beat QT interval variability: novel evidence for repolarization lability in

ischemic and nonischemic dilated cardiomyopathy. Circulation 96:1557– 1565. PMID: 9315547, doi: 10.1161/01.CIR.96.5.1557.

14. Berger, R.D. 2003. QT variability. J Electrocardiol. 36 Suppl: 83-87. PMID: 14716597, doi: 10.1016/j.jelectrocard.2003.09.019.
15. Bers DM (2001). Excitation-contraction coupling and cardiac contractile force. 2nd edn. Kluwer Academic Publishers, Dordrecht-Boston-London. doi: 10.1007/978-94-010-0658-3.
16. Biliczki P, Virág L, Iost N, Papp JG, Varró A. 2002 Interaction of different potassium channels in cardiac repolarization in dog ventricular preparations: role of repolarization reserve. Br J Pharmacol. 137(3):361-8. PMID: 12237256 doi: 10.1038/sj.bjp.0704881
17. Boyett MR, Harrison SM, Janvier NC, McMorn SO, Owen JM, Shui Z. 1996. A list of vertebrate cardiac ionic currents nomenclature, properties, function and cloned equivalents. Cardiovasc Res. 32(3):455-81. PMID: 8881508, doi: 10.1016/S0008-6363(95)00228-6.
18. Brennan M, Palaniswami M, Kamen P. 2001. Do existing measures of Poincaré plot geometry reflect nonlinear features of heart rate variability? IEEE Trans Biomed Eng. 48(11):1342-7. PMID: 11686633, doi: 10.1109/10.959330.
19. Brunet S, Aimond F, Guo W, Li H, Eldstrom J, Fedida D, et al. 2004. Heterogeneous expression of repolarizing, voltage-gated K+ currents in adult mouse ventricles. J Physiol. 559(Pt 1):103–20. doi: 10.1113/jphysiol.2004.063347
20. Bundgaard H, Kjeldsen K. 1996. Human myocardial Na,K-ATPase concentration in heart failure. Mol Cell Biochem 163–164: 277–283. PMID: 8974067,
21. Carmeliet E. 2006. Action potential duration, rate of stimulation, and intracellular sodium. J Cardiovasc Electrophysiol 17: S2–S7. PMID: 16686677, doi: 10.1111/j.1540-8167.2006.00378.x.
22. Carmeliet E. 1993. Mechanisms and control of repolarization. Eur Heart J. 14 Suppl H:3-13. Review. PMID: 8293752, doi: 10.1093/eurheartj/14.suppl_H.3.
23. Carmeliet E. 1987. Slow inactivation of the sodium current in rabbit cardiac Purkinje fibres. Pflugers Arch. 408(1):18-26. PMID: 2434919, doi: 10.1007/BF00581835.
24. Chézalviel-Guilbert F, Davy JM, Poirier JM, Weissenburger J. 1995. Mexiletine antagonizes effects of sotalol on QT interval duration and its proarrhythmic effects in a canine model of torsade de pointes. J Am Coll Cardiol. 26(3):787-92. PMID: 7642874, doi: 10.1016/0735-1097(95)00234-U.
25. Dhamoon AS, Pandit SV, Sarmast F, Parisian KR, Guha P, Li Y, Bagwe S, Taffet SM, Anumonwo JM. 2004. Unique Kir2.x properties determine regional and species differences in the cardiac inward rectifier K+ current. Circ Res. 94(10):1332-9. PMID: 15087421, doi: 10.1161/01.RES.0000128408.66946.67.
26. Dhamoon, A.S. and Jalife, J. 2005. The inward rectifier current (IK1) controls cardiac excitability and is involved in arrhythmogenesis. Heart Rhythm. 2:316-324. PMID: 15851327, doi: 10.1016/j.hrthm.2004.11.012.
27. Dhamoon, A.S., Pandit, S.V., Sarmast, F., Parisian, K.R., Guha, P., Li, Y., Bagwe, S., Taffet, S.M. and Anumonwo, J.M. 2004. Unique Kir2.x properties determine regional and species differences in the cardiac inward rectifier K+ current. Circ. Res. 94:1332-1339. PMID: 15087421, doi: 10.1161/01.RES.0000128408.66946.67.
28. Eisner DA, Dibb KM, Trafford AW. 2009. The mechanism and significance of the slow changes of ventricular action potential duration following a change of heart rate. Exp Physiol 94: 520–528. PMID: 19270038, doi: 10.1113/expphysiol.2008.044008.

29. Faber GM, Rudy Y. 2000. Action potential and contractility changes in [Na]i overloaded cardiac myocytes: a simulation study. Biophys J 78: 2392– 2404, 2000. PMID: 10777735, doi: 10.1016/S0006-3495(00)76783-X.

30. Farkas A, Batey AJ, Coker SJ. 2004. How to measure electrocardiographic QT interval in the anaesthetized rabbit. J Pharmacol Toxicol Methods. 50(3):175-85. PMID: 15519904, doi: 10.1016/j.vascn.2004.05.002

31. Follmer CH, ten Eick RE, Yeh JZ. 1987. Sodium current kinetics in cat atrial myocytes. J Physiol. 384:169-97. PMID: 2443658.

32. Foster PR, Elharrar V, Zipes DP. 1977. Accelerated ventricular escapes induced in the intact dog by barium, strontium and calcium. J Pharmacol Exp Ther. 200(2): 373-383. PMID: 839442.

33. Fozzard HA, January CT, Makielski JC. 1985. New studies of the excitatory sodium currents in heart muscle. Circ Res. 56(4):475-85. Review. PMID: 2579746, doi: 10.1161/01.RES.56.4.475.

34. Furukawa T, Kimura S, Furukawa N, Bassett AL, Myerburg RJ. 1992. Potassium rectifier currents differ in myocytes of endocardial and epicardial origin. Circ Res. 70(1):91-103. PMID: 1727690, doi: 10.1161/01.RES.70.1.91

35. Giles WR, Imaizumi Y. 1988. Comparison of potassium currents in rabbit atrial and ventricular cells. J Physiol. 405:123-45. PMID: 2855639

36. Gilmour RF Jr, Otani NF &Watanabe MA. 1997. Memory and complex dynamics in cardiac Purkinje fibers. Am J Physiol Heart Circ Physiol 272, H1826–H1832. PMID: 9139969,

37. Gintant GA. 1995. Regional differences in IK density in canine left ventricle: role of IK,s in electrical heterogeneity. Am J Physiol. 268(2 Pt 2):H604-13. PMID: 7864185.

38. Gintant GA. 1996. Two components of delayed rectifier current in canine atrium and ventricle. Does IKs play a role in the reverse rate dependence of class III agents? Circ Res. 78(1):26-37. PMID: 8603502, doi: 10.1161/01.RES.78.1.26.

39. Grom A, Faber TS, Brunner M, Bode C, Zehender M. 2005. Delayed adaptation of ventricular repolarization after sudden changes in heart rate due to conversion of atrial fibrillation. A potential risk factor for proarrhythmia? Europace. 7(2):113-21. PMID: 15763525 doi: 10.1016/j.eupc.2005.01.001

40. Guo J, Massaeli H, Xu J, Jia Z, Wigle JT, Mesaeli N, Zhang S. 2009. Extracellular K+ concentration controls cell surface density of IKr in rabbit hearts and of the HERG channel in human cell lines. J Clin Invest. 119(9):2745-57. PMID: 19726881, doi: 10.1172/JCI39027

41. Han W, Wang Z, Nattel S. 2001. Slow delayed rectifier current and repolarization in canine cardiac Purkinje cells. Am J Physiol Heart Circ Physiol. 280(3):H1075-80. PMID: 11179049.

42. Harvey RD, Ten Eick RE. 1988. Characterization of the inward-rectifying potassium current in cat ventricular myocytes. J Gen Physiol. 91(4):593-615. PMID: 2455768, doi: 10.1085/jgp.91.4.593

43. Hinterseer M, Beckmann BM, Thomsen MB, et al. 2009. Relation of increased short term variability of QT interval to congenital long-QT syndrome. Am J Cardiol. 103:1244 –1248. PMID: 19406266, doi: 10.1016/j.amjcard.2009.01.011.

44. Hinterseer M, Beckmann BM, Thomsen MB, Pfeufer A, Ulbrich M, Sinner MF et al. 2010. Usefulness of short-term variability of QT intervals as a predictor for electrical

remodeling and proarrhythmia in patients with nonischemic heart failure. Am J Cardiol 106: 216–220. PMID: 20599006, doi: 10.1016/j.amjcard.2010.02.033.

45. Hinterseer M, Thomsen MB, Beckmann BM, et al. 2008. Beat-to-beat variability of QT intervals is increased in patients with drug-induced long-QT syndrome: a case control pilot study. Eur Heart J. 29:185–190. PMID: 18156612, doi: 10.1093/eurheartj/ehm586.
46. Hinterseer, M., Beckmann, B.M., Thomsen, M.B., Pfeufer, A., Ulbrich, M., Sinner, M.F., Perz, S., Wichmann, H.E., Lengyel, C., Schimpf, R., Maier, S.K., Varró, A., Vos, M.A., Steinbeck, G. and Kääb, S. 2010. Usefulness of short-term variability of QT intervals as a predictor for electrical remodeling and proarrhythmia in patients with nonischemic heart failure. Am. J. Cardiol. 106: 216–220. PMID: 20599006, doi: 10.1016/j.amjcard.2010.02.033.
47. Hirano Y, Fozzard HA, January CT. 1989. Characteristics of L- and T-type Ca2+ currents in canine cardiac Purkinje cells. Am J Physiol. 256(5 Pt 2):H1478-92. PMID: 2470265.
48. Hondeghem LM, Lu HR, van Rossem K, De Clerck F. 2003. Detection of proarrhythmia in the female rabbit heart: blinded validation. J Cardiovasc Electrophysiol. 14:287–294. PMID: 12716112, doi: 10.1046/j.1540-8167.2003.02466.x
49. Isenberg G, Klöckner U. 1982. Calcium currents of isolated bovine ventricular myocytes are fast and of large amplitude. Pflugers Arch. 395(1):30-41. PMID: 6294586, doi: 10.1007/BF00584965.
50. Ishihara K, Sarai N, Asakura K, Noma A, Matsuoka S. 2009. Role of Mg(2+) block of the inward rectifier K(+) current in cardiac repolarization reserve: A quantitative simulation. J Mol Cell Cardiol. 47(1):76-84. PMID: 19303883, doi: 10.1016/j.yjmcc.2009.03.008.
51. January CT, Riddle JM. 1989. Early afterdepolarizations: mechanism of induction and block. A role for L-type Ca2+ current. Circ Res. 64(5):977-90. PMID: 2468430, doi: 10.1161/01.RES.64.5.977.
52. Johnson DM, Heijman J, Pollard CE, Valentin JP, Crijns HJ, Abi-Gerges N, Volders PG. 2010. I(Ks) restricts excessive beat-to-beat variability of repolarization during beta-adrenergic receptor stimulation. J Mol Cell Cardiol. 48(1):122-30. PMID: 19744496, doi: 10.1016/j.yjmcc.2009.08.033.
53. Jost N, Papp JG, Varró A. 2007. Slow delayed rectifier potassium current (IKs) and the repolarization reserve. Ann Noninvasive Electrocardiol. 12(1):64-78. Review. PMID: 17286653, doi: 10.1111/j.1542-474X.2007.00140.x.
54. Jost N, Varró A, Szűts V, Kovacs PP, Seprenyi G, Biliczki P et al. 2008. Molecular basis of repolarization reserve differences between dogs and man. Circulation 118 Suppl: 342. Circulation. 118: S_342.
55. Jost N, Virág L, Bitay M, Takács J, Lengyel C, Biliczki P, Nagy Z, Bogáts G, Lathrop DA, Papp JG, Varró A. 2005. Restricting excessive cardiac action potential and QT prolongation: a vital role for IKs in human ventricular muscle. Circulation. 112(10):1392-9. PMID: 16129791, doi: 10.1161/CIRCULATIONAHA.105.550111.
56. Jost, N., Kohajda, Zs., Corici, C., Horvath, A., Bitay, M., Bogats, G., Papp, J.G., Varró, A. and Virag, L. 2013. The comparative study of rapid and slow delayed rectifier currents in undiseased human, dog, rabbit and guinea pig ventricular myocytes. Europace, 15 Suppl 2: ii1-ii9. doi: 10.1093/europace/eut170.

57. Jost. N,, Virág, L., Comtois, P., Ördög, B., Szűts, V., Seprényi, G., Bitay, M., Kohajda, Z., Koncz, I., Nagy, N., Szél, T., Magyar, J., Kovács, M., Puskás, L.G., Lengyel, C., Wettwer, E., Ravens, U., Nánási, P.P., Papp, J.G., Varró, A. and Nattel, S. 2013. Ionic mechanisms limiting cardiac repolarization reserve in humans compared to dogs. J. Physiol. 591: 4189- 4206. PMID: 23878377 doi: 10.1113/jphysiol.2013.261198.

58. Lawrence CL, Pollard CE, Hammond TG, Valentin JP. 2005. Nonclinical proarrhythmia models: predicting Torsades de Pointes. J Pharmacol Toxicol Methods. 52(1):46-59. Review. PMID: 15975832, doi: 10.1016/j.vascn.2005.04.011.

59. Lengyel C, Iost N, Virág L, Varró A, Lathrop DA, Papp JG. 2001. Pharmacological block of the slow component of the outward delayed rectifier current (I(Ks)) fails to lengthen rabbit ventricular muscle QT(c) and action potential duration. Br J Pharmacol. 132(1):101-10. PMID: 11156566, doi: 10.1038/sj.bjp.0703777.

60. Lengyel C, Orosz A, Hegyi P, Komka Z, Udvardy A, Bosnyák E, Trájer E, Pavlik G, Tóth M, Wittmann T, Papp JG, Varró A, Baczkó I. 2011. Increased short-term variability of the QT interval in professional soccer players: possible implications for arrhythmia prediction. PLoS One. 6(4):e18751. doi: 10.1371/journal.pone.0018751. PMID: 21526208, doi: 10.1371/journal.pone.0018751.

61. Lengyel C, Varró A, Tábori K, Papp JG, Baczkó I. 2007. Combined pharmacological block of I(Kr) and I(Ks) increases short-term QT interval variability and provokes torsades de pointes. Br J Pharmacol. 151(7):941-51. PMID: 17533421, doi: 10.1038/sj.bjp.0707297.

62. Lu, Z., Kamiya, K., Opthof, T., Yasui, K. and Kodama, I. 2001. Density and kinetics of I(Kr) and I(Ks) in guinea pig and rabbit ventricular myocytes explain different efficacy of I(Ks) blockade at high heart rate in guinea pig and rabbit: implications for arrhythmogenesis in humans. Circulation. 104: 951-956. PMID: 11514385, doi: 10.1161/hc3401.093151.

63. Matsuda H, Saigusa A, Irisawa H. 1987. Ohmic conductance through the inwardly rectifying K channel and blocking by internal Mg2+. Nature. 325(7000):156-9. PMID: 2433601, doi: 10.1038/325156a0.

64. Melnyk P, Zhang L, Shrier A, Nattel S. 2002. Differential distribution of Kir2.1 and Kir2.3 subunits in canine atrium and ventricle. Am J Physiol Heart Circ Physiol. 283(3):H1123-33. PMID: 12181143, doi: 10.1152/ajpheart.00934.2001

65. Mitra R, Morad M. 1986. Two types of calcium channels in guinea pig ventricular myocytes. Proc Natl Acad Sci U S A. 83(14):5340-4. PMID: 2425366, doi: 10.1073/pnas.83.14.5340.

66. Nattel S, Quantz MA. 1988. Pharmacological response of quinidine induced early afterdepolarisations in canine cardiac Purkinje fibres: insights into underlying ionic mechanisms. Cardiovasc Res. 22(11):808-17. PMID: 3256422, doi: 10.1093/cvr/22.11.808

67. Nichols CG, Lopatin AN. 1997. Inward rectifier potassium channels. Annu Rev Physiol. 59:171-91. Review. PMID: 9074760, doi: 10.1146/annurev.physiol.59.1.171

68. Obreztchikova MN, Patberg KW, Plotnikov AN, Ozgen N, Shlapakova IN, Rybin AV, Sosunov EA, Danilo P Jr, Anyukhovsky EP, Robinson RB, Rosen MR 2006. I(Kr) contributes to the altered ventricular repolarization that determines long-term cardiac memory. Cardiovasc Res. 71(1):88-96. PMID: 16626671, doi: 10.1016/j.cardiores.2006.02.028

69. Oros A, Houtman MJ, Neco P, Gomez AM, Rajamani S, Oosterhoff P, Attevelt NJ, Beekman JD, van der Heyden MA, Ver Donck L, Belardinelli L, Richard S, Antoons G, Vos MA; CONTICA investigators. 2010. Robust anti-arrhythmic efficacy of verapamil and flunarizine against dofetilide-induced TdP arrhythmias is based upon a shared and a different mode of action. Br J Pharmacol. 161(1):162-75. PMID: 20718748, doi: 10.1111/j.1476-5381.2010.00883.x.

70. Oros A, Volders PG, Beekman JD, van der Nagel T, Vos MA. 2006. Atrial-specific drug AVE0118 is free of torsades de pointes in anesthetized dogs with chronic complete atrioventricular block. Heart Rhythm. 3(11):1339-45. PMID: 17074641, doi: 10.1016/j.hrthm.2006.07.017.

71. Panama BK, McLerie M, Lopatin AN. 2007. Heterogeneity of IK1 in the mouse heart. Am JPhysiol, Heart Circ Physiol. 293(6):H3558–67. PMID: 17890431 doi: 10.1152/ajpheart.00419.2007.

72. Plotnikov AN, Yu H, Geller JC, Gainullin RZ, Chandra P, Patberg KW, Friezema S, Danilo P Jr, Cohen IS, Feinmark SJ, Rosen MR 2003. Role of L-type calcium channels in pacing-induced short-term and long-term cardiac memory in canine heart. Circulation. 107(22):2844-9. PMID: 12756152, doi: 10.1161/01.CIR.0000068376.88600.41

73. Pueyo E, Husti Z, Hornyik T, Baczkó I, Laguna P, Varró A, Rodríguez B. 2010. Mechanisms of ventricular rate adaptation as a predictor of arrhythmic risk. Am J Physiol Heart Circ Physiol. 298(5):H1577-87. PMID: 20207815, doi: 10.1152/ajpheart.00936.2009

74. Pueyo E, Smetana P, Caminal P, de Luna AB, Malik M, Laguna P. 2004. Characterization of QT interval adaptation to RR interval changes and its use as a risk-stratifier of arrhythmic mortality in amiodarone-treated survivors of acute myocardial infarction. IEEE Trans Biomed Eng. 51(9):1511-20. PMID: 15376499, doi: 10.1109/TBME.2004.828050

75. Roden DM, Viswanathan PC. 2005. Genetics of acquired long QT syndrome. J Clin Invest. 115(8):2025-32. Review. PMID: 16075043, doi:10.1172/JCI25539.

76. Roden DM. 1998. Taking the "idio" out of "idiosyncratic": predicting torsades de pointes. Pacing Clin Electrophysiol. 21(5):1029-34. PMID: 9604234, doi: 10.1111/j.1540-8159.1998.tb00148.x.

77. Rosenbaum MB, Blanco HH, Elizari MV, Lbzzari JO & Davidenko JM 1982. Electrotonic modulation of the T wave and cardiac memory. Am J Cardiol 50, 213–222. PMID: 7102553, doi: 10.1016/0002-9149(82)90169-2

78. Sanguinetti MC, Jurkiewicz NK. 1992. Role of external Ca2+ and K+ in gating of cardiac delayed rectifier K+ currents. Pflugers Arch. 420(2):180-6. PMID: 1620577, doi: 10.1007/BF00374988.

79. Schwartz PJ, Priori SG, Locati EH, Napolitano C, Cantù F, Towbin JA, Keating MT, Hammoude H, Brown AM, Chen LS. 1995. Long QT syndrome patients with mutations of the SCN5A and HERG genes have differential responses to Na+ channel blockade and to increases in heart rate. Implications for gene-specific therapy. Circulation. 92(12):3381-6. PMID: 8521555, doi: 10.1161/01.CIR.92.12.3381

80. Shvilkin A, Danilo P Jr,Wang J, Burkhoff D, Anyukhovsky EP, Sosunov EA, Hara M & Rosen MR 1998. Evolution and resolution of long-term cardiac memory. Circulation 97, 1810–1817. PMID: 9603536, doi: 10.1161/01.CIR.97.18.1810

81. Smetana P, Pueyo E, Hnatkova K, Batchvarov V, Laguna P, Malik M. 2004.Individual patterns of dynamic QT/RR relationship in survivors of acute myocardial infarction and their relationship to antiarrhythmic efficacy of amiodarone. J Cardiovasc Electrophysiol 15: 1147–1154. PMID: 15485438, doi: 10.1046/j.1540-8167.2004.04076.x.

82. Spector PS, Curran ME, Zou A, Keating MT, Sanguinetti MC. 1996. Fast inactivation causes rectification of the IKr channel. J Gen Physiol. 107(5):611-9. PMID: 8740374, doi: 10.1085/jgp.107.5.611.

83. Tattersall ML, Dymond M, Hammond T, Valentin JP 2006. Correction of QT values to allow for increases in heart rate in conscious Beagle dogs in toxicology assessment. J Pharmacol Toxicol Methods 53: 11–19. PMID: 15886026, doi: 10.1016/j.vascn.2005.02.005.

84. Thomsen MB, Beekman JD, Attevelt NJ, Takahara A, Sugiyama A, Chiba K, Vos MA. 2006. No proarrhythmic properties of the antibiotics Moxifloxacin or Azithromycin in anaesthetized dogs with chronic-AV block. Br J Pharmacol. 149(8):1039-48. PMID: 17088870, doi: 10.1038/sj.bjp.0706900.

85. Thomsen MB, Oros A, Schoenmakers M, van Opstal JM, Maas JN, Beekman JD, Vos MA. 2007. Proarrhythmic electrical remodelling is associated with increased beat-to-beat variability of repolarisation. Cardiovasc Res. 73(3):521-30. PMID: 17196569, doi: 10.1016/j.cardiores.2006.11.025

86. Thomsen MB, Verduyn SC, Stengl M, Beekman JD, de Pater G, van Opstal J, Volders PG, Vos MA. 2004. Increased short-term variability of repolarization predicts d-sotalol-induced torsades de pointes in dogs. Circulation. 110(16):2453-9. PMID: 15477402, doi: 10.1161/01.CIR.0000145162.64183.C8.

87. Van de Water A, Verheyen J, Xhonneux R, Reneman RS. 1989. An improved method to correct the QT interval of the electrocardiogram for changes in heart rate. J Pharmacol Methods. 22(3):207-17. PMID: 2586115, doi: 10.1016/0160-5402(89)90015-6.

88. van Opstal JM, Schoenmakers M, Verduyn SC, de Groot SH, Leunissen JD, van Der Hulst FF, Molenschot MM, Wellens HJ, Vos MA. 2001.Chronic amiodarone evokes no torsade de pointes arrhythmias despite QT lengthening in an animal model of acquired long-QT syndrome. Circulation. 104(22):2722-7. PMID: 11723026, doi: 10.1161/hc4701.099579.

89. Varkevisser, R., Wijers, S.C., van der Heyden, M.A., Beekman, J.D., Meine, M. and Vos, M.A. 2012. Beat-to-beat variability of repolarization as a new biomarker for proarrhythmia in vivo. Heart Rhythm 9:1718-1726. PMID: 22609158, doi: 10.1016/j.hrthm.2012.05.016.

90. Varró A, Baczkó I. 2011 Cardiac ventricular repolarization reserve: a principle for understanding drug-related proarrhythmic risk. Br J Pharmacol. 164(1):14-36. Review. PMID: 21545574, doi: 10.1111/j.1476-5381.2011.01367.x.

91. Varró A, Baláti B, Iost N, Takács J, Virág L, Lathrop DA, Csaba L, Tálosi L, Papp JG. 2000. The role of the delayed rectifier component IKs in dog ventricular muscle and Purkinje fibre repolarization. J Physiol. 523 Pt 1:67-81. PMID: 10675203 doi: 10.1111/j.1469-7793.2000.00067.x.

92. Varró A, Lathrop DA, Hester SB, Nánási PP, Papp JG. 1993. Ionic currents and action potentials in rabbit, rat, and guinea pig ventricular myocytes. Basic Res Cardiol. 88(2):93-102. PMID: 8389123 doi: 10.1007/BF00798257.

93. Varró A, Papp JG. 1992. The impact of single cell voltage clamp on the understanding of the cardiac ventricular action potential. Cardioscience. 3(3):131-44. Review. PMID: 1384746.

94. Virág L, Acsai K, Hála O, Zaza A, Bitay M, Bogáts G, Papp JG, Varró A. 2009. Self-augmentation of the lengthening of repolarization is related to the shape of the cardiac action potential: implications for reverse rate dependency. Br J Pharmacol. 156(7):1076-84. PMID: 19226285, doi: 10.1111/j.1476-5381.2009.00116.x.

95. Virág L, Iost N, Opincariu M, Szolnoky J, Szécsi J, Bogáts G, Szenohradszky P, Varró A, Papp JG. 2001. The slow component of the delayed rectifier potassium current in undiseased human ventricular myocytes. Cardiovasc Res. 49(4):790-7. PMID: 11230978, doi: 10.1016/S0008-6363(00)00306-0.

96. Virág, L., Jost, N., Papp, R., Koncz, I., Kristóf, A., Kohajda, Z., Harmati, G., Carbonell- Pascual, B., Ferrero, J.M. Jr, Papp, J.G., Nánási, P.P. and Varró, A. 2011. Analysis of the contribution of Ito to repolarization in canine ventricular myocardium. Br J Pharmacol. 164: 93-105. PMID: 21410683, doi: 10.1111/j.1476-5381.2011.01331.x.

97. Volders PG, Sipido KR, Vos MA, Spätjens RL, Leunissen JD, Carmeliet E, Wellens HJ. 1999. Downregulation of delayed rectifier K(+) currents in dogs with chronic complete atrioventricular block and acquired torsades de pointes. Circulation. 100(24):2455-61. PMID: 10595960, doi:10.1161/01.CIR.100.24.2455.

98. Volders PG, Stengl M, van Opstal JM, Gerlach U, Spätjens RL, Beekman JD, Sipido KR, Vos MA. 2003. Probing the contribution of IKs to canine ventricular repolarization: key role for beta-adrenergic receptor stimulation. Circulation. 107(21):2753-60. PMID: 12756150, doi: 10.1161/01.CIR.0000068344.54010.B3.

99. Vos MA, Verduyn SC, Gorgels AP, Lipcsei GC, Wellens HJ. 1995. Reproducible induction of early afterdepolarizations and torsade de pointes arrhythmias by d-sotalol and pacing in dogs with chronic atrioventricular block. Circulation. 91(3):864-72. PMID: 7828315, doi: 10.1161/01.CIR.91.3.864.

100. Walsh KB, Kass RS. 1991. Distinct voltage-dependent regulation of a heart-delayed IK by protein kinases A and C. Am J Physiol. 261(6 Pt 1):C1081-90. PMID: 1662903.

101. Wang, Z., Yue, L., White, M., Pelletier, G. and Nattel, S. 1998. Differential distribution of inward rectifier potassium channel transcripts in human atrium versus ventricle. Circulation 98: 2422-8. PMID: 9832487 doi: 10.1161/01.CIR.98.22.2422.

102. Wegener FT, Ehrlich JR, 2006. Hohnloser SH. Dronedarone: an emerging agent with rhythm- and rate-controlling effects. J Cardiovasc Electrophysiol 17: S17–S20. PMID: 16939434, doi: 10.1111/j.1540-8167.2006.00583.x

103. Whalley DW, Wendt DJ, Grant AO. 1995. Basic concepts in cellular cardiac electrophysiology: Part I: Ion channels, membrane currents, and the action potential. Pacing Clin Electrophysiol. 18(8):1556-74. Review. PMID: 7479177, doi: 10.1111/j.1540-8159.1995.tb06742.x.

104. Wu R & Patwardhan A 2004. Restitution of action potential duration during sequential changes in diastolic intervals shows multimodal behavior. Circ Res 94, 634–641. PMID: 14752029, doi: 10.1161/01.RES.0000119322.87051.A9.

105. Yang T, Snyders DJ, Roden DM. 1997. Rapid inactivation determines the rectification and [K+]o dependence of the rapid component of the delayed rectifier K+

current in cardiac cells. Circ Res. 80(6):782-9. PMID: 9168780, doi: 10.1161/01.RES.80.6.782.

106. Yazawa K, Kameyama M. 1990. Mechanism of receptor-mediated modulation of the delayed outward potassium current in guinea-pig ventricular myocytes. J Physiol. 421:135-50. PMID: 2161457.

107. Zhang, L., Benson, D.W., Tristani-Firouzi, M., Ptacek, L.J., Tawil, R., Schwartz, P.J., George, A.L., Horie, M., Andelfinger, G., Snow, G.L., Fu, Y.H., Ackerman, M.J. and Vincent, G.M.. 2005. Electrocardiographic features in Andersen-Tawil syndrome patients with KCNJ2 mutations: characteristic T-U-wave patterns predict the KCNJ2 genotype. Circulation 111: 2720–2726. PMID: 15911703, doi: 10.1161/CIRCULATIONAHA.104.472498.

108. Zicha, S., Moss, I., Allen, B., Varró, A., Papp, J.G., Dumaine, R., Antzelevich, C. and Nattel S. 2003. Molecular basis of species-specific expression of repolarizing K+ currents in the heart. Am. J. Physiol. Heart Circ. Physiol. 285: H1641–H1649. PMID: 12816752 doi: 10.1152/ajpheart.00346.2003.

109. Zobel, C., Cho, H.C., Nguyen, T.T., Pekhletski, R., Diaz, R.J., Wilson, G.J. and Backx, P.H. 2003.Molecular dissection of the inward rectifier potassium current (IK1) in rabbit cardiomyocytes: evidence for heteromeric co-assembly of Kir2.1 and Kir2.2. J Physiol. 550: 365-72. PMID: 12794173, doi: 10.1113/jphysiol.2002.036400.

Canadian Journal of Physiology and Pharmacology

Decision Letter (cjpp-2014-0514.R1)

From: cjpp@nrcresearchpress.com

To: husti.zoltan@gmail.com, taborikata@gmail.com, juhasz.viktor@med.u-szeged.hu, hornyik.tibor@med.u-szeged.hu, varro.andras@med.u-szeged.hu, ibaczko@gmail.com

CC: cjpp@nrcresearchpress.com

Subject: Canadian Journal of Physiology and Pharmacology - Decision on Manuscript ID cjpp-2014-0514.R1

Body: 23-Dec-2014

Dear Dr. Husti,

It is a pleasure to accept your manuscript entitled "Combined inhibition of key potassium currents differently affects cardiac repolarization reserve and arrhythmia susceptibility in dogs and rabbits" in its current form for publication in the Canadian Journal of Physiology and Pharmacology. The comments of the reviewer(s) who reviewed your manuscript are included at the foot of this letter.

The Editorial Office will contact the corresponding author about publication.

OpenArticle, an open access option for published research articles, allows individual authors or their funding agencies to sponsor open availability of their articles on the journal Web site for a fee of $3000. For further information, please see http://www.nrcresearchpress.com/page/authors/services/openarticle. If you wish to take advantage of the OpenArticle option, you must submit a completed form (also available on that Web site). You will be billed for the fee upon submission of the completed form.

Thank you for your fine contribution. On behalf of the Editors of the Canadian Journal of Physiology and Pharmacology, we look forward to your continued contributions to the Journal.

Sincerely,

Drs. Grant Pierce & Donald Smyth
Editors in Chief, Canadian Journal of Physiology and Pharmacology

****
Maximize your article's potential!

Download your Author Checklist and take advantage of opportunities to expand the reach of your work, sign up for e-alerts, provide valuable feedback, and more.
http://www.cdnsciencepub.com/learning-centre/publishing-technology/Author-Checklist.aspx

****

Reviewer(s)' Comments to Author:

** If applicable, Reviewer File Attachments may be found in Manuscript Central in your Author Center. Click on "Manuscripts Accepted for First Look". Click on View Decision Letter. Reviewer File Attachments are located at the bottom of the screen.**

Reviewer: 1

General
The authors handled the criticism adequately, the improved manuscript is suitable for publication in Canadian J Physiol Pharmacol.

Reviewer: 2

General
Much improved. Nice work. No further comments

Date Sent: 23-Dec-2014

Close Window

Combined inhibition of key potassium currents differently affects cardiac repolarization reserve and arrhythmia susceptibility in dogs and rabbits

Zoltán Husti[1], Katalin Tábori[1], Viktor Juhász[1], Tibor Hornyik[1], András Varró[1,2], István Baczkó[1]

[1] Department of Pharmacology and Pharmacotherapy, University of Szeged; H-6720, Dóm tér 12, P.O. Box 427, Szeged, Hungary

[2] MTA-SZTE Research Group of Cardiovascular Pharmacology, Hungarian Academy of Sciences, H-6720, Dóm tér 12, P.O. Box 427, Szeged, Hungary

Address for correspondence:

Zoltán Husti, M.D.

Department of Pharmacology and Pharmacotherapy,

Faculty of Medicine, University of Szeged,

H-6720 Szeged, Dóm tér 12, Hungary

Phone: +36.62.545-682; Fax: +36.62.545-680

E-mail: husti.zoltan@gmail.com

Abstract

The reliable assessment of the pro-arrhythmic potential of drugs in development remains elusive. Rabbits and dogs are commonly used in pro-arrhythmia models. Species differences in repolarizing potassium currents are poorly understood. We investigated the incidence of drug-induced Torsades de Pointes, measured conventional ECG parameters and the short-term variability of the QT interval (STV_{QT}) following combined pharmacological inhibition of I_{K1} + I_{Ks} and I_{K1} + I_{Kr} in conscious dogs and anesthetized rabbits. A high TdP incidence was observed following inhibition of I_{K1} + I_{Ks} in dogs (67% vs 14% in rabbits). Rabbits exhibited higher TdP incidence after I_{K1} + I_{Kr} inhibition (72% vs 14% in dogs). Increased TdP incidence was associated with significantly larger STV_{QT} in both models. The different relative roles of I_{K1} and I_{Ks} in dog and rabbit repolarization reserve should be taken into account when extrapolating the results of animal pro-arrhythmia models to humans. A stronger repolarization reserve in dogs (likely due to stronger I_{K1} and I_{Ks}) and a more human-like arrhythmia susceptibility of rabbits argues for the preferred use of rabbit in the evaluation of pro-arrhythmic adverse effects.

Key words

Repolarization, repolarization reserve, electrophysiology, potassium channels, Torsades de Pointes, I_{K1}, I_{Ks}, I_{Kr}

Introduction

The proper assessment of the pro-arrhythmic potential of candidate compounds is a major concern for drug development (Haverkamp et al. 2000), since drug-induced arrhythmias, including Torsades de Pointes (TdP), can lead to sudden cardiac death (Fenichel et al. 2004). The prediction of TdP in clinical setting is very difficult since the incidence of drug-induced TdP is very low (1:100 000), however, drug associated sudden cardiac deaths have led to the withdrawal of several compounds in the past. Therefore, the reliable preclinical assessment of pro-arrhythmic side effects is essential. Importantly, current methods mostly concentrate on testing the hERG blocking and/or ventricular repolarization prolonging effects of these compounds mostly in healthy tissues and animals, and these cardiac safety tests are not sensitive enough (International Conference on Harmonisation, guidance E14 2005; International Conference on Harmonisation, guidance S7B 2005; Thomsen et al. 2006; Farkas and Nattel 2010).

The inhibition of cardiac potassium channels prolongs repolarization and refractoriness, leading to Class III antiarrhythmic effects (Sing and Vaughan-Williams 1970). However, excessive repolarization prolongation by Class III antiarrhythmic drugs, seen as marked QT interval prolongation on the ECG, can result in drug-induced TdP (Hondeghem and Snyders 1990; El-Sherif 1992). On the other hand, experimental and clinical studies suggest that the degree of repolarization prolongation does not show a close correlation with subsequent ventricular arrhythmia development (van Opstal et al. 2001; Thomsen et al. 2004; Lengyel et al. 2007; Hinterseer et al. 2009; Hinterseer et al. 2010). In these cases, without marked prolongation of the QT interval, repolarization reserve may be reduced with a consequent increase in arrhythmia susceptibility. According to the concept of repolarization reserve, normal cardiac repolarization is controlled by different potassium currents in a redundant way, and congenital or acquired (e.g. mild potassium current inhibition by a non-

cardiovascular drug) decrease in the function of a single repolarizing current does not always lead to marked repolarization prolongation, since other currents can compensate for the lost function (Roden 1998; Varró and Baczkó 2011). In the case of reduced repolarization reserve, additional inhibition of another repolarizing current can result in excessive prolongation of repolarization and can provoke serious ventricular arrhythmias.

Experimental evidence from studies on both animal and human ventricular myocardium point to a critically important role for the slow component of the delayed rectifier potassium current (I_{Ks}) in ventricular repolarization reserve (Volders et al. 1999; Varró et al. 2000; Lengyel et al. 2001; Volders et al. 2003; Jost et al. 2005; Abi-Gerges et al. 2006; Lengyel et al. 2007). In addition to I_{Ks}, however, other ventricular repolarizing potassium currents may significantly contribute to repolarization reserve, including I_{to} (Virág et al. 2011) and I_{K1} (Biliczki et al. 2002). There is considerable variation in the expression of key repolarizing potassium channels in different mammalian species (Zicha et al. 2003.). The dog and rabbit are frequently used species in various *in vitro* and *in vivo* pro-arrhythmia models. Therefore, it is reasonable to assume that species specific ion channel expression profiles may result in species dependent alterations in responses to potassium channel blockers (Nerbonne and Kass 2005). Such differences may significantly influence the value of data obtained in these models for human extrapolation. Indeed, a very recent study found similar I_{Kr} densities and significantly lower I_{K1} and I_{Ks} densities in human ventricular myocytes compared to their canine counterparts, suggesting that humans may exhibit a reduced repolarization reserve and might be more susceptible to the pro-arrhythmic adverse effects of I_{Kr} blocking drugs (Jost et al. 2013). It is not clear, however, how species specific potassium channel expressions translate into differences in arrhythmia development in dogs and rabbits. We have shown previously that repolarization reserve impairment by pharmacological block of I_{Ks} increased

arrhythmia susceptibility during subsequent I_{Kr} inhibition in dogs and rabbits in a similar degree (Lengyel et al. 2007).

In the present study, we studied the effects of combined pharmacological inhibition of I_{K1} and I_{Ks}, as well as I_{K1} and I_{Kr} on ECG parameters and the incidence of TdP in conscious dogs and anesthetized rabbits. We also investigated whether TdP development was paralleled by increased short-term variability of the QT interval, a novel ECG parameter suggested for more reliable prediction of drug-induced ventricular arrhythmias.

Materials and methods

Ethical issues

All experiments were carried out in compliance with the Guide for the Care and Use of Laboratory Animals (U.S.A. NIH publication No 85-23, revised 1996) and the protocol had been approved by the Ethical Committee for the Protection of Animals in Research of the University of Szeged, Szeged, Hungary (approval number I-74-5-2012); and by the Department of Animal Health and Food Control of the Ministry of Agriculture (authority approval number XIII/1211/2012).

Conscious dogs

Beagle dogs of either sex weighing 10-15 kg were used for the experiments. The animals were allowed to accomodate to experimental personnel and equipment, every day for a week before the start of the actual studies. After a 20 min equilibration period, baseline recordings were obtained. The animals were then randomly assigned to the following groups: the first group of dogs (n=7) were first administered the I_{K1} inhibitor $BaCl_2$ (3 mg/kg) followed by the I_{Kr} inhibitor dofetilide (25 μg/kg) intravenously after a 20 min equilibration period and in the second group (n=6) the animals received the I_{Ks} inhibitor HMR 1556 (1 mg/kg) first followed by the I_{K1} inhibitor $BaCl_2$ (3 mg/kg) intravenously after a 20 min equilibration period. The drugs were administered during a 5 min continuous i.v. infusion (Terufusion TE-3, Terumo Europe, Leuven, Belgium). The electrocardiogram was obtained using precordial leads and was digitized and stored on a computer for later analysis using National Instruments data acquisition hardware (National Instruments, Austin, TX, USA) and SPEL Advanced Haemosys software (v3.2, Experimetria Ltd., Budapest, Hungary; MDE Heidelberg GMBH, Heidelberg, Germany). The PQ, RR, QT intervals were measured as the average of 30 consecutive beats (the minimum number of beats required for the calculation of

beat-to-beat short-term variability of an interval, see below) and the frequency corrected QT interval (QTc) was calculated using a formula recommended specifically for Beagle dogs: QTc = QT – (0,087 ∗ (RR-1000)) (Tattersall et al. 2006; Van de Water et al. 1989). The intervals were measured at the following time points during the experiments: (i) 2 min before the start of drug infusion (baseline); (ii) 5 min after the end of drug infusions and (iii) the ECG section directly preceding the arrhythmia still in sinus rhythm if TdP (**Figure 1**) or other ventricular arrhythmias occurred.

Anesthetized rabbits

Male New Zealand white rabbits (2-3 kg) were anesthetized with thiopentone (50 mg/kg i.v.) given into the marginal vein of the right ear. A catheter filled with isotonic saline containing 500 IU/mL heparin was inserted into the left carotid artery for the measurement of arterial blood pressure. The right jugular vein was cannulated for subsequent i.v. drug administration. The animals were allowed to stabilize for 20 min and baseline measurements were taken. The first group (n=7) was administered the I_{K1} inhibitor $BaCl_2$ (0.3 mg/kg, in a volume of 2 ml/kg during a 5 min infusion) followed by the I_{Kr} inhibitor dofetilide (25 μg/kg), 20 min after $BaCl_2$ administration. The second group (n=7) received the I_{Ks} inhibitor HMR 1556 (0.1 mg/kg) followed by the I_{K1} inhibitor $BaCl_2$ (0.3 mg/kg) intravenously 20 min after HMR 1556 administration.

The blood pressure and the electrocardiogram (leads I, II and III) were continuously recorded (at 200 Hz), digitized and stored on a computer for analysis using National Instruments data acquisition hardware (National Instruments, Austin, TX, USA) and SPEL Advanced Haemosys software (v3.2, Experimetria Ltd., Budapest, Hungary; MDE Heidelberg GMBH, Heidelberg, Germany). The PQ, RR, QT intervals were measured as the average of 30 beats (the minimum number of beats required for the calculation of short-term variability

of an interval, see below). During the measurement of the QT interval in anaesthetized rabbits, the guidelines described by Farkas et al. (2004) were followed. In rabbits with a significantly faster heart rate than that of humans, QTc calculated with Bazett's formula does not accurately reflect the heart rate dependent changes in QT interval. Accordingly, QTc was calculated by a formula specifically suggested for anaesthetized rabbits by Batey and Coker (2002) as follows: $QTc = QT - (0.704 * (RR-250))$.

Short-term beat-to-beat variability of the RR (STV_{RR}) and QT intervals (STV_{QT})

Temporal instability of beat-to-beat heart rate and repolarization can be quantitatively characterized by the calculation of the beat-to-beat short-term variability (STV) of RR or QT intervals, respectively. The calculation of STV is based on previous detailed mathematical analysis (Brennan et al. 2001), and was calculated as follows: $STV = \sum|D_{n+1}-D_n| \ (30x\sqrt{2})^{-1}$, where D is the duration of the QT or RR interval. The intervals used in the calculation were the result of 30 consecutive interval measurements in sinus rhythm at a given time point during the experiments. In the case of experiments where TdP occurred, the measurements were taken in sinus rhythm prior to the development of TdP. To illustrate temporal instability of the QT interval, Poincaré plots of the QT intervals were constructed where each QT value was plotted against its former value (**Figures 3 and 5, panel B**). The STV represents the mean orthogonal distance to the line-of-identity on the Poincaré plot.

Compounds

HMR 1556 (Aventis Pharma, Frankfurt am Main, Germany) was dissolved in dimethylsulfoxide (DMSO, 0.1%) as a stock solution of 10 μM. Dofetilide (Gedeon Richter Ltd., Budapest, Hungary) was dissolved in saline as a stock solution of 5 μM. $BaCl_2$ was

dissolved in distilled water as a stock solution of 100 mM. Each stock solution was diluted immediately before use.

Statistical analysis

The incidence of TdP (%) was compared by using the χ^2 test with Yates' correction. All other data are expressed as means $\pm$ SD. Data within groups were compared after analysis of variance (repeated measures one-way ANOVA) by Bonferroni's post test and the groups were compared in pairs by means of Student's "*t*" test. A level of $p<0.05$ was considered to be statistically significant.

Results

Effect of combined I_{K1} and I_{Kr} inhibition on RR and QTc intervals in conscious dogs and anesthetized rabbits

Both in dogs and rabbits, the administration of the I_{K1} inhibitor $BaCl_2$ alone did not change heart rate and the RR intervals (**Figure 2A**). However, infusion of the I_{Kr} inhibitor dofetilide significantly increased RR intervals (**Figure 2A**) and decreased heart rate (dogs: 66.9±16.96 vs. 80.5±12.12 beats/min in control; rabbits: 213.9±1.92 vs. 258.6±1.26 beats/min in control, $p<0.05$) in both species. In our previous study, the I_{Kr} inhibitor dofetilide administered alone did not alter the RR interval but as expected, significantly prolonged the QTc interval in conscious dogs and anesthetized rabbits (Lengyel et al. 2007).

In conscious dogs, I_{K1} inhibition significantly prolonged the frequency corrected QT interval, calculated with the Van de Water formula (Van de Water et al., 1989), and dofetilide infusion caused a further, significant prolongation of the QTc interval (**Figure 3A left panel**). The uncorrected QT intervals yielded similar prolongation: 317.4±47.9 ms after I_{K1} block and 373.5±37.8 ms after combined I_{K1}+I_{Kr} inhibition vs. 221.4±11.7 ms in controls, ($p<0.05$). In anesthetized rabbits, only the combination of I_{K1} and I_{Kr} inhibition resulted in significant QTc interval prolongation (**Figure 3A right panel**). Again, the uncorrected QT intervals showed a similar prolongation only after combined I_{K1}+I_{Kr} inhibition (150.6±5.88 ms after I_{K1} inhibition and 167.8±6.27 ms after $BaCl_2$ and dofetilide combination vs. 147.2±5.46 ms in control).

Effect of combined I_{K1} and I_{Kr} inhibition on the short-term variability of RR (STV_{RR}) and QT intervals (STV_{QT}) in conscious dogs and anesthetized rabbits

Since heart rate affects repolarization duration, the short-term variability of the RR intervals were also calculated in addition to STV_{QT}, the ECG parameter recently suggested for more reliable prediction of ventricular arrhythmias. In conscious dogs, STV_{RR} did not change

significantly following I_{K1} and combined I_{K1}+I_{Kr} inhibition (**Figure 2B left panel**). In anesthetized rabbits, the combination of $BaCl_2$ and dofetilide slightly, but significantly increased STV_{RR}, however, the magnitude of these changes (less than 0.5 ms) makes it very unlikely that this STV_{RR} change markedly influenced repolarization variability (**Figure 2B right panel**). The I_{Kr} inhibitor dofetilide administered alone did not alter STV_{RR} in conscious dogs and anesthetized rabbits in our previous study (Lengyel et al. 2007).

The Poincaré plots on **Figure 3B** illustrate repolarization temporal instability in two individual animals, a conscious dog (left panel) and an anesthetized rabbit (right panel) following I_{K1} and combined I_{K1}+I_{Kr} inhibition. Both animals exhibited TdP arrhythmia as a result of $BaCl_2$ and dofetilide combination, and the scatter of data points covering a large area on the plot following this combination represents large STV_{QT} values in these animals (15.8 ms in the dog and 4.9 ms in the rabbit). Grouped STV_{QT} data showed a significant increase in both species following combined I_{K1}+I_{Kr} inhibition (**Figure 3C**). Dofetilide alone did not increase STV_{QT} in conscious dogs, however, it significantly increased STV_{QT} in anesthetized rabbits in our previous study (Lengyel et al. 2007).

Effect of combined I_{Ks} and I_{K1} block on RR and QTc intervals in conscious dogs and anesthetized rabbits

The I_{Ks} inhibitor HMR 1556 did not change the RR interval significantly in conscious dogs or anesthetized rabbits, and this result was in good agreement with our previous observations (Lengyel et al., 2007). The combined inhibition of I_{Ks}+I_{K1}, however, caused a significant increase in RR intervals and decrease in heart rate in rabbits only (**Figure 4A right panel**).

In conscious dogs, I_{Ks} inhibition significantly increased the frequency corrected QT interval, similarly to our previous observations in conscious dogs (Lengyel et al., 2007). In

these animals, subsequent infusion of $BaCl_2$ caused a further, significant QTc prolongation (**Figure 5A left panel**). The uncorrected QT intervals showed similar prolongation: 317.5±35.2 ms after I_{Ks} block and 387.4±45.4 ms after combined I_{Ks}+I_{K1} inhibition vs. 230.5±7.6 ms in controls, ($p<0.05$). In anesthetized rabbits, I_{Ks} inhibition did not alter QTc, and combined I_{Ks}+I_{K1} inhibition only had a slight tendency to increase QTc but this change did not prove to be statistically significant (**Figure 5A right panel**).

Effect of combined I_{Ks} and I_{K1} inhibition on the short-term variability of RR (STV_{RR}) and QT (STV_{QT}) intervals in conscious dogs and anesthetized rabbits

HMR 1556 did not alter STV_{RR} in conscious dogs or anesthetized rabbits. The combined inhibition of I_{Ks}+I_{K1} caused a significant, but again, very small (less than 1 ms) increase in STV_{RR} in anesthetized rabbits (**Figure 4B right panel**).

The Poincaré plots on **Figure 5B** illustrate repolarization temporal instability in two individual animals, a conscious dog (left panel) and an anesthetized rabbit (right panel) following I_{Ks} and combined I_{Ks}+I_{K1} inhibition. The shift of QT interval data points to the right and upward direction in the conscious dog represent the above described QT prolongation following HMR 1556 administration. Careful observation of the plot reveals that in this animal, that later developed TdP after combined I_{Ks}+I_{K1} inhibition, the QT variability only increased after HMR 1556 and $BaCl_2$ combination (**Figure 5B left panel**). In accordance with grouped STV_{QT} data represented on **Figure 5C** (**right panel**), in the representative rabbit on **Figure 5B** STV_{QT} did not increase significantly after HMR 1556 or HMR 1556+$BaCl_2$ combination in anesthetized rabbits. In contrast, in conscious dogs this combination led to a significant increase in STV_{QT} (Figure 2E left panel). Importantly, in parallel to this STV_{QT} increase, conscious dogs responded to combined I_{Ks}+I_{K1} inhibition with significantly

increased TdP incidence, while only one of 7 rabbits developed TdP following this combination, and the rabbit grouped data did not show elevated STV_{QT} (**Figure 5C**).

Effect of combinations of I_{K1} and I_{Kr} inhibition, and I_{Ks} and I_{K1} inhibition on the incidence of TdP in conscious dogs and anesthetized rabbits

As shown on **Figure 6A and 6B**, inhibition of I_{K1} or I_{Ks} alone did not provoke TdP in any of the animals. We have shown previously that the I_{Kr} inhibitor dofetilide alone did not cause TdP in conscious dogs and caused TdP in 25% of anesthetized rabbits (Lengyel et al., 2007). Combined inhibition of repolarizing currents, however, led to a significant amount of TdP episodes in both species, albeit in a different manner.

Interestingly, conscious dogs and anesthetized rabbits exhibited different TdP incidence following the combined inhibition of key potassium currents: a significant amount of conscious dogs developed TdP following I_{Ks}+I_{K1} inhibition, while only one rabbit developed TdP after this combination. On the other hand, TdP incidence increased significantly following I_{K1}+I_{Kr} inhibition in rabbits, while only one dog exhibited TdP following $BaCl_2$+dofetilide administration (**Figures 6A and 6B**).

Discussion

Dogs and rabbits are frequently used species for pro-arrhythmia studies, and we previously established a pro-arrhythmia model based on repolarization reserve impairment achieved by pharmacological inhibition of I_{Ks}, a key potassium current in repolarization reserve (Lengyel et al., 2007). Recently, other potassium channels were also implicated in repolarization reserve, including I_{K1} (for a recent review see Varró and Baczkó, 2011). Species differences exist in the expression of important ion channels carrying repolarizing current (Zicha et al. 2003), most likely leading to species-specific differences in repolarization

reserve and in responses to compounds with even mild potassium channel inhibitory properties (Nerbonne and Kass 2005). Therefore, further characterization of the roles different potassium currents play in canine and rabbit pro-arrhythmia models are needed to assist in the proper extrapolation of data obtained in these models to human subjects.

In the present study we investigated the effects of repolarization reserve impairment by pharmacological inhibition of I_{K1} in combination with I_{Ks} and I_{Kr} on the incidence of the typical drug-induced arrhythmia, TdP, and different ECG parameters, in a similar experimental setup to our previous study where the effects of the combined pharmacological inhibition of I_{Ks} and I_{Kr} were characterized in conscious dogs and anesthetized rabbits (Lengyel et al., 2007). Here we show that combined pharmacological inhibition of other potassium currents leads to repolarization reserve impairment and high incidence of TdP in conscious dogs and anesthetized rabbits. However, dogs and rabbits exhibited markedly different patterns of TdP development in response to combined I_{K1}+I_{Kr} and I_{Ks}+I_{K1} inhibition suggesting that at least some of these currents may play different relative roles in repolarization reserve in the two species. In contrast, we previously showed that both species responded with a high incidence of TdP paralleled by significant increases of short-term variability of the QT interval, irrespective of the sequence of I_{Ks} and I_{Kr} inhibitor administration (Lengyel et al., 2007).

The key role of I_{Ks} in ventricular repolarization reserve is well established in different animal species as well as in humans (Volders et al. 1999; Varró et al. 2000; Lengyel et al. 2001; Volders et al. 2003; Jost et al. 2005; Abi-Gerges et al. 2006; Lengyel et al. 2007; Jost et al., 2007; Johnson et al., 2010). However, a recent study highlighted that due to lower I_{Ks} densities in human hearts, repolarization reserve may be reduced in humans compared to dogs (Jost et al., 2013). Attributed to low-level I_{Ks} beta-subunit minK expression, a small I_{Ks} and increased TdP susceptibility were described in rabbits (Lu et al., 2001; Zicha et al., 2003). In a

recent comparative study, the kinetics of rabbit I_{Ks} have been found more human-like compared to I_{Ks} in guinea-pigs and dogs (Jost et al., 2013b). These data indicate that despite the relatively well characterized role of I_{Ks} in repolarization reserve, the significant differences described in I_{Ks} subunit expression, current densities and kinetics in rabbits and dogs make human extrapolation of results somewhat difficult.

The roles other repolarizing potassium currents may play in repolarization reserve are poorly understood. Among these repolarizing potassium currents, possible roles for I_{to} (Virag et al., 2011) and I_{K1} (Biliczki et al., 2002; Varró and Baczkó, 2011) in repolarization reserve have been suggested. In LQT7 (Andersen-Tawil syndrome), loss of function mutations in Kir2.1 channels may significantly decrease I_{K1} current, however, the substantially increased pro-arrhythmic risk in these patients is not accompanied by marked QTc prolongation on the ECG (Zhang et al., 2005). Computer modelling studies also support a key role for I_{K1} in ventricles: in these models, reduction of I_{K1} in addition to I_{Kr} block led to early afterdepolarizations (Ishihara et al., 2009). A variety of channel subtypes can be responsible for the I_{K1} current, including alpha-subunits Kir2.1, Kir2.2, Kir2.3, Kir2.4 (for a recent review see Anumonwo and Lopatin, 2010). Significant species-specific differences in the expression of Kir2.x proteins have been reported previously (Wang et al., 1998; Melnyk et al., 2002; Dhamoon and Jalife, 2005). Different heteromeric assembly of Kir2.x proteins leads to different I_{K1} characteristics (Dhamoon et al., 2004) and most likely, to altered overall cardiac electrophysiological responses to drugs. In rabbit cardiomyocytes, a heteromeric assembly of Kir2.1 and Kir2.2 was reported (Zobel et al., 2003). In dogs, Kir2.2 and Kir2.4 levels were minimal, while in humans, Kir2.3 mRNA expression was on a similar level to Kir2.1 and Kir2.1 mRNA expression was three times higher in dogs compared to human (Jost et al., 2013).

Based on these studies and also supported by the present study, due to stronger I_{K1} and I_{Ks} in dogs compared to rabbits and humans, dogs may exhibit larger repolarization reserve compared to the other two species. Therefore, rabbit pro-arrhythmia models based on pharmacologically impaired repolarization reserve may represent greater arrhythmia susceptibility and may be more useful than canine models in predicting human electrophysiological responses to drugs affecting cardiac ventricular repolarization.

In this study, the short-term variability of the QT interval was calculated in order to assess temporal instability of repolarization following pharmacological inhibition of repolarizing potassium currents. The STV_{QT} characterizes differences in the QT intervals of consecutive heart beats and has been suggested as a more reliable measure of pro-arrhythmic risk associated with impaired repolarization reserve compared to conventional ECG parameters of repolarization (Berger at al 2003; Varkevisser et al 2012). In this regard, a number of previous *in vivo* and *in vitro* animal experimental and clinical studies (van Opstal et al., 2001; Thomsen et al., 2004; Lengyel et al 2007; Hinterseer et al., 2009; Hinterseer et al., 2010) found that STV_{QT} was increased and showed a better correlation with subsequent arrhythmias than QT prolongation in animals or individuals with decreased repolarization reserve later exhibiting serious ventricular arrhythmias. We found in this study that combined inhibition of I_{K1}+I_{Kr} and I_{Ks}+I_{K1} led to increased STV_{QT} in parallel with increased incidence of TdP in most cases, further supporting the role of STV_{QT} determination in ventricular arrhythmia risk estimation. It should be noted that in dogs, following I_{K1}+I_{Kr} inhibition a significant increase in STV_{QT} was found with only one animal showing TdP, however, very short episodes of nonsustained monomorphic ventricular tachycardia were observed in three additional animals.

In conclusion, both rabbits and dogs are susceptible to pharmacological impairment of repolarization reserve and concomitant ventricular arrhythmia induction by compounds that

inhibit repolarizing currents. This study has further confirmed that STV_{QT} may be a better predictor of subsequent drug-induced TdP development than conventional ECG parameters characterizing repolarization prolongation. Importantly, however, rabbits are more susceptible to combined inhibition of I_{K1}+I_{Kr} than dogs, and dogs are more susceptible to combined inhibition of I_{K1}+I_{Ks} than rabbits, suggesting different relative roles of I_{K1} and I_{Ks} in repolarization reserve in these species. These results warrant cautious evaluation of the potential proarrhythmic adverse effects and cardiovascular safety of candidate compounds in rabbit and dog models. The different relative roles of repolarizing potassium currents in these species need to be considered when extrapolating rabbit and canine proarrhythmia study results to humans.

Acknowledgements

This study was supported by grants from the Hungarian National Research Foundation (OTKA K 109610, OTKA NN 110896, OTKA NK 104331), by the Hungarian Academy of Sciences and by the National Development Agency, the European Union and co-funded by the European Social Fund (TÁMOP-4.2.2A-11/1/KONV-2012-0073). This research was also supported in the framework of TÁMOP 4.2.4. A/2-11-1-2012-0001 „National Excellence Program - Elaborating and operating an inland student and researcher personal support system" key project. The project was subsidized by the European Union and co-financed by the European Social Fund to Dr Baczkó.

Figure legends

Figure 1. Representative Torsades de Pointes (TdP) recording from (**A**) conscious dog following combined inhibition of I_{Ks} + I_{K1} and from (**B**) an anesthetized rabbit following the combined inhibition of I_{K1}+I_{Kr}.

Figure 2. Effect of I_{K1} inhibition (i.v. $BaCl_2$) and combined I_{K1}+I_{Kr} (i.v. $BaCl_2$+dofetilide) inhibition on (**A**) RR interval and (**B**) short-term variability of the RR interval (STV_{RR}) in conscious dogs and anesthetized rabbits. N=7 dogs and 7 rabbits/group; *p<0.05 vs. control values; #p<0.05 vs. I_{K1} inhibition.

Figure 3. Effect of I_{K1} inhibition (i.v. $BaCl_2$) and combined I_{K1}+I_{Kr} (i.v. $BaCl_2$+dofetilide) inhibition on (**A**) frequency corrected QT interval (QTc); (**B and C**) short-term variability of the QT interval (STV_{QT}) in conscious dogs and anesthetized rabbits. For details on Poincaré plot (**B**) description see text. N=7 dogs and 7 rabbits/group; *p<0.05 vs. control values; #p<0.05 vs. I_{K1} inhibition.

Figure 4. Effect of I_{Ks} inhibition (i.v. HMR 1556) and combined I_{Ks}+I_{K1} (i.v. HMR 1556+$BaCl_2$) inhibition on (**A**) RR interval and (**B**) short-term variability of the RR interval (STV_{RR}) in conscious dogs and anesthetized rabbits. N=6 dogs and 7 rabbits/group; *p<0.05 vs. control values; #p<0.05 vs. I_{Ks} inhibition.

Figure 5. Effect of I_{Ks} inhibition (i.v. HMR 1556) and combined I_{Ks}+I_{K1} (i.v. HMR 1556+$BaCl_2$) inhibition on (**A**) frequency corrected QT interval (QTc); (**B and C**) short-term variability of the QT interval (STV_{QT}) in conscious dogs and anesthetized rabbits. For details

on Poincaré plot (**B**) description see text. N=6 dogs and 7 rabbits/group; *p<0.05 vs. control values; #p<0.05 vs. I_{Ks} inhibition.

Figure 6. Effect of (**A**) I_{K1} inhibition (i.v. $BaCl_2$) and combined I_{K1}+I_{Kr} (i.v. $BaCl_2$+dofetilide) inhibition and (**B**) I_{Ks} inhibition (i.v. HMR 1556) and combined I_{Ks}+I_{K1} (i.v. HMR 1556+$BaCl_2$) inhibition on incidence of Torsades de Pointes (TdP) chaotic ventricular arrhythmia in conscious dogs (left panels) and anesthetized rabbits (right panels). N=7 and 6 dogs, and 7 rabbits/group; *p<0.05 vs. control values.

References

Abi-Gerges, N., Small, B.G., Lawrence, C.L., Hammond, T.G., Valentin, J.P. and Pollard, C.E. 2006. Gender differences in the slow delayed (I_{Ks}) but not in inward (I_{K1}) rectifier K^+ currents of canine Purkinje fibre cardiac action potential: key roles for I_{Ks} , β-adrenoceptor stimulation, pacing rate and gender. Br. J. Pharmacol. **147**: 653–660. doi: 10.1038/sj.bjp.0706491 PMID: 16314855.

Anumonwo, J.M. and Lopatin, A.N. 2010. Cardiac strong inward rectifier potassium channels. J Mol Cell Cardiol **48**: 45–54. doi: 10.1016/j.yjmcc.2009.08.013, PMID: 19703462.

Berger, R.D. 2003. QT variability. J Electrocardiol. **36** Suppl: 83-87. doi: 10.1016/j.jelectrocard.2003.09.019, PMID: 14716597.

Biliczki, P., Virág, L., Iost, N., Papp, J.Gy. and Varró, A. 2002. Interaction of different potassium channels in cardiac repolarization in dog ventricular preparations: role of the repolarization reserve. Br. J. Pharmacol. **137**: 361–368. doi: 10.1038/sj.bjp.0704881, PMID: 12237256.

Brennan, M., Palaniswami, M. and Kamen, P. 2001. Do existing measures of Poincare´ plot geometry reflect nonlinear features of heart rate variability? IEEE Trans. Biomed. Eng. **48**: 1342–1347. doi: 10.1109/10.959330, PMID: 11686633

Dhamoon, A.S., Pandit, S.V., Sarmast, F., Parisian, K.R., Guha, P., Li, Y., Bagwe, S., Taffet, S.M. and Anumonwo, J.M. 2004. Unique Kir2.x properties determine regional and species differences in the cardiac inward rectifier K+ current. Circ. Res. **94**:1332-1339. doi: 10.1161/01.RES.0000128408.66946.67, PMID: 15087421

Dhamoon, A.S. and Jalife, J. 2005. The inward rectifier current (IK1) controls cardiac excitability and is involved in arrhythmogenesis. Heart Rhythm. **2**:316-324. doi: 10.1016/j.hrthm.2004.11.012, PMID: 15851327

El-Sherif, N. 1992. The proarrhythmic mechanism of drugs that prolong repolarisation. Role of early afterdepolarisation. New Trends in Arrhythmias **8**: 617–626.

Farkas, A., Batey, A.J. and Coker, S.J. 2004. How to measure electrocardiographic QT interval in the anaesthetized rabbit. J. Pharmacol. Toxicol. Methods **50**: 175–185. doi: 10.1016/j.vascn.2004.05.002, PMID: 15519904

Farkas, A.S. and Nattel, S. 2010. Minimizing repolarization-related proarrhythmic risk in drug development and clinical practice. Drugs **70**: 573–603. doi: 10.2165/11535230-000000000-00000, PMID: 20329805

Fenichel, R.R., Malik, M., Antzelevitch, C., Sanguinetti, M., Roden, D.M., Priori, S.G., Ruskin, J.N., Lipicky, R.J. and Cantilena, L.R. Independent Academic Task Force. 2004. Independent Academic Task Force. Drug-induced torsades de pointes and implications for drug development. J. Cardiovasc. Electrophysiol. **15**: 475–495. doi: 10.1046/j.1540-8167.2004.03534.x, PMID: 15090000

Haverkamp, W., Breithardt, G., Camm, A.J, Janse, M.J., Rosen, M.R., Antzelevitch, C., Escande, D., Franz, M., Malik, M., Moss, A. and Shah R. 2000. The potential for QT prolongation and pro-arrhythmia by non-anti-arrhythmic drugs: clinical and regulatory implications. Report on a Policy Conference of the European Society of Cardiology. Cardiovasc Res **47**: 219–233. doi: http://dx.doi.org/10.1016/S0008-6363(00)00119-X, PMID: 10947683

Hinterseer, M., Beckmann, B.M., Thomsen, M.B., Pfeufer, A., Dalla Pozza, R., Loeff, M., Netz, H., Steinbeck, G., Vos, M.A. and Kääb, S. 2009. Relation of increased short-term variability of QT interval to congenital long-QT syndrome. Am. J. Cardiol. **103**: 1244–1248. doi: 10.1016/j.amjcard.2009.01.011, PMID: 19406266

Hinterseer, M., Beckmann, B.M., Thomsen, M.B., Pfeufer, A., Ulbrich, M., Sinner, M.F., Perz, S., Wichmann, H.E., Lengyel, C., Schimpf, R., Maier, S.K., Varró, A., Vos, M.A., Steinbeck, G. and Kääb, S. 2010. Usefulness of short-term variability of QT intervals as a predictor for electrical remodeling and proarrhythmia in patients with nonischemic heart failure. Am. J. Cardiol. **106**: 216–220. doi: 10.1016/j.amjcard.2010.02.033, PMID: 20599006

Hondeghem, L.M. and Snyders, D.J. 1990. Class III antiarrhythmic agents have a lot of potential but a long way to go. Reduced effectiveness and dangers of reverse use dependence. Circulation **81**: 686–690. doi: 10.1161/01.CIR.81.2.686, PMID: 2153477

International Conference on Harmonisation; guidance on E14 Clinical Evaluation of QT/QTc Interval Prolongation and Proarrhythmic Potential for Non-Antiarrhythmic Drugs. availability. 2005. Notice. Fed Regist **70**: 61134–61135. PMID: 16237860

International Conference on Harmonisation; guidance on S7B Nonclinical Evaluation of the Potential for Delayed Ventricular Repolarization (QT Interval Prolongation) by Human Pharmaceuticals; availability. Notice. Fed Reg 2005; **70**:61133–61134. PMID: 16237859

Ishihara. K,, Sarai. N,, Asakura, K., Noma, A. and Matsuoka, S. 2009. Role of Mg^{2+} block of the inward rectifier K^+ current in cardiac repolarization reserve: A quantitative simulation. J. Mol. Cell. Cardiol. **47**: 76–84. doi: 10.1016/j.yjmcc.2009.03.008, PMID: 19303883

Johnson, D.M., Heijman, J., Pollard, C.E., Valentin, J.P., Crijns, H.J., Abi-Gerges, N. and Volders, P.G. 2010 I(Ks) restricts excessive beat-to-beat variability of repolarization during beta-adrenergic receptor stimulation. J. Mol. Cell. Cardiol. **48**: 122-130. doi: 10.1016/j.yjmcc.2009.08.033, PMID: 19744496

Jost, N., Papp, J,G. and Varró, A. (2007) Slow delayed rectifier potassium current (I_{Ks}) and the repolarization reserve. Ann Noninvasive Electrocardiol 12: 64–78. doi: 10.1111/j.1542-474X.2007.00140.x, PMID: 17286653

Jost, N., Virág, L., Bitay, M., Takács, J., Lengyel, C., Biliczki, P., Nagy, Z., Bogáts, G., Lathrop, D.A., Papp, J.G. and Varró, A. 2005. Restricting excessive cardiac action potential and QT prolongation: a vital role for I_{Ks} in human ventricular muscle. Circulation **112**: 1392-1399. doi: 10.1161/CIRCULATIONAHA.105.550111, PMID: 16129791

Jost. N,, Virág, L., Comtois, P., Ördög, B., Szűts, V., Seprényi, G., Bitay, M., Kohajda, Z., Koncz, I., Nagy, N., Szél, T., Magyar, J., Kovács, M., Puskás, L.G., Lengyel, C., Wettwer, E.,

Ravens, U., Nánási, P.P., Papp, J.G., Varró, A. and Nattel, S. 2013. Ionic mechanisms limiting cardiac repolarization reserve in humans compared to dogs. J. Physiol. **591**: 4189-4206. doi: 10.1113/jphysiol.2013.261198, PMID: 23878377

Jost, N., Kohajda, Zs., Corici, C., Horvath, A., Bitay, M., Bogats, G., Papp, J.G., Varró, A. and Virag, L. 2013. The comparative study of rapid and slow delayed rectifier currents in undiseased human, dog, rabbit and guinea pig ventricular myocytes. Europace, **15** Suppl 2: ii1-ii9. doi: 10.1093/europace/eut170.

Lengyel, C., Iost, N., Virág, L., Varró, A., Lathrop, A.D. and Papp, J.G. 2001. Pharmacological block of the slow component of the outward delayed rectifier current (I_{Ks}) fails to lengthen rabbit ventricular muscle QT c and action potential duration. Br. J. Pharmacol. **132**: 101-110. doi: 10.1038/sj.bjp.0703777, PMID: 11156566

Lengyel, C,, Varró, A., Tábori, K., Papp, J.G. and Baczkó, I. 2007. Combined pharmacological block of I_{Kr} and I_{Ks} increases short-term QT interval variability and provokes torsades de pointes. Br. J. Pharmacol. **151**: 941–951. doi: 10.1038/sj.bjp.0707297, PMID: 17533421.

Lu, Z., Kamiya, K., Opthof, T., Yasui, K. and Kodama, I. 2001. Density and kinetics of I(Kr) and I(Ks) in guinea pig and rabbit ventricular myocytes explain different efficacy of I(Ks) blockade at high heart rate in guinea pig and rabbit: implications for arrhythmogenesis in humans. Circulation **104**: 951-956. doi: 10.1161/hc3401.093151, PMID: 11514385

Melnyk, P., Zhang, L., Shrier, A. and Nattel, S. 2002. Differential distribution of Kir2.1 and Kir2.3 subunits in canine atrium and ventricle. Am J Physiol Heart Circ Physiol. **283**: H1123-1133. doi: 10.1152/ajpheart.00934.2001, PMID: 12181143

Nerbonne, M. and Kass, R.S. 2005. Molecular physiology of cardiac repolarization. Physiol. Rev. **85**: 1205–1253. doi: 10.1152/physrev.00002.2005, PMID: 16183911

Roden, D.M. 1998. Taking the idio out of idiosyncratic – predicting torsades de pointes. Pacing Clin. Electrophysiol. **21**: 1029–1034. doi: 10.1111/j.1540-8159.1998.tb00148.x, PMID: 9604234,

Singh, B.N. and Vaughan Williams, E.M. 1970. A third class of anti-arrhythmic action. Effects on atrial and ventricular intracellular potentials, and other pharmacological actions on cardiac muscle, of MJ 1999 and AH 3474. Br J Pharmacol. **39**: 675-687. PMID: 5485144.

Tattersall, M.L., Dymond, M., Hammond, T. and Valentin, J.P. 2006. Correction of QT values to allow for increases in heart rate in conscious Beagle dogs in toxicology assessment. J Pharmacol Toxicol Methods **53**: 11–19. doi: 10.1016/j.vascn.2005.02.005, PMID: 15886026

Thomsen, M.B., Matz, J., Volders, P.G. and Vos, M.A. 2006. Assessing the proarrhythmic potential of drugs: current status of models and surrogate parameters of torsades de pointes arrhythmias. Pharmacol. Therapeut. **112**: 150–170. doi: 10.1016/j.pharmthera.2005.04.009, PMID: 16714061

Thomsen, M.B., Verduyn, S.C., Stengl, M., Beekman, J.D., de Pater, G, van Opstal, J. Volders,P.G,,. and Vos M.A. 2004. Increased short-term variability of repolarization predicts

d-sotalol-induced torsades de pointes in dogs. Circulation **110**: 2453–2459. doi: 10.1161/01.CIR.0000145162.64183.C8, PMID: 15477402

Van de Water, A., Verheyen, J., Xhonneux, R. and Reneman, R.S. 1989. An improved method to correct the QT interval of the electrocardiogram for changes in heart rate. J. Pharmacol. Methods **22**: 207–217. doi: 10.1016/0160-5402(89)90015-6, PMID: 2586115

van Opstal, J.M., Schoenmakers, M., Verduyn, S.C., de Groot, S.H., Leunissen, J.D., van Der Hulst, F.F. Molenschot, M.M., Wellens, H.J. and Vos, M.A. 2001. Chronic amiodarone evokes no torsade de pointes arrhythmias despite QT lengthening in an animal model of acquired long-QT syndrome. Circulation **104**: 2722–2727. doi: 10.1161/hc4701.099579, PMID: 11723026

Varkevisser, R., Wijers, S.C., van der Heyden, M.A., Beekman, J.D., Meine, M. and Vos, M.A. 2012. Beat-to-beat variability of repolarization as a new biomarker for proarrhythmia in vivo. Heart Rhythm **9**:1718-1726. doi: 10.1016/j.hrthm.2012.05.016. PMID: 22609158

Varró, A., Baláti, B., Iost, N., Takács, J., Virág, L., Lathrop, D.A., Lengyel, C., Tálosi, L, and Papp J,G. 2000. The role of the delayed rectifier component I_{Ks} in dog ventricular muscle and Purkinje fibre repolarization. J Physiol **523**: 67–81. doi: 10.1111/j.1469-7793.2000.00067.x, PMID: 10675203

Varró, A. and Baczkó, I. 2011. Cardiac ventricular repolarization reserve: a principle for understanding drug-related proarrhythmic risk. Br J Pharmacol. 1**64**: 14-36. doi: 10.1111/j.1476-5381.2011.01367.x., PMID: 21545574

Virág, L., Jost, N., Papp, R., Koncz, I., Kristóf, A., Kohajda, Z., Harmati, G., Carbonell-Pascual, B., Ferrero, J.M. Jr, Papp, J.G., Nánási, P.P. and Varró, A. 2011. Analysis of the contribution of I_{to} to repolarization in canine ventricular myocardium. Br J Pharmacol. **164**: 93-105. doi: 10.1111/j.1476-5381.2011.01331.x., PMID: 21410683

Volders, P.G., Sipido, K.R., Vos, M.A., Spatjens, R.L., Leunissen, J.D., Carmeliet, E. and Wellens, H.J. 1999. Downregulation of delayed rectifier K^+ currents in dogs with chronic complete atrioventricular block and acquired torsades de pointes. Circulation **100**: 2455–2461. doi: 10.1161/01.CIR.100.24.2455, PMID: 10595960

Volders, P.G., Stengl, M., van Opstal, J.M., Gerlach, U., Spatjens, R.L., Beekman, J.D., Sipido, K.R. and Vos, M.A. 2003. Probing the contribution of I_{Ks} to canine ventricular repolarization: key role for β-adrenergic receptor stimulation. Circulation **107**: 2753–2760. doi: 10.1161/01.CIR.0000068344.54010.B3, PMID: 12756150

Wang, Z., Yue, L., White, M., Pelletier, G. and Nattel, S. 1998. Differential distribution of inward rectifier potassium channel transcripts in human atrium versus ventricle. Circulation **98**: 2422-8. doi: 10.1161/01.CIR.98.22.2422, PMID: 9832487

Zhang, L., Benson, D.W., Tristani-Firouzi, M., Ptacek, L.J., Tawil, R., Schwartz, P.J., George, A.L., Horie, M., Andelfinger, G., Snow, G.L., Fu, Y.H., Ackerman, M.J. and Vincent, G.M. 2005. Electrocardiographic features in Andersen-Tawil syndrome patients with KCNJ2 mutations: characteristic T-U-wave patterns predict the KCNJ2 genotype. Circulation **111**: 2720–2726. doi: 10.1161/CIRCULATIONAHA.104.472498, PMID: 15911703

Zicha, S., Moss, I., Allen, B., Varró, A., Papp, J.G., Dumaine, R., Antzelevich, C. and Nattel S. 2003. Molecular basis of species-specific expression of repolarizing K^+ currents in the heart. Am. J. Physiol. Heart Circ. Physiol. **285**: H1641–H1649. doi: 10.1152/ajpheart.00346.2003, PMID: 12816752

Zobel, C., Cho, H.C., Nguyen, T.T., Pekhletski, R., Diaz, R.J., Wilson, G.J. and Backx, P.H. 2003. Molecular dissection of the inward rectifier potassium current (IK1) in rabbit cardiomyocytes: evidence for heteromeric co-assembly of Kir2.1 and Kir2.2. J Physiol. **550**: 365-72. doi: 10.1113/jphysiol.2002.036400, PMID: 12794173

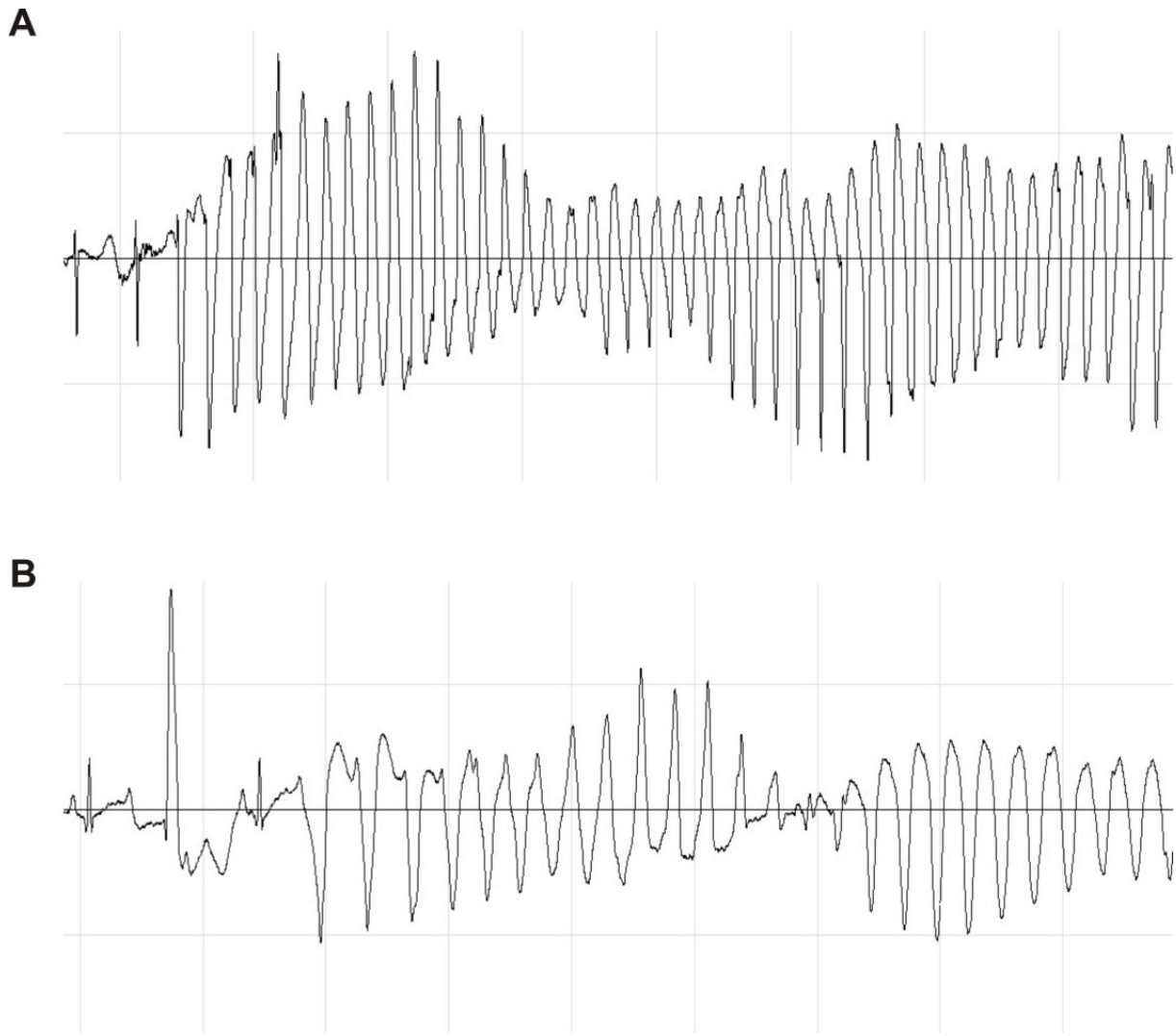

Figure 1. Representative Torsades de Pointes (TdP) recording from (**A**) conscious dog following combined inhibition of I_{Ks} + I_{K1} and from (**B**) an anesthetized rabbit following the combined inhibition of I_{K1}+I_{Kr}.

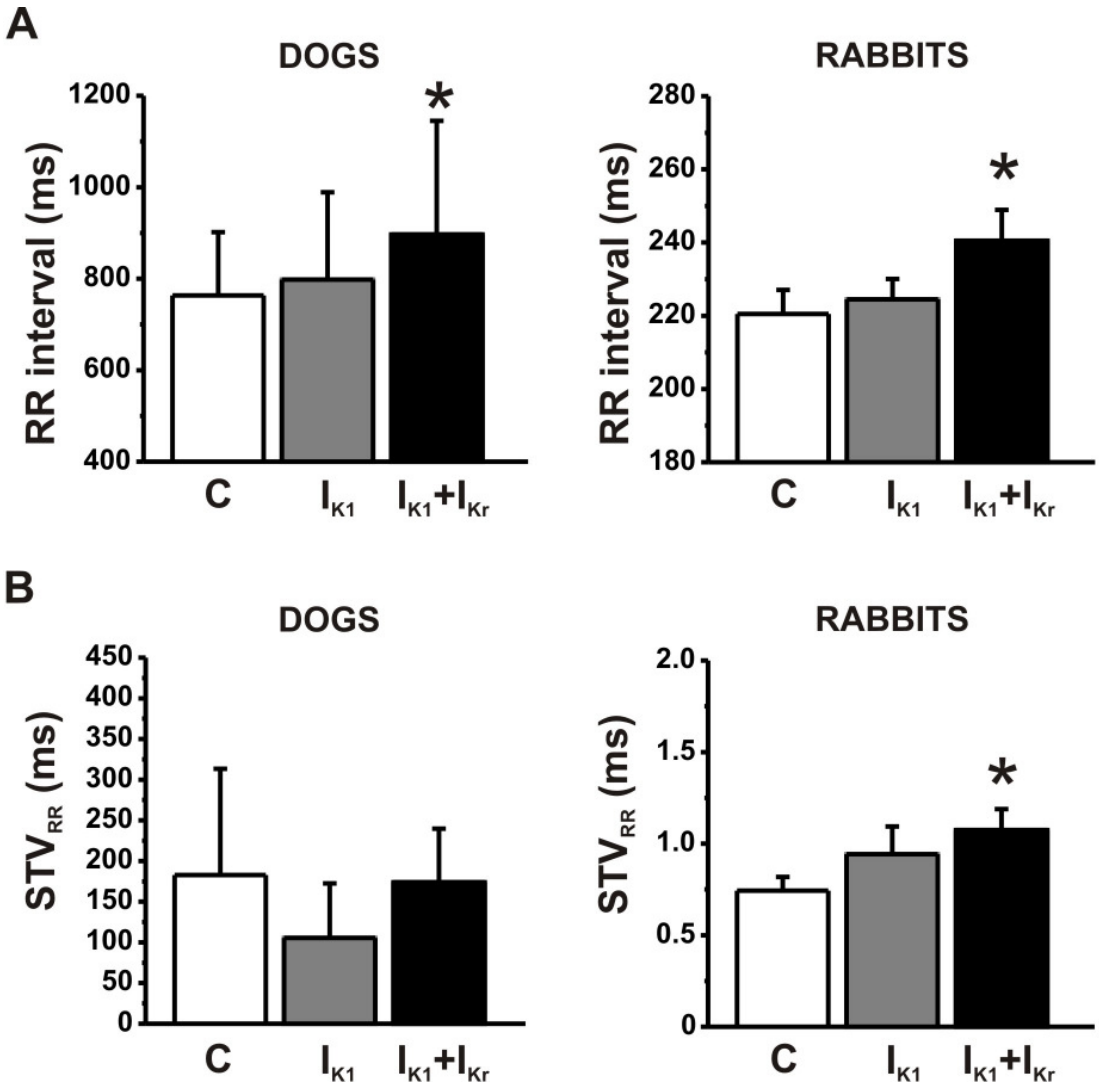

Figure 2. Effect of I_{K1} inhibition (i.v. $BaCl_2$) and combined $I_{K1}+I_{Kr}$ (i.v. $BaCl_2$+dofetilide) inhibition on (**A**) RR interval and (**B**) short-term variability of the RR interval (STV_{RR}) in conscious dogs and anesthetized rabbits. N=7 dogs and 7 rabbits/group; *p<0.05 vs. control values; #p<0.05 vs. I_{K1} inhibition.

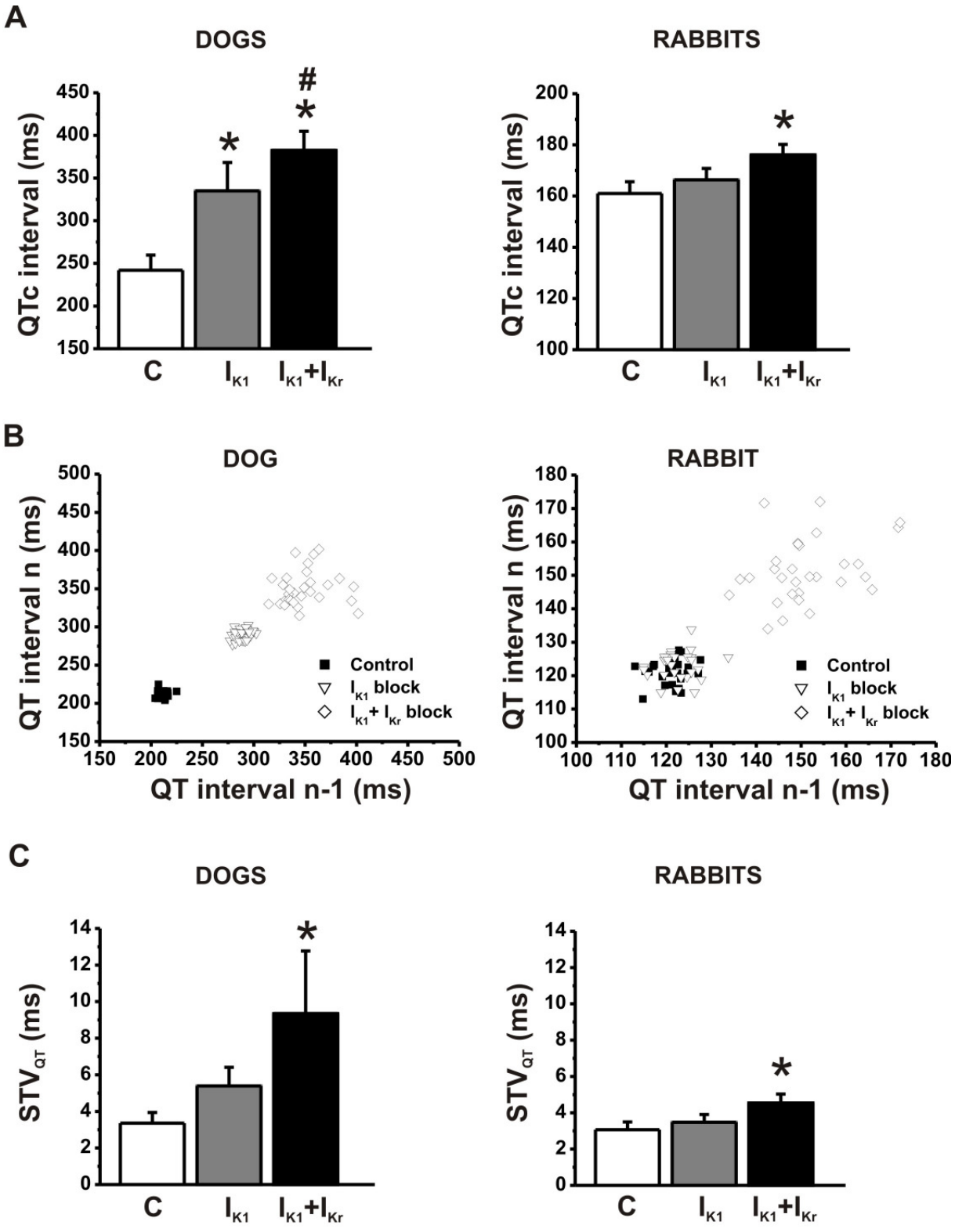

Figure 3. Effect of I_{K1} inhibition (i.v. $BaCl_2$) and combined $I_{K1}+I_{Kr}$ (i.v. $BaCl_2$+dofetilide) inhibition on (**A**) frequency corrected QT interval (QTc); (**B and C**) short-term variability of the QT interval (STV_{QT}) in conscious dogs and anesthetized rabbits. For details on Poincaré plot (**B**) description see text. N=7 dogs and 7 rabbits/group; *p<0.05 vs. control values; #p<0.05 vs. I_{K1} inhibition.

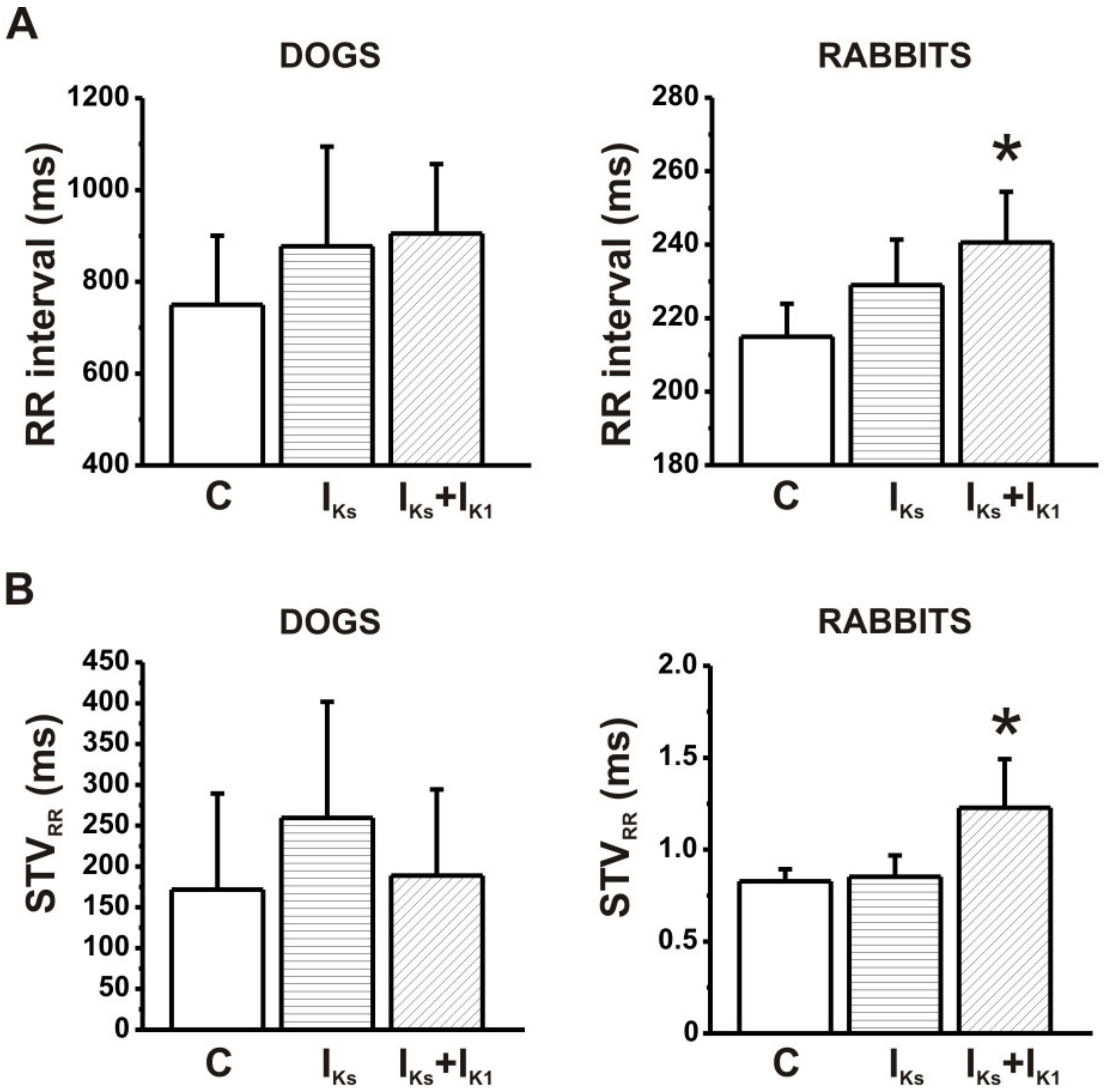

Figure 4. Effect of I_{Ks} inhibition (i.v. HMR 1556) and combined $I_{Ks}+I_{K1}$ (i.v. HMR 1556+$BaCl_2$) inhibition on (**A**) RR interval and (**B**) short-term variability of the RR interval (STV_{RR}) in conscious dogs and anesthetized rabbits. N=6 dogs and 7 rabbits/group; *p<0.05 vs. control values; #p<0.05 vs. I_{Ks} inhibition.

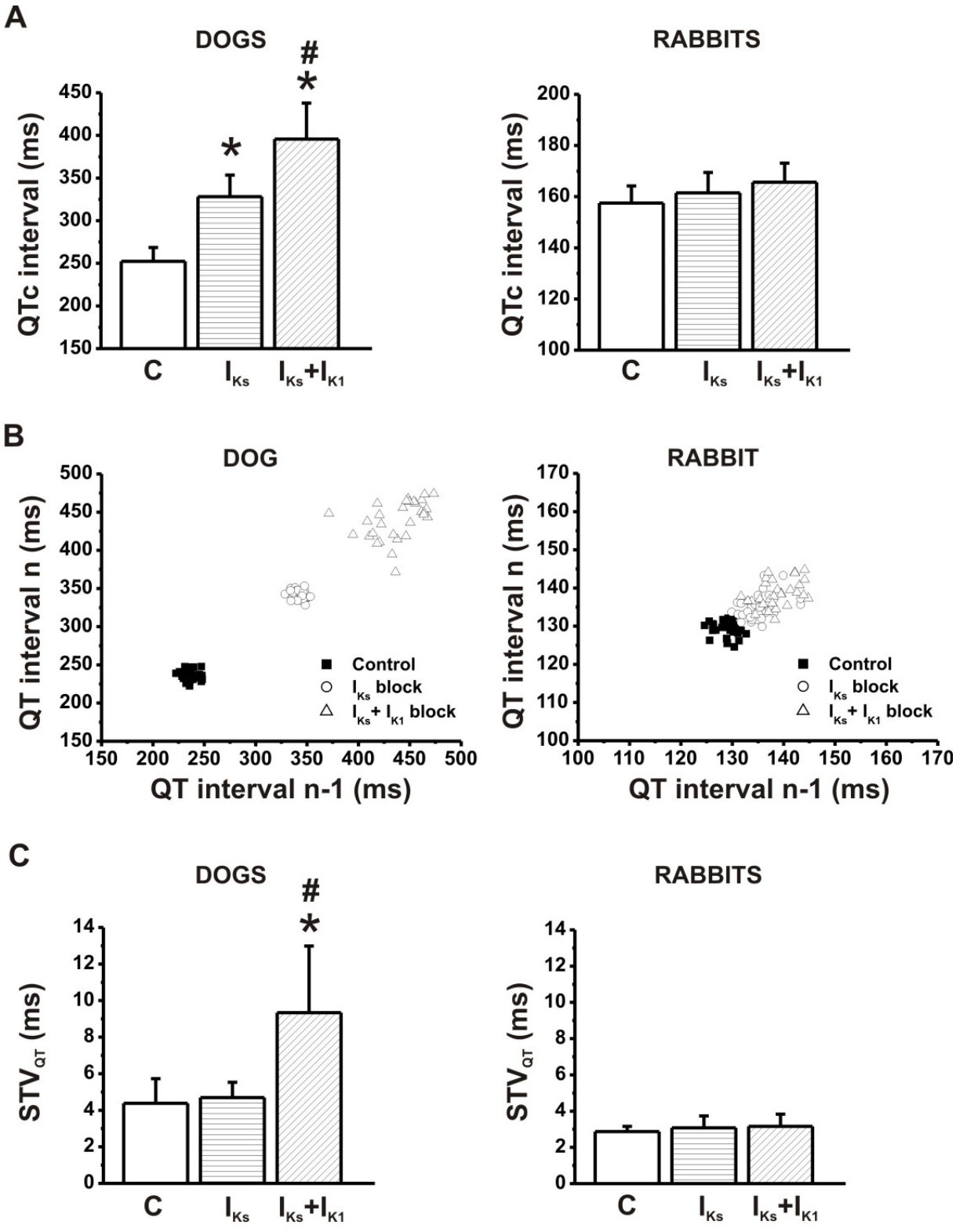

Figure 5. Effect of I_{Ks} inhibition (i.v. HMR 1556) and combined $I_{Ks}+I_{K1}$ (i.v. HMR 1556+$BaCl_2$) inhibition on (**A**) frequency corrected QT interval (QTc); (**B and C**) short-term variability of the QT interval (STV_{QT}) in conscious dogs and anesthetized rabbits. For details on Poincaré plot (**B**) description see text. N=6 dogs and 7 rabbits/group; *p<0.05 vs. control values; #p<0.05 vs. I_{Ks} inhibition.

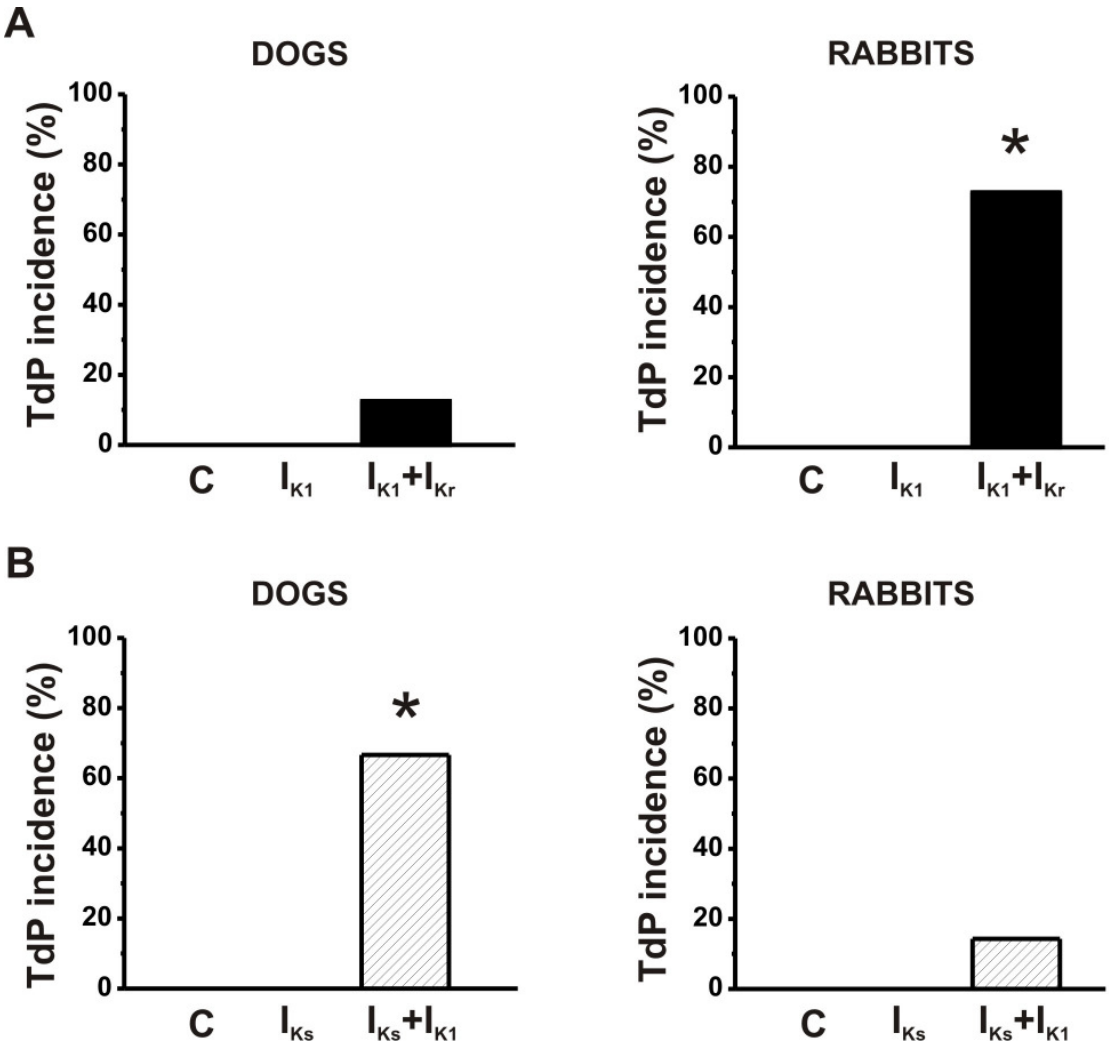

Figure 6. Effect of (**A**) I_{K1} inhibition (i.v. $BaCl_2$) and combined $I_{K1}+I_{Kr}$ (i.v. $BaCl_2$+dofetilide) inhibition and (**B**) I_{Ks} inhibition (i.v. HMR 1556) and combined $I_{Ks}+I_{K1}$ (i.v. HMR 1556+$BaCl_2$) inhibition on incidence of Torsades de Pointes (TdP) chaotic ventricular arrhythmia in conscious dogs (left panels) and anesthetized rabbits (right panels). N=7 and 6 dogs, and 7 rabbits/group; *$p<0.05$ vs. control values.

Am J Physiol Heart Circ Physiol 298: H1577–H1587, 2010.
First published March 5, 2010; doi:10.1152/ajpheart.00936.2009.

Mechanisms of ventricular rate adaptation as a predictor of arrhythmic risk

Esther Pueyo,[1,2,3] Zoltán Husti,[4] Tibor Hornyik,[4,5] István Baczkó,[4] Pablo Laguna,[2,3] András Varró,[4,5] and Blanca Rodríguez[1]

[1]*Oxford University Computing Laboratory, University of Oxford, Oxford, United Kingdom;* [2]*Instituto de Investigación en Ingeniería de Aragón, Universidad de Zaragoza, Zaragoza, Spain;* [3]*Centro de Investigación Biomédica En Red de Bioingeniería, Biomateriales y Nanomedicina, Zaragoza, Spain; and* [4]*Department of Pharmacology and Pharmacotherapy, University of Szeged, and* [5]*Research Unit for Cardiovascular Pharmacology, Hungarian Academy of Sciences, Szeged, Hungary*

Submitted 5 October 2009; accepted in final form 23 February 2010

Pueyo E, Husti Z, Hornyik T, Baczkó I, Laguna P, Varró A, Rodríguez B. Mechanisms of ventricular rate adaptation as a predictor of arrhythmic risk. *Am J Physiol Heart Circ Physiol* 298: H1577–H1587, 2010. First published March 5, 2010; doi:10.1152/ajpheart.00936.2009.—Protracted QT interval (QTI) adaptation to abrupt heart rate (HR) changes has been identified as a clinical arrhythmic risk marker. This study investigates the ionic mechanisms of QTI rate adaptation and its relationship to arrhythmic risk. Computer simulations and experimental recordings in human and canine ventricular tissue were used to investigate the ionic basis of QTI and action potential duration (APD) to abrupt changes in HR with a protocol commonly used in clinical studies. The time for 90% QTI adaptation is 3.5 min in simulations, in agreement with experimental and clinical data in humans. APD adaptation follows similar dynamics, being faster in midmyocardial cells (2.5 min) than in endocardial and epicardial cells (3.5 min). Both QTI and APD adapt in two phases following an abrupt HR change: a fast initial phase with time constant < 30 s, mainly related to L-type calcium and slow-delayed rectifier potassium current, and a second slow phase of >2 min driven by intracellular sodium concentration ($[Na^+]_i$) dynamics. Alterations in $[Na^+]_i$ dynamics due to Na^+/K^+ pump current inhibition result in protracted rate adaptation and are associated with increased proarrhythmic risk, as indicated by action potential triangulation and faster L-type calcium current recovery from inactivation, leading to the formation of early afterdepolarizations. In conclusion, this study suggests that protracted QTI adaptation could be an indicator of altered $[Na^+]_i$ dynamics following Na^+/K^+ pump inhibition as it occurs in patients with ischemia or heart failure. An increased risk of cardiac arrhythmias in patients with protracted rate adaptation may be due to an increased risk of early afterdepolarization formation.

action potentials; ventricles; ion channels; arrhythmia; computers

CLINICAL, EXPERIMENTAL, AND theoretical studies have shown that an abrupt change in heart rate (HR) results in the progressive adaptation of the QT interval (QTI) in the ECG because of short-term cardiac memory effects (2, 3, 22, 29, 35, 36). Patients exhibiting protracted QTI HR adaptation dynamics have been identified as at increased risk of experiencing cardiac arrhythmias and sudden cardiac death (22, 35). Furthermore, clinical data also suggest that the extent of amiodarone-induced acceleration of QTI HR adaptation could be used as a therapeutic marker of drug efficacy (37). However, despite strong evidence suggesting an important role of short-term cardiac memory in arrhythmogenesis, the underlying mechanisms are still controversial.

Address for reprint requests and other correspondence: E. Pueyo, Oxford Univ. Computing Lab., Wolfson Bldg., Parks Rd., Oxford OX1 3QD, UK (e-mail: epueyo@unizar.es).

The present study investigates the ionic basis of QTI rate adaptation in human ventricular tissue and its link to proarrhythmic mechanisms. Computer simulations and experiments were conducted to identify the specific mechanisms of ionic transport that determine QTI rate adaptation and how alterations in those mechanisms might result in arrhythmic events. Key simulation predictions were evaluated using experimental and clinical data from the literature and a limited set of experiments in humans performed in this study. Ionic mechanisms underlying HR adaptation were further investigated using simulations and experiments in both humans and dogs because of their similar repolarization mechanisms and the greater availability of canine tissue compared with that of humans (41).

MATERIALS AND METHODS

Computer Modeling and Simulation

Human (38) and canine (10) ventricular cell models were used to investigate short-term memory mechanisms. Computer simulations of electrical propagation and pseudo-ECG (pECG) (21) were conducted using a transmural one-dimensional fiber model, consisting of 100 cells [30% endocardial (Endo), 30% midmyocardial (Mid), and 40% epicardial (Epi) cells (12, 38)]. A 1-ms square stimulus pulse of 1.5 times diastolic threshold was applied to the endocardium. Integration was performed using the forward Euler method with a 0.02-ms time step and 0.015-cm space step. pECG peaks and boundaries were identified using an automatic wavelet transform-based delineation system (33). pECG QTI was measured as the time interval between the QRS complex onset and the T-wave end.

Characterization of Ventricular HR Adaptation Dynamics

The rate adaptation of QTI and action potential (AP) duration (APD) at 90% repolarization was evaluated (18, 29): pacing at a cycle length (CL) of 1,000 ms was applied until steady state, followed by a CL of 600 ms for 10 min and back to a CL of 1,000 ms for an additional 10 min. Fast and slow phases in QTI and APD rate adaptation were identified, and time constants (τ) of their dynamics were obtained by fitting to: $f(t) = a + be^{-(t-c)/\tau}$.

Time constants τ_{fast} and τ_{slow}, characterizing each of the two adaptation phases, were obtained, both after the CL increase and decrease. In cases where the fast phase consisted of only two data points, then $f(t) = be^{-t/\tau}$ was used to derive τ_{fast}.

QTI or APD adaptation is defined as protracted when the associated time constant τ_{slow} is abnormally long (see RESULTS for a detailed description), which is related to irregularities in APD adaptation dynamics and the generation of afterdepolarizations.

Evaluation of Proarrhythmic Risk in Simulation

To investigate the ionic mechanisms of rate adaptation and its relationship to risk, adaptation dynamics and arrhythmic risk markers

were quantified for control and also following ±15 and ±30% changes in specific model parameters. The arrhythmic risk markers (30) considered were *1*) AP triangulation, quantified as $\delta = APD/APD_{50}$, where APD_{50} denotes APD at 50% repolarization, considered to be an indicator of an early afterdepolarization (EAD) occurrence (34); *2*) APD restitution (APDR) curve slope at a diastolic interval of 60 ms (26), determined using both S1-S2 and dynamic protocols (38), $S_{S1\text{-}S2}$ and S_{dyn}, respectively; and *3*) calcium current reactivation, as the product ρ of the inactivation gates [f, f_2, and f_{cass} (38)] of the L-type calcium current (I_{CaL}) computed at 90% repolarization for steady state at a CL of 1,000 ms (42).

Experimental Methods

Experiments were performed to validate key simulation results, when specific data were not available in the literature. Experiments were conducted in human ventricular tissue when available ($n = 2$ tissue samples); otherwise, right ventricle papillary muscles isolated from adult mongrel dogs hearts ($n = 21$) were used (8–20 kg, either sex) (40). All animal experiments were conducted in compliance with the *Guide for the Care and Use of Laboratory Animals* (NIH Publication No. 85-23, Revised 1996), and the protocol was approved by the Ethical Committee for the Protection of Animals in Research of the University of Szeged, Hungary (I-74-125-2007) and by the Department of Animal Health and Food Control of the Ministry of Agriculture and Rural Development (XIII/01031/000/2008). Regarding human experiments, undiseased human hearts that were technically not usable for transplantation (based on logistical and not on patient-related reasons) were obtained from general organ donors. Before cardiac explantation, organ donor patients did not receive medication except dobutamine, furosemide, and plasma expanders. The investigations conform with the principles outlined in the *Declaration of Helsinki* of the World Medical Association. The experimental procedures and protocols were approved by the Ethical Review Board of the Medical Center of the University of Szeged, Hungary (No. 51-57/1997 OEJ). Human right ventricular papillary muscle preparations were dissected from donor hearts stored in cardioplegic solution at 4°C for 3 to 4 h before placing them into oxygenated modified Locke's solution containing (in mM) 120 NaCl, 4 KCl, 1.0 $CaCl_2$, 1 $MgCl_2$, 22 $NaHCO_3$, and 11 glucose. The pH of this solution was set to 7.4 ± 0.05 when saturated with the mixture of 95% O_2 and 5% CO_2 at 37°C.

Transmembrane APs were recorded using the conventional microelectrode technique as described previously (40). APD HR adaptation was evaluated using the same protocol as in the simulations, both in control (in humans and dogs) and in the presence of the following drug concentrations (in dogs): 0.2 and 0.6 μM strophanthin G ($n = 5$ and 7), 1 and 3 μM nisoldipine ($n = 1$), 30 μM $BaCl_2$ ($n = 2$), 0.25 μM HMR-1556 ($n = 3$), and 0.1 μM dofetilide ($n = 3$). Strophanthin G and $BaCl_2$ were dissolved in distilled water to give stock solution concentrations of 1 and 50 mM, respectively. Nisoldipine was dissolved in 100% ethanol stock solution (1 mM). HMR-1556 was dissolved in DMSO stock solution (1 mM).

RESULTS

Ventricular Rate Adaptation

QTI adaptation. Figure 1*A* illustrates QTI adaptation kinetics in humans from simulations (*left*) and clinical data (29) (*right*). Figure 1*B* shows simulated pECG for the first beat following HR acceleration (*left*) and deceleration (*right*) and when the new steady state is reached. QTI adaptation after a

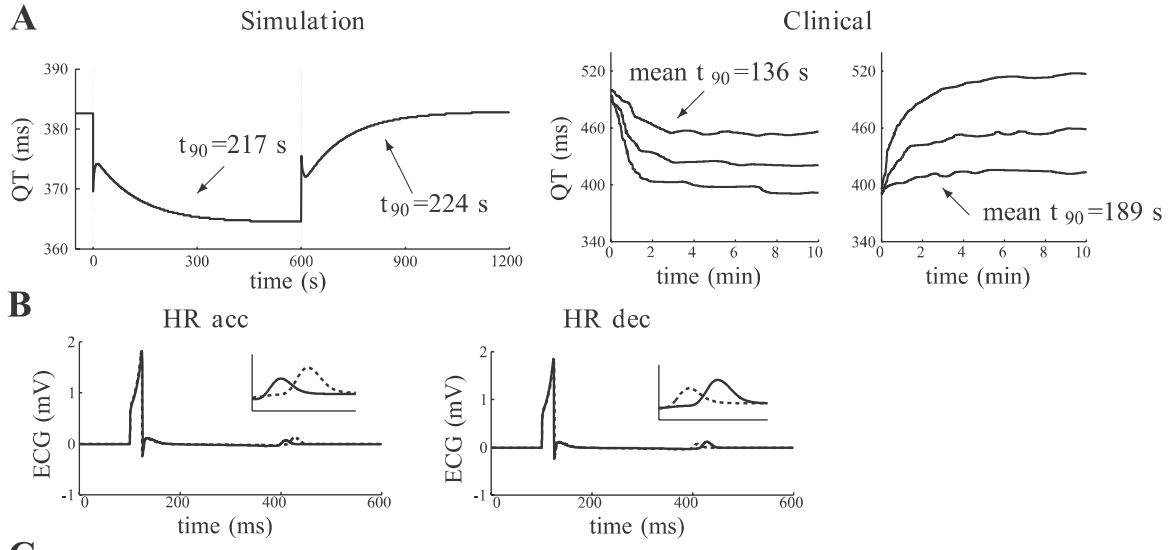

Simulation	TP06	HRacc: 217 s	HRdec: 224s
Clinical	Lau et al	HRacc, mean ± SEM: 136 ± 16 s	HRdec, mean ± SEM: 189 ± 25 s
	Seed et al	> 180 s	
	Attwell et al	~ 180 s	
	Grom et al	60 s – 300 s	
	Pueyo et al	10 s – 240 s	

Fig. 1. *A*, *left*: simulated QT interval (QTI) adaptation in human pseudo-ECG for cycle length (CL) of 1,000 to 600 to 1,000 ms. *A*, *right*: QTI adaptation in human ECG recordings for 50 or 110 beats/min in increments or decrements of 20, 40, and 60 beats/min (modified and redrawn from original graphs from Ref. 29). Time required for 90% QTI rate adaptation (t_{90}) is presented. *B*: simulated pseudo-ECGs corresponding to first (dotted line) and last (solid line) beats after CL decrease (*left*) and CL increase (*right*). *C*: t_{90} values for simulated pseudo-ECGs and clinical human ECGs. HR, heart rate; Acc, acceleration; Dec, deceleration; TP06, human ventricular cell model developed by ten Tusscher and Panfilov (38) in 2006.

step CL decrease/increase begins with a fast QTI shortening/lengthening during the initial beats after the HR change (τ_{fast} = 17/34 s), followed by a second slow accommodation (τ_{slow} = 122/122 s). In the simulations, the time (t_{90}) required for QTI to complete 90% of its adaptation in humans is 217/224 s following HR acceleration/deceleration. As shown in Fig. 1*C*, simulation values for t_{90} are within the wide range reported clinically.

A sensitivity analysis was performed to assess the dependence of QTI rate adaptation dynamics on CL change magnitude (m_{CL}) and on the initial CL (i_{CL}). Values for m_{CL} considered were 200, 400, and 600 ms, and values for i_{CL} were 1,000 and 1,400 ms. No statistically significant differences (analysis of variance, $P > 0.05$) in t_{90} are observed when varying m_{CL} or i_{CL}.

APD adaptation. Figure 2, *A* and *B*, illustrates APD HR adaptation in simulated Endo (*top*), Mid (*middle*), and Epi (*bottom*) human ventricular cells. Figure 2*A* shows the time course of APD adaptation, and Fig. 2*B* illustrates the AP corresponding to the first beat and the new steady state follow-

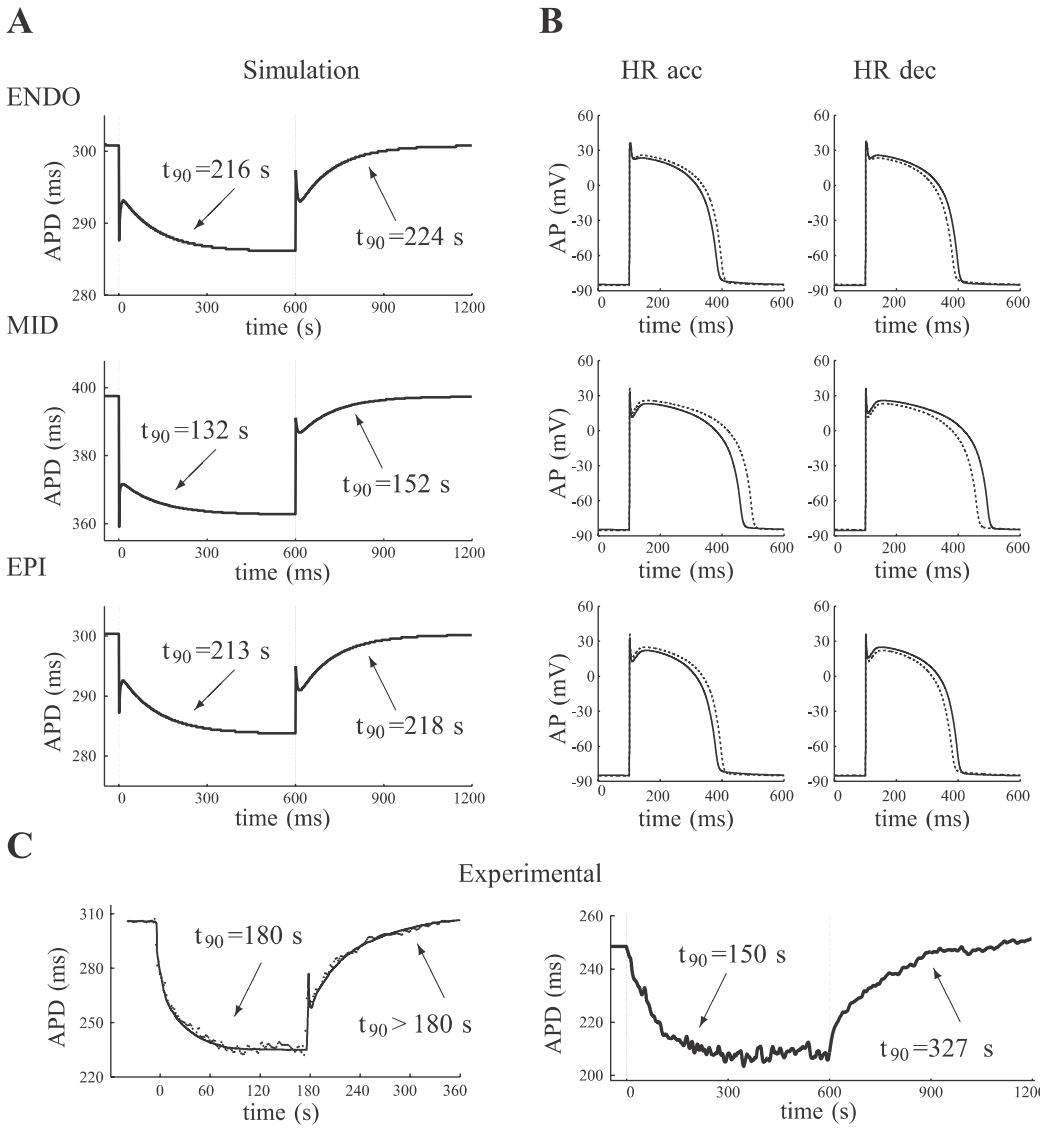

D

Simulation	TP06	Endo	HRacc: 216 s	HRdec: 224 s
		Mid	HRacc: 132 s	HRdec: 152 s
		Epi	HRacc: 213 s	HRdec: 218 s
Experimen tal	Franz et al	Endo	HRacc: 108 s – 192 s	
	Seed et al	Endo	HRacc: > 180 s	
	This study	Papillary Muscle	HRacc: 89 s – 150 s	HRdec: 159 s – 327 s

Fig. 2. *A*: simulated action potential (AP) duration (APD) adaptation in humans for CL of 1,000 to 600 to 1,000 ms for endocardial (Endo; *top*), midmyocardial (Mid; *middle*), and epicardial (Epi; *bottom*) cardiomyocytes. *B*: simulated APs corresponding to first (dotted line) and last (solid line) beats after CL decrease (*left*) and CL increase (*right*) for human Endo (*top*), Mid (*middle*), and Epi (*bottom*) cardiomyocytes. *C*: experimental APD adaptation in humans for CL of 750–410 ms (*left*, modified and redrawn from original graphs from Ref. 18) and for CL of 1,000–600 ms (*right*, this study). *D*: t_{90} values for simulated and experimental human APs.

ing HR acceleration (*left*) and deceleration (*right*) for the three cell types. Figure 2*C* presents experimental APD adaptation measured in human ventricular endocardium (18), as well as in human papillary muscle, measured in this study.

It is clear that APD HR adaptation dynamics are similar in human simulations and experiments (18) and comparable with QTI HR adaptation dynamics (shown in Fig. 1), consisting of a fast and slow phase (τ_{fast} = 13/26 s after CL decrease/increase for Endo, 6/14 s for Mid, and 13/26 s for Epi cells; and τ_{slow} = 126/122 s after CL decrease/increase for Endo, 128/122 s for Mid, and 126/123 s for Epi cells). This suggests that QTI HR adaptation is a manifestation of cellular APD HR adaptation. As shown in Fig. 2*D*, simulation values for t_{90} are within the range observed experimentally. Furthermore, simulations with both the human and the dog models yield similar rate adaptation dynamics, although slightly slower in dog (t_{90} = 282/311 s in canine and t_{90} = 213/218 s in human Epi cells for HR acceleration/deceleration, respectively). Analogous to the results reported for QTI in this study, no statistically significant differences in t_{90} for APD adaptation are found when varying m_{CL} or i_{CL}.

Ionic Mechanisms of APD Rate Adaptation

Figures 3 and 4 illustrate the ionic mechanisms of APD HR adaptation in humans. Each panel in Fig. 3 represents the change in peak value of each ionic current [slow delayed rectifier potassium current (I_{Ks}), I_{CaL}, transient outward potassium current (I_{to}), rapid delayed rectifier potassium current (I_{Kr}), inward rectifier potassium current (I_{K1}), fast sodium current (I_{Na}), Na^+/Ca^{2+} exchanger current (I_{NaCa}), and Na^+/K^+ pump current (I_{NaK})] or intracellular sodium and calcium ion concentration ($[Na^+]_i$ and $[Ca^{2+}]_i$), as a function of APD for the beats following HR acceleration (analogous results were obtained for HR deceleration; graphics not shown). The numbers shown in each graph indicate the number of beats following the CL change. Bar graphs in Fig. 4 show the percentage of total change in peak values of each ionic current or intracellular ion concentration that occurred during the fast (*top*) and slow (*bottom*) phase of HR adaptation. The ionic mechanisms involved in each of the adaptation phases, fast and slow, are further described in the following.

Initial fast phase of adaptation. Figures 3 and 4 show that I_{CaL} and I_{Ks} experience the greatest percentage of total change during the initial phase of rate adaptation and are key mechanisms driving that phase. Other ionic currents, such as I_{to}, present a percentage of change similar to I_{Ks}, but these changes are a consequence (and not a cause) of APD adaptation, since variations in conductance and/or kinetics do not affect τ_{fast}.

Figure 5*A* further illustrates the role that the dynamics of the I_{CaL} slow voltage-dependent inactivation gate (*f*) and the I_{Ks}

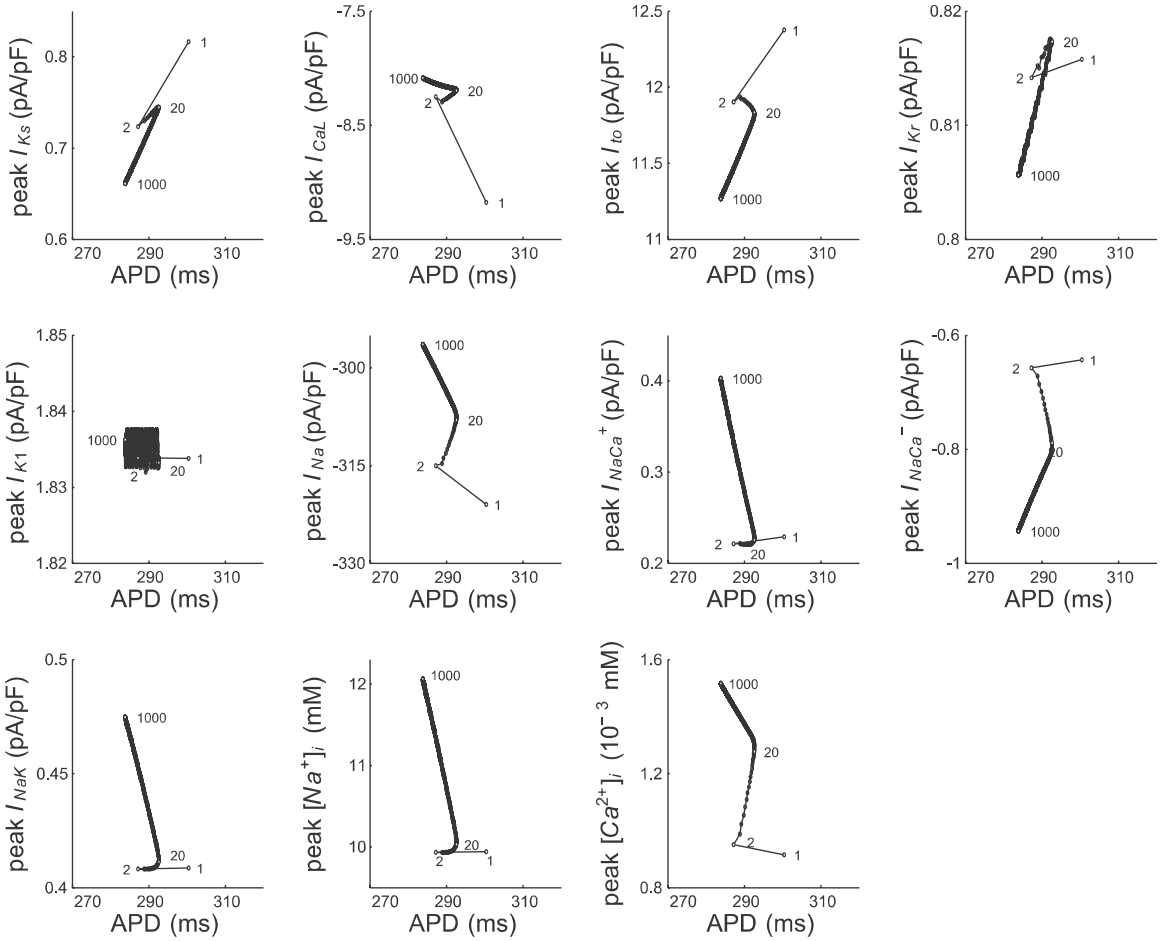

Fig. 3. Peak values for I_{Ks}, I_{CaL}, I_{to}, I_{Kr}, I_{K1}, I_{Na}, I_{NaCa}, I_{NaK}, $[Na^+]_i$, and $[Ca^{2+}]_i$ (see main text for definitions of abbreviations) as a function of APD during adaptation for CL varying from 1,000 to 600 ms in humans. Beat number after step CL change is shown.

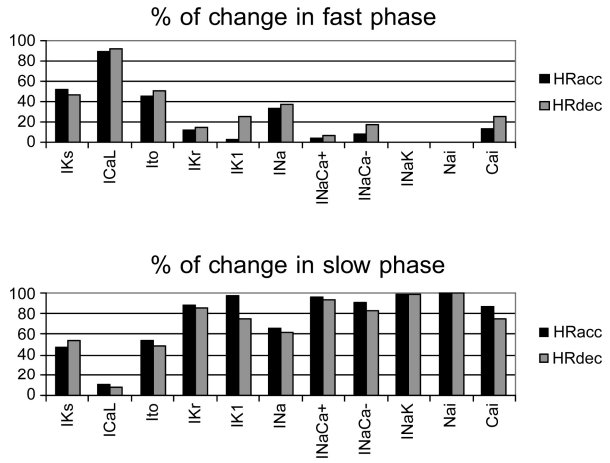

Fig. 4. Percentage of total change in peak value for each ionic current and concentration during fast (*top*) and slow (*bottom*) phases of APD adaptation for CL varying from 1,000 to 600 ms (HRacc) and from 600 to 1,000 ms (HRdec). Nai, $[Na^+]_i$; Cai, $[Ca^{2+}]_i$.

activation gate (*xs*) play in the fast phase of human APD adaptation. Indeed, a sudden decrease in CL results in an insufficient time for *f* to fully recover ($f < 1$) (Fig. 5*A*, *top*), whereas I_{Ks} is unable to completely deactivate ($xs > 0$) at the end of each beat. The resulting decrease in inward and increase in outward currents contribute to APD shortening following HR acceleration. To further illustrate the importance of *f* and *xs* in the initial adaptation phase, Fig. 5*A*, *right*, shows APD adaptation dynamics for control and for a simulation where beat-to-beat differences in *f* and *xs* are eliminated by fixing them to their steady-state values for a CL of 1,000 ms ($f = 0.9774$ and $xs = 0.003225$, respectively). Results show that eliminating beat-to-beat differences in *f* and *xs* leads to the abolishment of the fast phase of APD adaptation. Similar mechanisms are observed using the canine ventricular model (not shown).

Simulations were performed to evaluate the effect of moderate changes (±15–30%) in values of key parameters defining gate kinetics and conductances of all ionic currents in the human ventricular model. The effect of those changes on time constants for the fast and slow adaptation phases (τ_{fast} and τ_{slow}), as well as the arrhythmic risk indicators ρ, δ, $S_{S1\text{-}S2}$, and S_{dyn}, were quantified. Simulation results are shown in Fig. 6 for the parameters with greatest influence on human APD HR adaptation. As previously discussed and illustrated in Figs. 3–5, Fig. 6 (*first row*) also shows that τ_{fast} is greatly sensitive to I_{CaL} inactivation and I_{Ks} activation kinetics and thus moderate changes of up to 30% in τ_f and τ_{xs} significantly alter τ_{fast}. Changes of up to 30% in ionic current conductances have only a negligible effect on τ_{fast} (Fig. 6, *first row*). Additional simulations and experiments were conducted to evaluate whether large degrees (>70%) of ion channel block could affect τ_{fast}. Results for human ventricular myocyte simulations and canine experiments are shown in Fig. 7, *left* and *right*, respectively, for I_{CaL} (*A*), I_{Ks} (*B*), I_{K1} (*C*), and I_{Kr} (*D*). Results show that I_{CaL} block by 70–90% significantly increases τ_{fast} by 54–249/107–223% following HR acceleration/deceleration using the human model (Fig. 7*A*, *left*). Qualitatively similar results are obtained using the canine model (not shown), although the effects are more pronounced in dogs, reaching >500% change in τ_{fast} for full I_{CaL} block. In the experiments, I_{CaL} block using 1 or 3 μM nisoldipine also results in increased τ_{fast} in canine papillary muscle (Fig. 7*A*, *right*), although to a lower extent than in the simulations, i.e., by 33/72% and 54/94% following HR acceleration/deceleration, respectively.

Furthermore, simulated 90–100% I_{Ks} inhibition results in a significant decrease in τ_{fast} by 71–82/63–76% following HR acceleration/deceleration in humans (Fig. 7*B*, *left*), whereas in dogs, the simulated effect is <10%. In the canine experiments, I_{Ks} block by 0.25 μM HMR-1556 (~full block) led to 16/20% decrease in τ_{fast} following HR acceleration/deceleration (Fig. 7*B*, *right*). The effect of I_{K1} and I_{Kr} block on τ_{fast} was also explored. The results in Fig. 7*C*, *left*, show that simulated I_{K1} block by 80–90% results in a 6–40/3–22% increase in τ_{fast} following HR acceleration/deceleration in humans, whereas in dogs it results in a 39–67/41–67% decrease in τ_{fast}. In the experiments, 30 μM $BaCl_2$ (estimated 80% block) results in a 28/11% decrease in τ_{fast} (Fig. 7*C*, *right*). Full I_{Kr} block results in a 7/9% increase in τ_{fast} with the human model (Fig. 7*D*, *left*), but in the canine model this leads to EADs, making the τ_{fast} measurement impossible. In the canine experiments with 0.1 μM dofetilide, there is a 10/10% decrease in τ_{fast} following HR acceleration/deceleration (Fig. 7*D*, *right*). Overall, the simulations and experiments show a good qualitative agreement in the

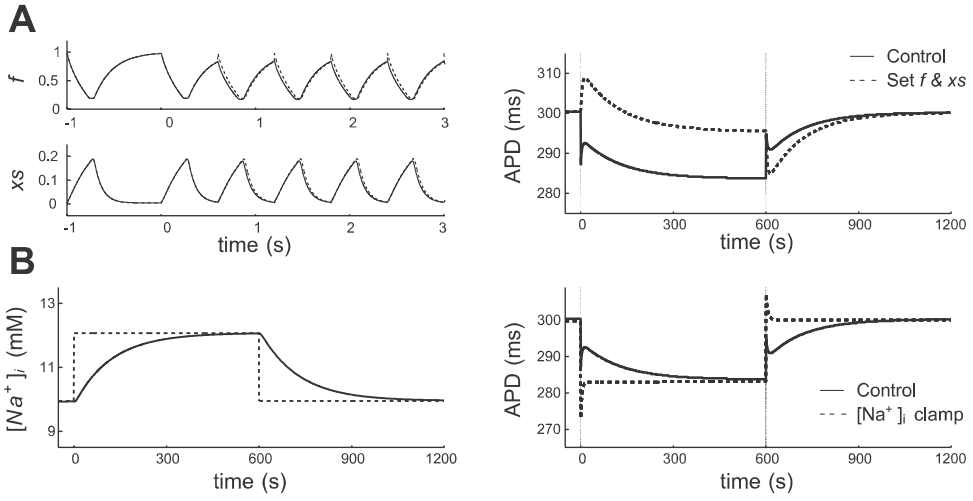

Fig. 5. Mechanisms of the fast and slow phases of APD adaptation after abrupt sustained CL changes (1,000 to 600 to 1,000 ms) in humans. *A*, *left*: time course of the I_{CaL} slow voltage-dependent inactivation gate *f* and the I_{Ks} activation gate *xs* for the first 5 beats after CL decrease for control (solid line) and when gate variables are preset to the steady-state value for CL of 1,000 ms at the beginning of each beat (dotted line). *A*, *right*: corresponding APD time courses. *B*, *left*: time course of $[Na^+]_i$ for control (solid line) and when clamped to its steady-state value for each CL (dotted line). *B*, *right*: corresponding APD time courses.

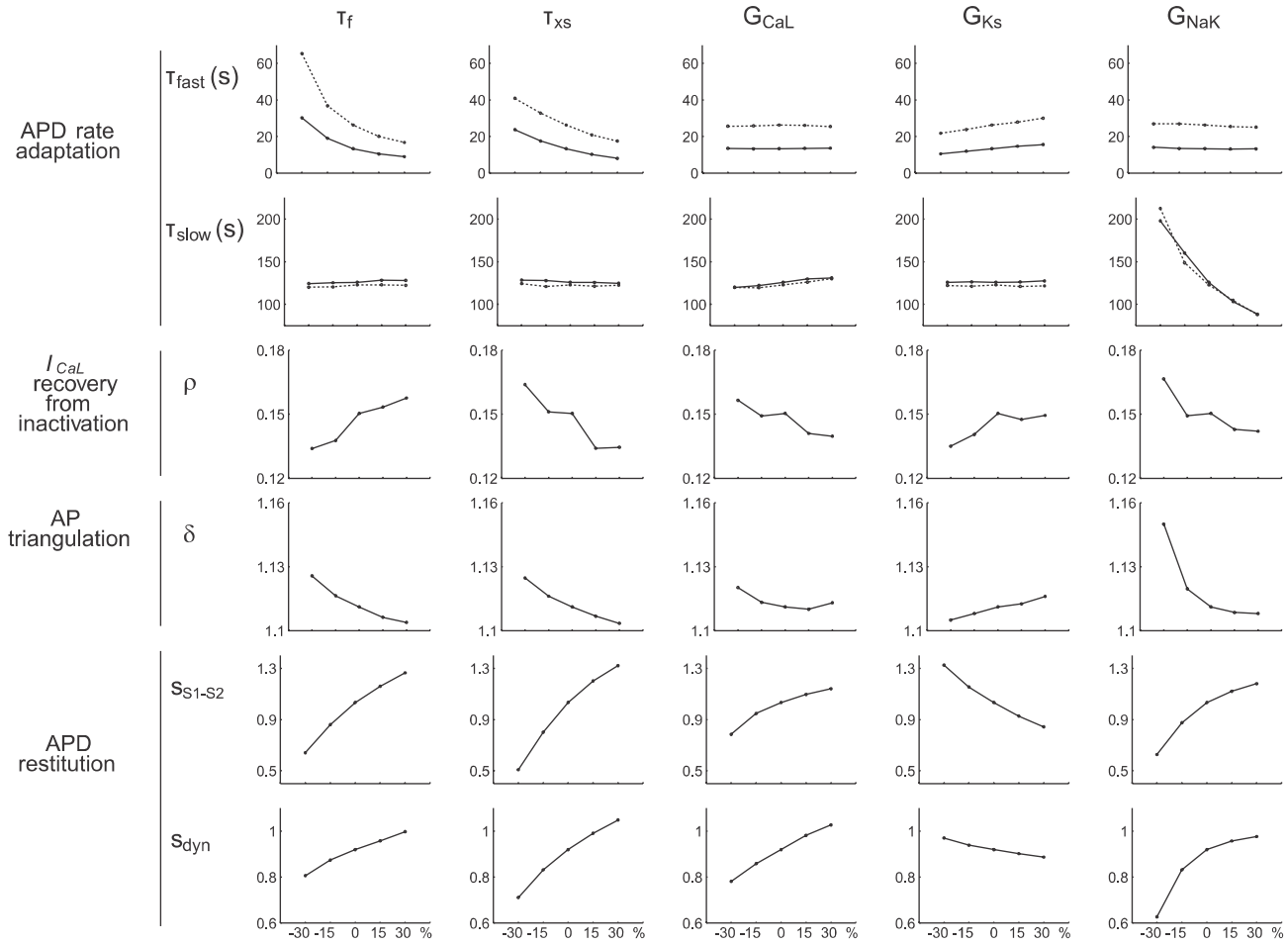

Fig. 6. Changes in time constants for fast (τ_{fast}, *first row*) and slow (τ_{slow}, *second row*) phases of APD adaptation (solid line for HR acceleration for CL of 1,000 to 600 ms, and dotted line for HR deceleration for CL of 600 to 1000 ms), degree of I_{CaL} recovery from inactivation at 90% repolarization (ρ, *third row*), AP triangulation (δ, *fourth row*), S1-S2 restitution slope ($S_{S1\text{-}S2}$, *fifth row*), and dynamic restitution slope (S_{dyn}, *sixth row*) induced by ± 15–30% variations in time constant of slow voltage-dependent I_{CaL} inactivation gate f (τ_f, *first column*), time constant of I_{Ks} activation gate xs (τ_{xs}, *second column*), I_{CaL} maximal conductance (G_{CaL}, *third column*), I_{Ks} maximal conductance (G_{Ks}, *fourth column*), and maximal I_{NaK} (G_{NaK}, *fifth column*).

effect of specific ionic current block on τ_{fast}, although specific quantitative differences are found, which are further analyzed in DISCUSSION.

Slow phase of adaptation. APD adaptation finishes with a slow phase, during which $[Na^+]_i$ and $[Ca^{2+}]_i$, as well as I_{NaK}, I_{NaCa}, and several potassium currents, experience important changes (Figs. 3 and 4). As shown in Fig. 5*B*, *left*, following HR acceleration, $[Na^+]_i$ slowly accumulates (control trace), which causes an increase in repolarization current via enhanced activity of I_{NaK} and I_{NaCa} (operating in reverse mode), resulting in a progressive APD shortening. With the use of both human and canine ventricular models, clamping $[Na^+]_i$ to its steady-state value eliminates the slow APD adaptation phase (Fig. 5*B*, $[Na^+]_i$ clamp in humans). This suggests that $[Na^+]_i$ dynamics determine the slow phase of adaptation and that changes in potassium currents depicted in Figs. 3 and 4 are secondary to APD alterations caused by sodium regulation.

The results in Fig. 6 confirm the importance of I_{NaK} in the slow phase of APD adaptation: I_{NaK} maximal conductance is the only model parameter that when altered moderately (up to 30%) exerts a significant influence in τ_{slow} in both humans and dogs. Figure 8*A* shows that I_{NaK} inhibition by 30% results in an increase in τ_{slow} by ~60% in virtual humans (Fig. 8*A*, *left*) and by ~150% in virtual canine Epi myocytes, whereas 0.6 μM strophanthin G results in an ~100% increase in τ_{slow} in canine experiments (Fig. 8*A*, *right*). I_{K1} and I_{Kr} block are also found to have an impact on the slow APD adaptation, although only in dogs, not in humans, and only for almost complete block. Specifically, 90% I_{K1} block leads to a >30% decrease in τ_{slow} in both simulations and experiments in dogs but only to a ~10% decrease in human simulations. Full I_{Kr} block is associated with >25% increase in τ_{slow} in experiments in dogs but results in <10% change in τ_{slow} in humans. The effects of I_{CaL} or I_{Ks} block on τ_{slow} are negligible.

APD HR Adaptation and Arrhythmic Risk

In this section, the link between protracted QTI and APD HR adaptation dynamics and arrhythmic risk suggested by clinical studies (19, 35) is investigated. As shown in Fig. 6, fast I_{CaL} inactivation and I_{Ks} activation (i.e., decrease in τ_f or τ_{xs}, respectively) lead to large τ_{fast} values and to a simultaneously flattening of restitution curves, an enhanced AP triangulation (associated with increased risk of EAD development), and a decrease and an increase in ρ, respectively (protection against and increased likelihood of I_{CaL} reactivation during AP repo-

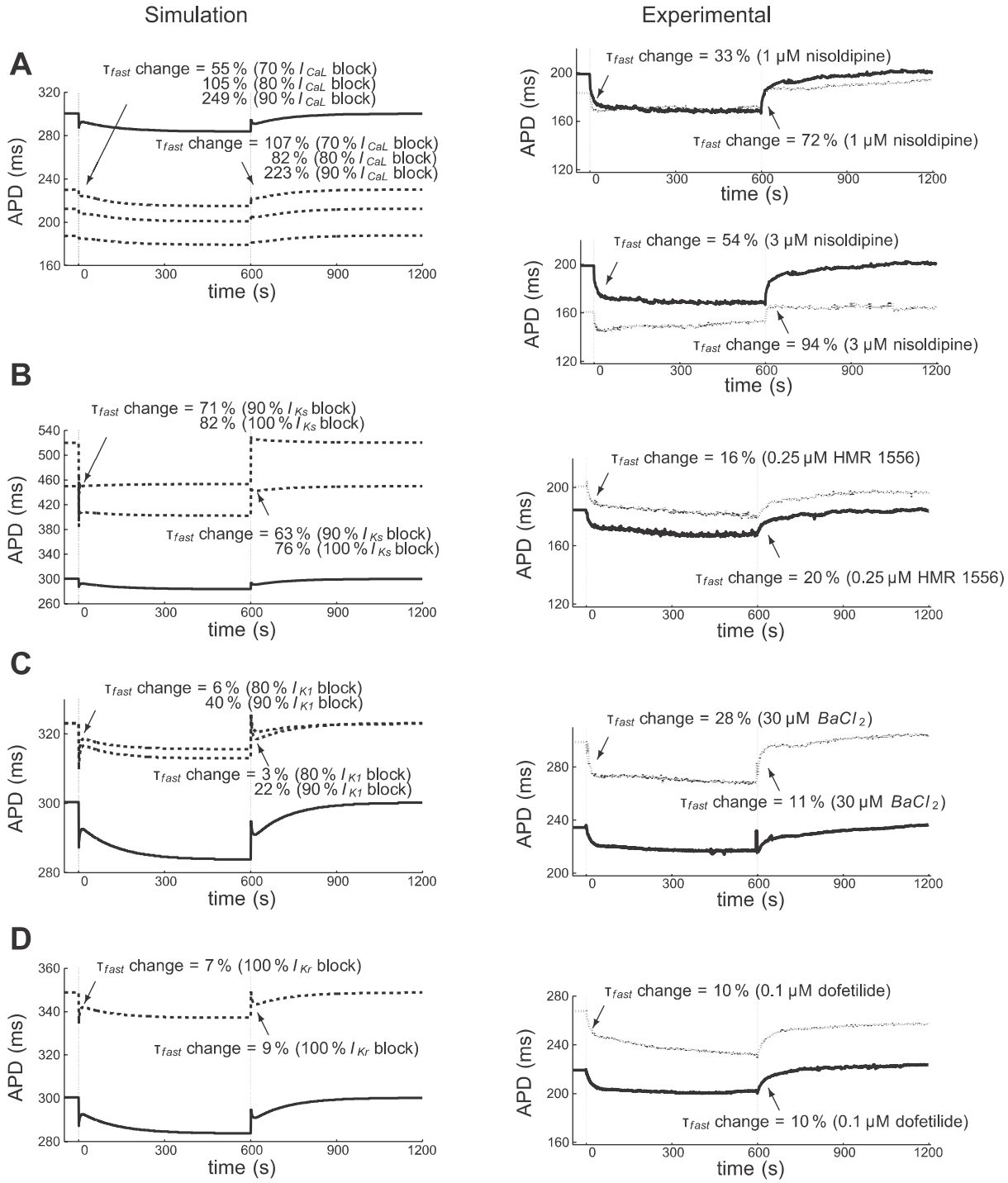

Fig. 7. Effect of ion channel block on APD rate adaptation dynamics. *Left*: simulation results in human ventricular cardiomyocyte. *Right*: experimental recordings in canine papillary muscle for control (solid lines) and for the following: I_{CaL} block by 70–80-90% in simulations and by 1 (*A*, *top*) and 3 μM (*A*, *bottom*) nisoldipine in experiments, I_{Ks} block by 90–100% in simulations and by 0.25 μM HMR-1556 in experiments (*B*), I_{K1} block by 80–90% in simulations and by 30 μM $BaCl_2$ in experiments (*C*), and I_{Kr} block by 100% in simulations and by 0.1 μM dofetilide in experiments (*D*). All experimental curves represent average over experiments. Values for percent changes in the time constant of the fast phase of APD rate adaptation (τ_{fast}) induced by each intervention are also shown.

larization, respectively). Despite the enhancement of AP triangulation associated with large τ_{fast} values, no afterdepolarizations were observed in the simulations for 60% changes in τ_f, τ_{xs}, I_{CaL} maximal conductance, and I_{Ks} maximal conductance, although a 10-fold increase in τ_{fast} was obtained for a 60% reduction in τ_f.

Regarding the slow phase of APD adaptation, Fig. 6 shows that I_{NaK} inhibition results in an increase in τ_{slow} and also an increased ρ and δ, suggesting the increased likelihood of EAD generation (24, 27, 42). Indeed, I_{NaK} inhibition by 30% in simulations and by 0.6 μM strophanthin G in experiments results in an increase in δ from 1.11 to 1.15 and from 1.20 to

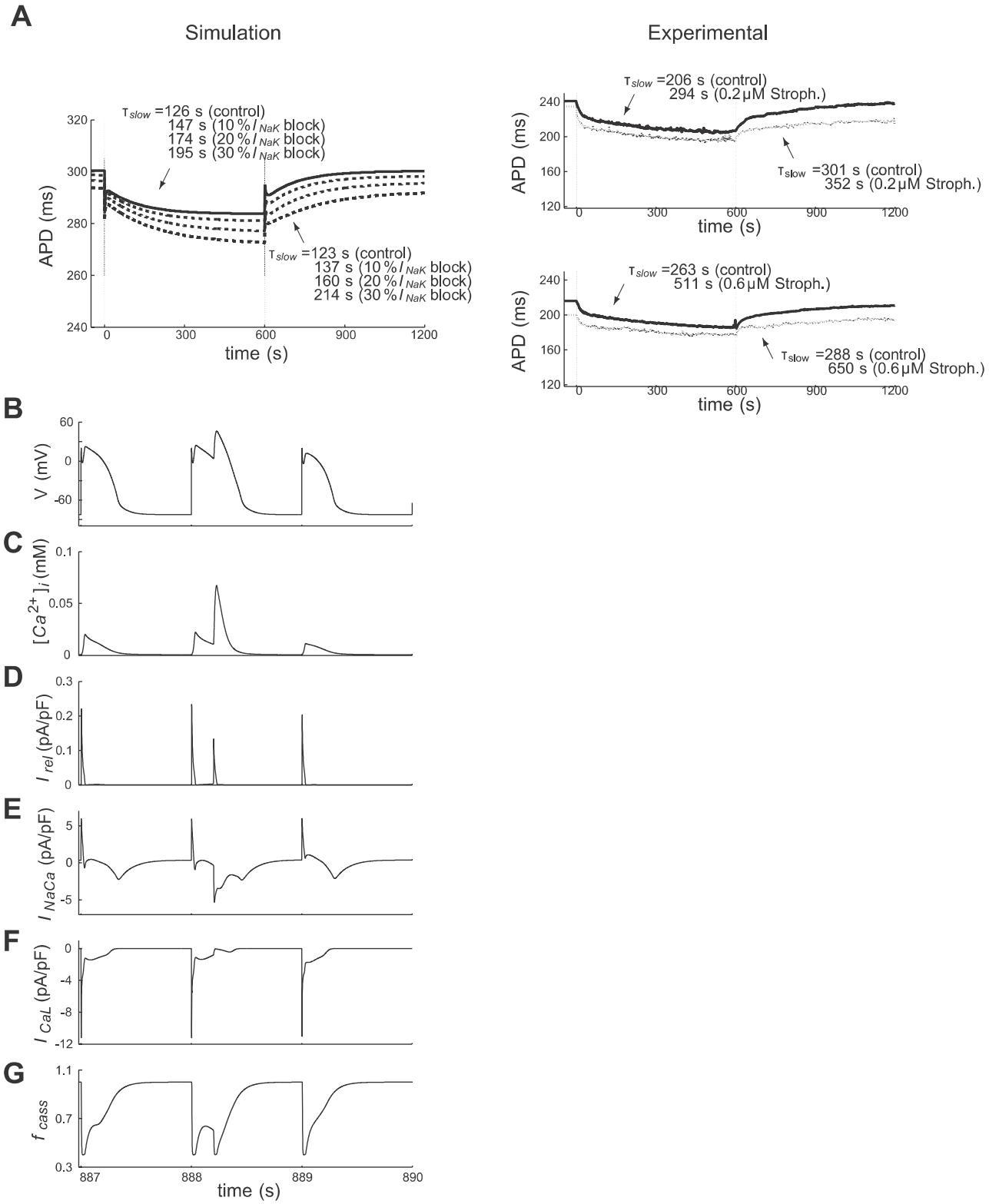

Fig. 8. *A*: effect of Na^+/K^+ pump inhibition on the slow phase of APD rate adaptation. *A*: simulated (*left*) and experimental (*right*) APD adaptation in control (solid line) and for Na^+/K^+ pump inhibition (dotted line) by 10–20-30% in simulated human ventricular cardiomyocytes and by 0.2 (*top*) and 0.6 μM (*bottom*) strophanthin G (Stroph) in canine experiments. Experimental curves represent average over experiments. *B*: early afterdepolarization generated following CL increase from 600 to 1,000 ms for simulated 60% I_{NaK} inhibition. *C–G*: corresponding time course of $[Ca^{2+}]_i$, I_{rel}, I_{NaCa}, I_{CaL}, and calcium-dependent inactivation gate f_{cass} of I_{CaL}. See main text for definitions of abbreviations. V, voltage.

1.33, respectively. EADs are observed in the simulations for I_{NaK} inhibition by 60% following HR deceleration, for all cell types in both humans and dogs. An example of EADs under those conditions in a simulated human ventricular myocyte is shown in Fig. 8*B*. Increasing the degree of I_{NaK} inhibition $>$ 35% results in a significant increase in τ_{slow}: τ_{slow} = 380 s and 1,610 s for 35 and 40% of I_{NaK} inhibition, respectively. In addition, I_{NaK} inhibition degrees $>$ 40% lead to oscillations in APD adaptation dynamics and EADs, which prevent its characterization using exponential functions. Based on our results, APD rate adaptation is defined as protracted when associated $\tau_{slow} > 380$ s. The mechanisms of EAD formation are the same in both humans and dogs: severe I_{NaK} inhibition results in an increase in $[Na^+]_i$ levels, and thus in I_{NaCa}-mediated calcium influx (Fig. 8*C*), which increases $[Ca^{2+}]_i$ and calcium release from the sarcoplasmic reticulum (I_{rel}, Fig. 8*D*). This gives rise to the enhanced depolarizing current via I_{NaCa} and I_{CaL} (Fig. 8, *E–G*) and, consequently, EAD formation.

DISCUSSION

The clinical relevance of ventricular rate adaptation has been emphasized in a number of studies (15, 22, 45) and is highlighted by the frequent involvement of sudden changes in CL in the initiation of lethal arrhythmias. In the present study, a synergistic combination of theoretical and experimental methods is used to investigate the ionic basis of QTI and APD HR adaptation and their link to proarrhythmic mechanisms. Simulation predictions on QTI and APD adaptation dynamics in humans were validated using experimental and clinical data available in the literature, and key ionic mechanisms of ventricular HR adaptation in humans were identified. Because of limitations in the availability of human tissue and similarities in repolarization mechanisms in humans and dogs, further investigations of the ionic basis of ventricular HR adaptation were performed using a combination of simulations and experiments in humans and dogs. The results show that both QTI and APD HR adaptation follow similar dynamics, consisting of two phases, fast and slow, driven by I_{CaL} and I_{Ks} kinetics and conductances, and $[Na^+]_i$ dynamics and I_{NaK}, respectively. Our results suggest that protracted QTI rate adaptation (defined by $\tau_{slow} > 380$ s), as measured from the surface ECG of patients at high arrhythmic risk, could be a reflection of adverse ionic changes involving I_{CaL}, I_{Ks}, and $[Na^+]_i$ dynamics that, upon further deterioration, may facilitate arrhythmia initiation via an increased likelihood of EAD generation.

Dynamics and Mechanisms of Ventricular HR Adaptation in Humans

This study shows that simulated QTI and APD HR adaptation dynamics in humans are in good qualitative and quantitative agreement with the results reported in experimental and clinical studies (3, 18, 22, 29, 35, 36). The simulation results report two phases, fast and slow, in QTI and APD adaptation dynamics, as previously reported in human experiments (18, 29, 35, 36) and also confirmed in experiments performed in this study. The time constants for the two phases in human are $\tau_{fast} <$ 30 s and $\tau_{slow} \geq 2$ min, respectively, in both simulations and experiments, in this study and in the literature (18, 36). Similar adaptation dynamics are found in dogs, with a slightly longer adaptation time compared with that in humans.

Our simulation results identify I_{CaL} and I_{Ks} properties as the main ionic determinants of the fast rate-dependent APD changes in humans, with I_{CaL} inactivation (Fig. 5*A*) playing a major role, as reported in previous studies for humans (31), for guinea pigs and rabbits (39), and for canine Purkinje fibers (6). In addition, our results show that I_{Ks} activation kinetics also contribute to the fast rate-dependent APD shortening (Fig. 5*A*), as previously suggested (8, 13, 14).

Importantly, we also demonstrate that $[Na^+]_i$ dynamics play a key role in the slow phase of APD adaptation (Fig. 5). I_{NaK} inhibition, as it occurs in ischemia and heart failure patients, results in slower $[Na^+]_i$ dynamics and delayed APD accommodation. The importance of I_{NaK} in the slow phase of APD adaptation was previously suggested in animal species such as dogs and guinea pigs (6, 10, 11, 14) but not in humans. Our study quantifies it and confirms it for humans. In addition, we show that it is primarily due to the role of I_{NaK} in regulating $[Na^+]_i$ dynamics, and, indirectly, $[Ca^{2+}]_i$ dynamics through the Na^+/Ca^{2+} exchanger, rather than to alterations in the electrogenic I_{NaK} current.

Ventricular rate adaptation as an indicator of arrhythmic risk. Following a thorough validation of the simulated rate adaptation dynamics described in *Ventricular Rate Adaptation*, computer simulations were used to explore the link between protracted HR adaptation and increased arrhythmic risk, as previously suggested (22, 35). The main preclinical arrhythmic risk biomarkers, namely, AP triangulation, probability of I_{CaL} reactivation, and APDR, were evaluated for conditions that lead to delayed APD adaptation, to quantify risk of occurrence of repolarization instabilities such as EADs and/or alternans (5, 44).

As discussed in *Ventricular Rate Adaption*, delayed APD adaptation could be caused by an increase in τ_{fast} (via a moderate reduction in τ_f or τ_{xs} or severe I_{CaL} maximal conductance block) or in τ_{slow} (via I_{NaK} inhibition). Reduced τ_f values have been reported in dogs with chronic atrioventricular block (1), which exhibit a high propensity for EADs and Torsades de Pointes, whereas reduced τ_{xs} is caused by a mutation in the KCNQ1 gene that causes short QT syndrome and is associated with high sudden cardiac death rate (4). Our simulations also show that a less-pronounced initial APD rate adaptation is associated with an increased AP triangulation and, in the case of reduced τ_{xs}, a higher probability of I_{CaL} reactivation, which facilitates EAD formation (25, 27, 30). Our results are also consistent with experimental results showing that the low incidence of EADs observed following the administration of amiodarone could be related to the ability of the drug to slow I_{CaL} (43) and decrease τ_{fast}. Furthermore, in patients who benefit from amiodarone therapy, the efficacy of the drug has been explained by its ability to accelerate QTI rate adaptation (37).

Reduced τ_f or τ_{xs}, and therefore increased τ_{fast}, are also associated with APDR slopes flattening, consistent with previous studies (23). The potential of APDR slopes as arrhythmic risk predictors is somewhat controversial. Both experimental and theoretical studies have shown that steep restitution slopes facilitate a spiral wave breakup and a transition from ventricular tachycardia to fibrillation (20, 32). However, conditions associated with flat restitution slopes also allow wave break (9, 16) and could favor reentrant wave stability (17, 19). Thus large τ_{fast} values could also be associated with an increased

arrhythmic risk due to the increased likelihood of the establishment of reentrant activity.

Both our simulation and experimental results show that I_{NaK} plays a key role in determining τ_{slow}. Large τ_{slow} due to I_{NaK} inhibition is associated with an increase in AP triangulation and in the likelihood of I_{CaL} reactivation (Fig. 6), indicating an increased risk of EAD formation. Large τ_{slow} values are also associated with flat APDR slopes, which could favor the stability of reentrant circuits and thus could increase arrhythmic risk.

Our simulations show that, both in humans and dogs, EADs develop for 60% I_{NaK} inhibition, a degree of inhibition observed in ischemic disease and heart failure patients treated with digitalis (7). In the experiments of I_{NaK} inhibition with 0.2 or 0.6 μM strophanthin G performed in the present study, no EADs were observed; however, the degree of drug-induced I_{NaK} inhibition is unknown and may be below 60%. Additionally, the lack of EADs in the experiments might be explained by the electrophysiological differences between the experimental (canine papillary muscle) and simulated preparations (canine Epi and human Endo/Mid/Epi tissue).

Limitations of the Study

In our study, a human ventricular model was used to explore ventricular rate adaptation dynamics and simulation predictions were validated using experimental and clinical data from the literature and in a limited set of experiments in humans performed in this study. Additional experiments and simulations were performed in dogs because of its similarities with humans in repolarization mechanisms. Our experimental and theoretical results obtained in dogs and humans are qualitatively similar, although quantitative differences exist that could be due to true animal species differences, differences in experimental conditions, or model limitations. First, differences exist in I_{K1} and I_{Ks} in canine versus human cardiac ventricular tissue (28), which would lead to differences in ventricular rate adaptation. Second, the human model (38) does not include a description of the late sodium current and its I_{Ks} conductance was defined based on APD measurements, which could explain a larger contribution of I_{Ks} to APD adaptation in simulations compared with experiments. Despite these limitations, the present study provides new insights into the mechanisms of ventricular rate adaptation and its link to proarrhythmic risk in humans through a challenging combination of theoretical and experimental work.

GRANTS

This study was financially supported by European Commission preDiCT Grant DG-INFSO-224381; a United Kingdom Medical Research Council Career Development award (to B. Rodríguez); a Royal Society Visiting Fellowship and International Joint Project (to E. Pueyo and B. Rodríguez); Ministerio de Ciencia e Innovación fellowships and from Caja de Ahorros de la Immaculada, Spain (to E. Pueyo); Ministerio de Ciencia e Innovación, Spain, Grant TEC-2007-68076-C02-02 (to E. Pueyo and P. Laguna); a János Bolyai research scholarship (to I. Baczkó); and Hungarian National Research Foundation Grant OTKA-CNK-77855.

DISCLOSURES

No conflicts to disclose.

REFERENCES

1. **Antoons G, Volders PG, Stankovicova T, Bito V, Stengl M, Vos MA, Sipido KR.** Window Ca^{2+} current and its modulation by Ca^{2+} release in hypertrophied cardiac myocytes from dogs with chronic atrioventricular block. *J Physiol* 579: 147–160, 2007.
2. **Arnold L, Page J, Attwell D, Cannell M, Eisner DA.** The dependence on heart rate of the human ventricular action potential duration. *Cardiovasc Res* 16: 547–551, 1982.
3. **Attwell D, Cohen I, Eisner DA.** The effects of heart rate on the action potential of guinea-pig and human ventricular muscle. *J Physiol* 313: 439–461, 1981.
4. **Béllocq C, van Ginneken AC, Bezzina CR, Alders M, Escande D, Mannens MM, Baró I, Wilde AA.** Mutation in the KCNQ1 gene leading to the short QT-interval syndrome. *Circulation* 109: 2394–2397, 2004.
5. **Binah O, Rosen MR.** Mechanisms of ventricular arrhythmias. *Circulation* 85: I25–I31, 1992.
6. **Boyett MR, Fedida D.** Changes in the electrical activity of dog cardiac Purkinje fibres at high heart rates. *J Physiol* 350: 361–391, 1984.
7. **Bundgaard H, Kjeldsen K.** Human myocardial Na,K-ATPase concentration in heart failure. *Mol Cell Biochem* 163–164: 277–283, 1996.
8. **Carmeliet E.** Action potential duration, rate of stimulation, and intracellular sodium. *J Cardiovasc Electrophysiol* 17: S2–S7, 2006.
9. **Clayton RH, Taggart P.** Regional differences in APD restitution can initiate wavebreak and re-entry in cardiac tissue: a computational study. *Biomed Eng Online* 20: 4–54, 2005.
10. **Decker KF, Heijman J, Silva JR, Hund TJ, Rudy Y.** Properties and ionic mechanisms of action potential adaptation, restitution, and accommodation in canine epicardium. *Am J Physiol Heart Circ Physiol* 296: H1017–H1026, 2009.
11. **Drake AJ, Noble MI, Schouten V, Seed A, Ter Keurs HE, Wohlfart B.** Is action potential duration of the intact dog heart related to contractility or stimulus rate? *J Physiol* 331: 499–510, 1982.
12. **Drouin E, Charpentier F, Gauthier C, Laurent K, Le Marec H.** Electrophysiologic characteristics of cells spanning the left ventricular wall of human heart: evidence for presence of M cells. *J Am Coll Cardiol* 26: 185–192, 1995.
13. **Eisner DA, Dibb KM, Trafford AW.** The mechanism and significance of the slow changes of ventricular action potential duration following a change of heart rate. *Exp Physiol* 94: 520–528, 2009.
14. **Faber GM, Rudy Y.** Action potential and contractility changes in $[Na^+]_i$ overloaded cardiac myocytes: a simulation study. *Biophys J* 78: 2392–2404, 2000.
15. **Fenichel RR, Malik M, Antzelevitch C, Sanguinetti M, Roden DM, Priori SG, Ruskin JN, Lipicky RJ, Cantilena LR; Independent Academic Task Force.** Drug-induced torsades de pointes and implications for drug development. *J Cardiovasc Electrophysiol* 15: 475–495, 2004.
16. **Fenton FH, Evans SJ, Hastings HM.** Memory in an excitable medium: a mechanism for spiral wave breakup in the low-excitability limit. *Phys Rev Lett* 83: 3964–3967, 1999.
17. **Frame LH, Simson MB.** Oscillations of conduction, action potential duration, and refractoriness. A mechanism for spontaneous termination of reentrant tachycardias. *Circulation* 78: 1277–1287, 1988.
18. **Franz MR, Swerdlow CD, Liem LB, Schaefer J.** Cycle length dependence of human action potential duration in vivo. Effects of single extrastimuli, sudden sustained rate acceleration and deceleration, and different steady-state frequencies. *J Clin Invest* 82: 972–979, 1988.
19. **Franz MR.** The electrical restitution curve revisited: steep or flat slope—which is better? *J Cardiovasc Electrophysiol* 14: S140–S147, 2003.
20. **Garfinkel A, Kim YH, Voroshilovsky O, Qu Z, Kil JR, Lee MH, Karagueuzian HS, Weiss JN, Chen PS.** Preventing ventricular fibrillation by flattening cardiac restitution. *Proc Natl Acad Sci USA* 97: 6061–6066, 2000.
21. **Gima K, Rudy Y.** Ionic current basis of electrocardiographic waveforms: a model study. *Circ Res* 90: 889–896, 2002.
22. **Grom A, Faber TS, Brunner M, Bode C, Zehender M.** Delayed adaptation of ventricular repolarization after sudden changes in heart rate due to conversion of atrial fibrillation. A potential risk factor for proarrhythmia? *Europace* 7: 113–121, 2005.
23. **Gudzenko V, Shiferaw Y, Savalli N, Vyas R, Weiss JN, Olcese R.** Influence of channel subunit composition on L-type Ca^{2+} current kinetics and cardiac wave stability. *Am J Physiol Heart Circ Physiol* 293: H1805–H1815, 2007.
24. **Guo D, Zhao X, Wu Y, Liu T, Kowey PR, Yan GX.** L-type calcium current reactivation contributes to arrhythmogenesis associated with action potential triangulation. *J Cardiovasc Electrophysiol* 18: 196–203, 2007.
25. **Guo D, Zhou J, Zhao X, Gupta P, Kowey PR, Martin J, Wu Y, Liu T, Yan GX.** L-type calcium current recovery versus ventricular repolariza-

tion: preserved membrane-stabilizing mechanism for different QT intervals across species. *Heart Rhythm* 5: 271–279, 2008.
26. **Hao SC, Christini DJ, Stein KM, Jordan PN, Iwai S, Bramwell O, Markowitz SM, Mittal S, Lerman BB.** Effect of β-adrenergic blockade on dynamic electrical restitution in vivo. *Am J Physiol Heart Circ Physiol* 287: H390–H394, 2004.
27. **Hondeghem LM, Carlsson L, Duker G.** Instability and triangulation of the action potential predict serious proarrhythmia, but action potential duration prolongation is antiarrhythmic. *Circulation* 103: 2004–2013, 2001.
28. **Jost N, Varró A, Szuts V, Kovacs PP, Seprényi GY, Biliczki P, Lengyel Cs Prorok J, Bitay M, Ördög B, Szabad J, Varga-Orvos Z, Puskas L, Cotella D, Papp JG, Virag L, Nattel S.** Molecular basis of repolarization reserve differences between dogs and man (Abstract). *Circulation* 118: S342, 2008.
29. **Lau CP, Freedman AR, Fleming S, Malik M, Camm AJ, Ward DE.** Hysteresis of the ventricular paced QT interval in response to abrupt changes in pacing rate. *Cardiovasc Res* 22: 67–72, 1988.
30. **Lawrence CL, Pollard CE, Hammond TG, Valentin JP.** Nonclinical proarrhythmia models: predicting Torsades de Pointes. *J Pharmacol Toxicol Methods* 52: 46–59, 2005.
31. **Li GR, Yang B, Feng J, Bosch RF, Carrier M, Nattel S.** Transmembrane I_{Ca} contributes to rate-dependent changes of action potentials in human ventricular myocytes. *Am J Physiol Heart Circ Physiol* 276: H98–H106, 1999.
32. **Mahajan A, Sato D, Shiferaw Y, Baher A, Xie LH, Peralta R, Olcese R, Garfinkel A, Qu Z, Weiss JN.** Modifying L-type calcium current kinetics: consequences for cardiac excitation and arrhythmia dynamics. *Biophys J* 94: 411–423, 2008.
33. **Martínez JP, Almeida R, Olmos S, Rocha AP, Laguna P.** A wavelet-based ECG delineator: evaluation on standard databases. *IEEE Trans Biomed Eng* 51: 570–581, 2004.
34. **Milberg P, Reinsch N, Wasmer K, Mönnig G, Stypmann J, Osada N, Breithardt G, Haverkamp W, Eckardt L.** Transmural dispersion of repolarization as a key factor of arrhythmogenicity in a novel intact heart model of LQT3. *Cardiovasc Res* 65: 397–404, 2005.
35. **Pueyo E, Smetana P, Caminal P, de Luna AB, Malik M, Laguna P.** Characterization of QT interval adaptation to RR interval changes and its use as a risk-stratifier of arrhythmic mortality in amiodarone-treated survivors of acute myocardial infarction. *IEEE Trans Biomed Eng* 51: 1511–1520, 2004.
36. **Seed WA, Noble MI, Oldershaw P, Wanless RB, Drake-Holland AJ, Redwood D, Pugh S, Mills C.** Relation of human cardiac action potential duration to the interval between beats: implications for the validity of rate corrected QT interval (QTc). *Br Heart J* 57: 32–37, 1987.
37. **Smetana P, Pueyo E, Hnatkova K, Batchvarov V, Laguna P, Malik M.** Individual patterns of dynamic QT/RR relationship in survivors of acute myocardial infarction and their relationship to antiarrhythmic efficacy of amiodarone. *J Cardiovasc Electrophysiol* 15: 1147–1154, 2004.
38. **ten Tusscher KH, Panfilov AV.** Alternans and spiral breakup in a human ventricular tissue model. *Am J Physiol Heart Circ Physiol* 291: H1088–H1100, 2006.
39. **Tolkacheva EG, Anumonwo JM, Jalife J.** Action potential duration restitution portraits of mammalian ventricular myocytes: role of calcium current. *Biophys J* 91: 2735–2745, 2006.
40. **Varró A, Baláti B, Iost N, Takács J, Virág L, Lathrop DA, Csaba L, Tálosi L, Papp JG.** The role of the delayed rectifier component I_{Ks} in dog ventricular muscle and Purkinje fibre repolarization. *J Physiol* 523: 67–81, 2000.
41. **Virág L, Acsai K, Hála O, Zaza A, Bitay M, Bogáts G, Papp JG, Varró A.** Self-augmentation of the lengthening of repolarization is related to the shape of the cardiac action potential: implications for reverse rate dependency. *Br J Pharmacol* 156: 1076–1084, 2009.
42. **Viswanathan PC, Rudy Y.** Pause induced early afterdepolarizations in the long QT syndrome: a simulation study. *Cardiovasc Res* 42: 530–542, 1999.
43. **Wegener FT, Ehrlich JR, Hohnloser SH.** Dronedarone: an emerging agent with rhythm- and rate-controlling effects. *J Cardiovasc Electrophysiol* 17: S17–S20, 2006.
44. **Weiss JN, Qu Z, Chen PS, Lin SF, Karagueuzian HS, Hayashi H, Garfinkel A, Karma A.** The dynamics of cardiac fibrillation. *Circulation* 112: 1232–1240, 2005.
45. **Zaza A, Malfatto G, Schwartz PJ.** Sympathetic modulation of the relation between ventricular repolarization and cycle length. *Circ Res* 68: 1191–1203, 1991.